AUTOMATED MONITORING OF LAUNCHING GIRDER OPERATIONS USING WIRELESS SENSOR NETWORK

A THESIS

submitted by

RANJITH K. S.

for the award of the degree of

MASTER OF SCIENCE

BUILDING TECHNOLOGY AND CONSTRUCTION MANAGEMENT DIVISION

DEPARTMENT OF CIVIL ENGINEERING

INDIAN INSTITUTE OF TECHNOLOGY MADRAS

NOVEMBER 2016

THESIS CERTIFICATE

This is to certify that the thesis titled **'AUTOMATED MONITORING OF LAUNCHING GIRDER OPERATIONS USING WIRELESS SENSOR NETWORK'**, submitted by **Ranjith K. S.**, to the Indian Institute of Technology Madras, for the award of the degree of Master of Science, is a bonafide record of the research work carried out by him under my supervision. The contents of this thesis, in full or in parts, have not been submitted to any other Institute or University for the award of any degree or diploma.

Dr. Benny Raphael
(Research Guide)
Associate Professor,
Department of Civil Engineering,
Indian Institute of Technology Madras,
Chennai - 600 036

Prof. Koshy Varghese
(Research Co-Guide)
Professor,
Department of Civil Engineering,
Indian Institute of Technology Madras,
Chennai - 600 036

Chennai, India
29 Nov, 2016

ACKNOWLEDGEMENT

This thesis is the end of my journey in obtaining my M. S. by Research degree. I have not traveled in a vacuum in this journey. This thesis has been kept on track and been seen through to completion with the support and encouragement of numerous people including my well-wishers, my friends, colleagues and various institutions. At the end of my thesis I would like to thank all those people who made this thesis possible and an unforgettable experience for me. At this point, it is a pleasant task to express my thanks to all those who contributed in many ways to the success of this study and made it an unforgettable experience for me.

I would like to express my sincere gratitude to all of them. First of all, I am extremely grateful to my research guide, Dr. Benny Raphael, for his valuable guidance, scholarly inputs and consistent encouragement I received throughout the research work. This feat was possible only because of the unconditional support provided by Sir. A person with an amicable and positive disposition, Sir has always made himself available to clarify my doubts despite his busy schedules and I consider it as a great opportunity to do my research under his guidance and to learn from his research expertise. He has been kind enough to take that extra effort and correct my papers and thesis even after me submitting it at the eleventh hour without any dejection. Thank you Sir, for all your help and support.

'A true mentor is one who inspires you to outdo yourself'. Nothing else describes my co- guide better. I would like to express my special appreciation and thanks to Professor Koshy Varghese, you have been a tremendous mentor for me. Little did I know, when I first met you, that you would change my life in such magnitude. I would like to thank you for encouraging my research and for allowing me to grow as a research scholar. Your advice on both research as well as on my career have been priceless.

Besides my advisor, I would like to thank the rest of my thesis committee: Prof. V. Kamakoti, and Dr. Saravanan U., for their insightful comments and encouragement, but also for the hard questions which incented me to widen my research from various perspectives. Faculty members of the Institute have been very kind enough to extend their help at various phases of this research, whenever I approached them, and I do hereby acknowledge all of them. The technical guidance offered at various phases of this project by Dr. Ashwin Mahalingam, Dr. Boby George, and Prof. Vellore Gopalaratnam is highly appreciated. . I thank Prof. Meher Prasad, Head of the

Department of Civil Engineering, for providing all necessary facilities and excellent technical support. I am also grateful to Prof. Ravishankar Kottada, Prof. Ravindra Gettu, and Dr. Radhakrishna G. Pillai for the technical assistance provided in the form of the access to various laboratories in IITM.

I take this opportunity to sincerely acknowledge the EDRC division of Larsen and Toubro for enabling me a platform for the validation study of my research. I am extremely thankful to Bhavani K, Suni K, Chandravanan L, Chaithanyam K B and Aqueel Mohammad for helping me get access to different sites of HMRL for my research. I would like to express my gratitude to the site engineers Santosh and Padarbinda Khuntiya at the Malakpet LG 1 site for providing all the necessary facilities at the site during the implementation. I am indebted to Hari Prasad and Madhu Sudhan for offering outstanding technical help for getting trained in embedded programming.

Most of the results described in this thesis would not have been obtained without a close collaboration with few laboratories and laboratory staff. I would like to thank Veera Balaji, Dominic and Benny Roger for the assistance in the lab and during the implementation of my research. I extend my sincere gratitude to the staffs of the Central Workshop in IITM and Central Fabrication Facility (CFF) to all the help offered in this project and the excellent quality of the work which deserves appreciation.

I thank my fellow lab mates Vinay Mathews, Jeevan Jacob and Amritha John for the stimulating discussions, for the sleepless nights we were working together, and for all the fun we have had in the last three years. I am indebted to my many student colleagues for providing a stimulating and fun filled environment. My thanks go in particular to Ranjitha R. with whom I started this M.S. programme and she had helped me a lot during the ups and downs of my research. I am ever indebted to Anna George and Sai Kiran and I admire their distinguished helping nature. I wish to thank my friends, Shyam, Shameeja, Abul and Sheetal for their love, care and moral support. Sanoop, Sooraj and Ram deserve special mention here for their constant support, motivation and help. I am also thankful to Pinky, Srinath, Marimuthu, Johan, and Jayachandran, for their support during my research work. My special thanks to Praveen for his advice to join for M.S. program in IITM which indeed turned out to be a life changing experience. I am greatly indebted to Dr. Radhakrishna G. Pillai for his timely advices and interventions which helped to approach my career in a better way and also changed my outlook towards life itself.

It’s my fortune to gratefully acknowledge the support of some special individuals. Words fail me to express my appreciation to Vani, Visakh, Madhumitha and Devi for their support, generous care and creating the homely feeling at IIT Madras. They were always beside me during the happy and hard moments to push me and motivate me. A journey is easier when you travel together. Thank you doesn't seem sufficient but it is said with appreciation and respect to them for their support, encouragement, care, understanding and precious friendship

I owe a lot to my parents, who encouraged and helped me at every stage of my personal and academic life, and longed to see this achievement come true. My mom has been the greatest support and the best of friends for every endeavor of my life including this. A huge thanks to Amma for enduring all my fretting and fuming when things were not going right and for making me strong and independent in the process. Thanks to Achan, for being the inspiring strong pillar he is and my brother Raghu for springing up to solve my problems in his own little ways. Last but not the least, I thank God almighty for showering his blessings on me, without which I would not have been able to become what I am today.

- Ranjith

2q

CONTENTS

LIST OF FIGURES

LIST OF TABLES

ABBREVIATIONS

LG	Launching Girder
WSN	Wireless Sensor Network
RSSI	Received Signal Strength Indicator
PDR	Packet Delivery Ratio
SI	System Identification
GSM	Global System for Mobile Communication
Wi-Fi	Wireless Fidelity
GPS	Global Positioning System
RFID	Radio Frequency Identification
CDMA	Code Division Multiple Access
LIDAR	Light Radar
LASER	Light Amplification by Stimulated Emission of Radiation
IoT	Internet of Things

NOTATIONS

$H(x)$	Shannon’s entropy for event x
$p(x)$	Probability of event x

CHAPTER 1

INTRODUCTION

The global construction industry contributes to around 11 percent of the global GDP in 2011 and it is predicted to cross 13.2 % by the year 2020. The share of the construction industry in the global economy in 2015 is US$8.5 trillion which is expected to climb to US$10.3 trillion by 2020. A significant portion of this development comes from the construction scene of emerging economies which shows a higher rate of growth. Increasing population, growing economy and urbanization in these nations necessitate investments in various infrastructure projects. Growing urbanization in emerging nations is resulting in the initiation of a large number of urban transport projects such as metro rail construction. The Delhi Metro Rail Project revolutionized transport for the 17 million residents of this city. Based on the success of this project several other cities in India have also initiated metro rail projects. It is estimated that $30 billion will be invested in these metro rail projects, which are to be completed before 2019.

The overall success of these projects depends heavily on completion of construction within planned time and cost. To ensure this, the progress of the project has to be monitored and controlled on a continuous basis. The broad objective of this work is to develop a framework for real time automated construction progress monitoring of viaduct construction in metro rail projects.

While manual monitoring is conventionally utilized, it is slow and inaccurate(Davidson & Skibniewski 1995). Further, there are overheads for manual monitoring, 2% of the work in construction is committed to tracking and recording progress data manually(Cheok *et al.* 2000). Also, construction supervisors spend about 30-50% of their time interpreting and analyzing field data, in many situations data for correct analysis is not available and the supervisors resort to optimistic reporting(Goldratt & Cox 2004). As a result of these inefficiencies in data collection and interpretation, appropriate corrective actions are not implemented in a timely fashion and which lead to delays in the implementation of control measures.

Theoretical frameworks for project monitoring and control are available with which precise project performance indices need to be computed(Navon 2005). However, massive amounts of accurate data need to be continuously generated for effective project performance monitoring. Traditional methods employing manual data collection are slow and inaccurate. One solution to the above problem is automated data collection(Kiziltas *et al*. 2008). The main objective of automated monitoring is to acquire data, convert it to information and deliver it on time so that timely detection of discrepancies are noted(Rebolj *et al*. 2008)and corrective actions could be taken. Automated data collection can be implemented using real time monitoring systems with the aid of advanced sensing and signal processing technologies which would contribute towards checking quality, accuracy and progress of the project. The use of automated data collection techniques is increasingly used both for health monitoring and construction progress monitoring of the built environment. In the area of health monitoring, structural & functional parameters of high-rise buildings, bridges, tunnels, and heritage structures are monitored and controlled with the aid of sensor networks, data acquisition and communication, signal processing and information management systems. Long-term health monitoring systems have been deployed on structures such as high-rise buildings (Kijewski-correa *et al*. 2013), heritage buildings(Ramos *et al*. 2013), tunnels (Ran *et al*. 2012) and bridges .

1.1 RESEARCH QUESTION

Automated data collection has already been employed in construction for productivity and progress monitoring. This is achieved using technologies such as imaging (Dimitrov & Golparvar-Fard 2014), RFID (Jaselskis & El-Misalami 2003; Jang & Skibniewski 2009), distributed sensor networks (Ye *et al*. 2012), LIDAR (Golparvar-Fard *et al*. 2011), accelerometers (Joshua & Varghese 2014) for progress monitoring, material tracking , safety monitoring, etc. These technologies have inherent limitations such as lack of mobility. For instance, an imaging technique for progress monitoring is constrained by its location and cannot be used for monitoring projects such as viaduct construction. Joshua & Varghese (2014) have addressed this issue to an extent by integrating a wearable sensor on workers to track productivity. Although this approach is suitable for productivity assessment, this might not be suitable to track progress, especially in large projects since it is challenging to consolidate the large amount of data from all the workers and finally evaluate progress from these data. These limitations could be overcome if the monitoring system is integrated with the equipment or supporting structure which is central to the construction activity. Therefore, as the construction progresses, the monitoring system travels integrally with the equipment / supporting structure to the location of the construction.

A monitoring system that measures structural responses is a potential technology which can be integrated with the equipment or temporary structure. However, construction monitoring using the responses from structural monitoring of construction equipment has not been explored yet. This study explores the feasibility of using structural responses from construction equipment to assess the productivity and progress of construction as shown in Figure 1.1. This study tests this hypothesis on a metro rail viaduct construction to evaluate the feasibility.

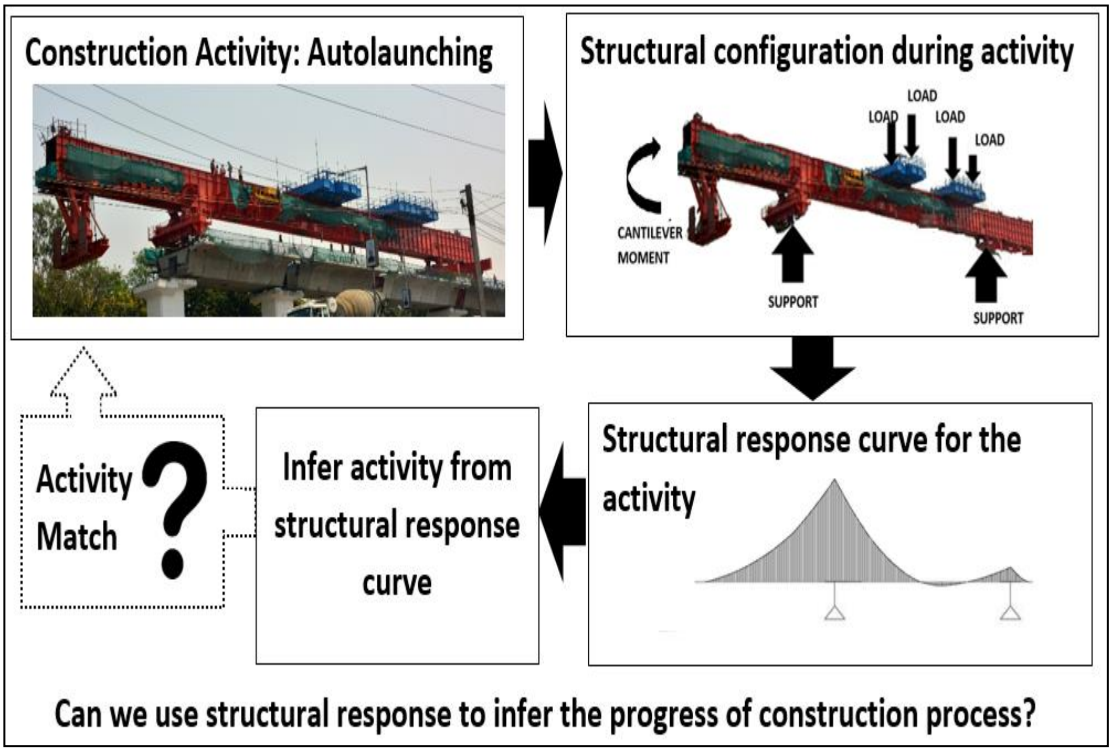

Figure 1.1: Figure illustrating the research question

1.2 NEED TO MONITOR LAUNCHING GIRDER

There are different methods for constructing via ducts. The most commonly used construction technique for viaduct is the incremental launching. When compared to other via duct construction methods, incremental launching have the advantages such

- Construction could be carried out in with less site area
- faster cycle time
- repetitive process

These advantages make it the best option for metro rail viaduct construction, which should be constructed on top of busy streets. Key component in the incremental launching construction method is the launching girder.

Launching Girder (LG) is an equipment used in metro rail construction to lift and assemble prefabricated concrete segments, which are then joined to create the span of the viaduct. Launching Girder is involved in several operations including the lifting of segments, pre-stressing, post-tensioning and loading of the span. Therefore, monitoring the state of this equipment should give direct information related to the progress of metro rail construction. Completion of each cycle of the launching girder operations can be considered as a milestone activity in the schedule of metro rail viaduct construction. Hence, by monitoring the operations of the launching girder we can, in turn, monitor the cycle times of the launching girder or in other words productivity of the construction, which if done manually would be slow and less accurate.

Although automation of launching girder has many advantages such as improved construction efficiency, reduction in accidents, smooth operation, etc., currently, there is limited automation in the operation of launching girders worldwide. To automate the construction process, real-time data pertaining to the state of the launching girder such as the current launch position, pressure in hydraulic pumps, internal forces, etc. are required. In addition, it is essential to ensure that assumptions made during the design phase are valid during the operation phase. Even though conservative assumptions are usually made, the impact of these assumptions is rarely studied. A sensing system capable of measuring structural responses of the launching girder aids in determining the state of the launching girder during the construction phase helps in progress and productivity monitoring, explores the possibility of automation and also serve as a feedback system for automation. It also helps to validate the assumptions made during the design phase. It is to be noted that assumptions made to cater to loads during the construction phase are generally taken by incorporating higher factor of safety. These assumptions are generally not validated during the construction phase. The proposed framework of the sensing system is capable of evaluating the assumptions made during the design by measuring actual strain during the construction and comparing with the designed strain limits.

1.3 LAUNCHING GIRDER AND ITS OPERATIONS

The LG is fabricated as a plate girder (box) and spans continuously over four supports as shown in Figure 1.2. This section describes the operations of a basic box type launching girder. It is observed that the overall progress of metro rail viaduct construction can be ascertained by monitoring the operations of the launching girder.

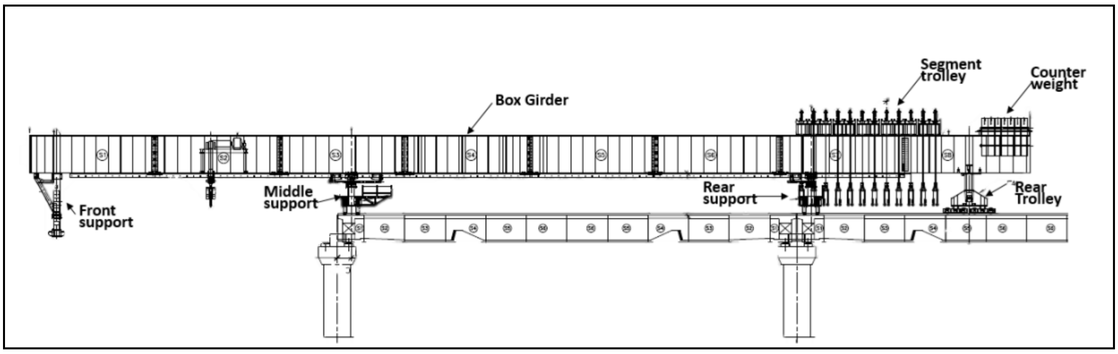

Figure 1.2 Different parts of Launching Girder

Figure 1.3: Launching girder during different operations
1. Auto Launching; 2: Segment Lifting; 3: Span Lowering

The LG consists primarily of five parts. Steel plate girder, front support, middle support, rear support and rear trolley as shown in Figure 1.2. The different stages (or state of launching girder) for the construction of a span and its associated bending moment diagram (BMD is for illustration purpose and may not be accurate on schematic) are as shown in Figure 1.4 and Figure 1.5 respectively.

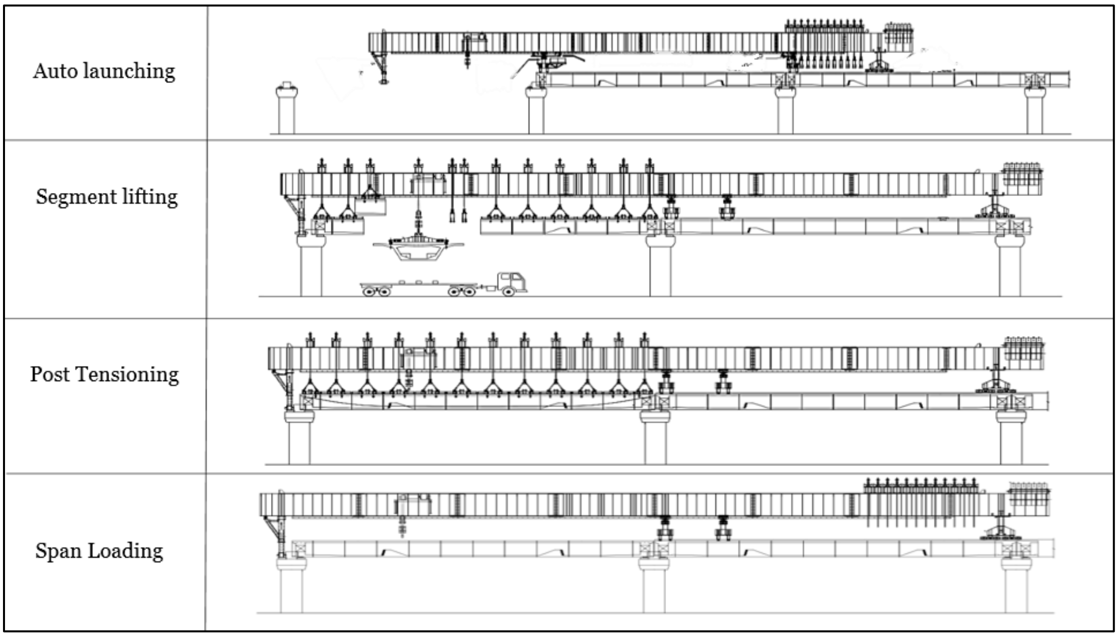

Figure 1.4:Launching Girder operations

Auto launching: Auto-launching is the process when the launching girder is moved from the ‘constructed span’ to the ‘next to be constructed’ span of the viaduct as shown in Figure 1.4. In this process, the front support of the launching girder is released and launching girder is supported by remaining supports. Launching Girder is launched to the subsequent span by pushing the plate girder forward to the next pier. Counterweight placed at the rear side of the LG balances cantilever moment created by the front portion until the front support reaches the next pier. The support is then rested on the pier which marks the end of Autolaunching operation. The BMD of the operation is shown in Figure 1.5 and characterized by the high negative moment at the cantilever support. Photograph of this operation is shown in Figure 1.3

Segment Lifting: This operation takes place after the auto-launching. It involves lifting each prefabricated segment from the ground sequentially and assembling it along the span to form the viaduct as shown in Figure 1.4. Once all the segments are lifted, they are then aligned and moved into position to be joined and placed on the piers. All the segments lifted remain suspended on the front portion of LG. Typical BMD of the operation is shown in Figure 1.5. There is a positive sagging moment on the front side of the LG while having a negative moment on the rear side. Please note that the BMD doesn’t correspond accurately to the schematic of the operation shown. Photograph of this operation is shown in Figure 1.3

Post-tensioning: This process, which takes place after the segment lifting involves joining all the segments through a post-tensioning process as shown in Figure 1.4.

Cables are run through the segments and then tensioned to the designed stress with a hydraulic jack while the segments are suspended on the front portion of LG. Once the stressing is done, the assembled segments act as a single structure. Load of the segments is still borne by the front portion of the LG. The bending moment is similar to segment lifting, however, the moment on the front side is partly negative in this case since the launching girder is fully loaded.

Span lowering: The post-tensioned span is lowered onto the piers in this process. Once the span rests on the pier, Segments are released from the launching girder. The span transfers its self-weight to the piers. LG is free from the load of the segments. Once this process is done, LG is ready for auto launch to the next to be constructed span. Schematic of this stage is shown in Figure 1.4. The bending moment during this stage is similar to the beginning of segment lifting but with a higher magnitude of the negative moment on the rear side. Photograph of this operation is shown in Figure 1.3

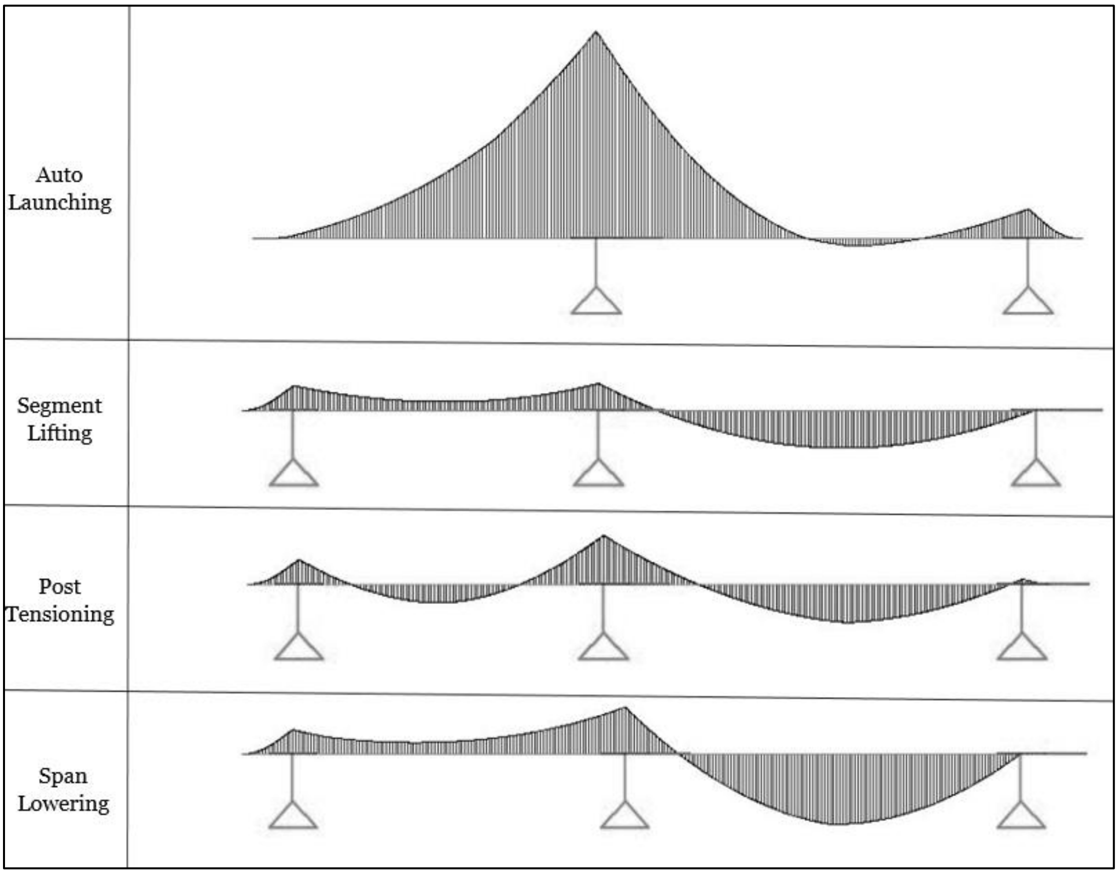

Figure 1.5: Bending moment associated with launching girder activities

The bending moment changes continuously with respect to the operation. It starts with a BMD similar to span lowering as shown in Figure 1.5. When the support is released during launching. BMD on the front will have a negative moment which increases with the increase in the distance launched. Finally, when front support rests on the girder, BMD corresponds to the one at the start of launching. Then, during the start of launching front side of the launching girder will have a positive moment which progresses to negative moment as the no of segment lifted progress, Post-Tensioning and the end of segment lifting would have the maximum negative moment on the front side of the LG. However these can be differentiated since the end of segment lifting will have a sudden change in slopes of BMD while that of Post-tensioning would have gradual changes. Once the span is lowered on to piers, the BMD changes to the initial state before the launch.

These changes in stress patterns can be identified in real time by measuring the structural parameters using sensors such as strain gauges, load cells etc. Once the strain pattern is obtained, the state of the LG can be recognized based on the strain pattern across the length of the LG. However, the operations of LG has its own uncertainties such as support settlement, variations in counter weights, variations in the weight of segments etc. Due to these field uncertainties, the results from the base analytical model will not be the same as the field measurements. In addition, uncertainties in measurements and errors in sensing may arise due to the nature of field conditions. The system identification algorithm should cater to these uncertainties while identifying the state of the launching girder.

1.4 THESIS ORGANISATION

The thesis is organized into six chapters. Each subchapter is further divided into the further section. A brief explanation of various chapters in the thesis is given below.

- Chapter 2 starts with a discussion on the work done in the area of wireless sensors followed by measurement system design and system identification. The chapter is concluded with research gaps found in the previous works.

- Chapter 3 presents the objectives of the work and its scope. It also discusses the methodology followed to conduct this research.

- Chapter 4 provides details on the wireless sensor network design, sensor placement methodology and the system identification methodologies used in this study.

- Chapter 5 discusses the implementation of the monitoring system on a launching girder, hardware components used for the same.

- Chapter 6 presents the results from the implementation of the launching girder. Performance of the WSN, comparative efficiency of the sensor placement methodology and relative accuracies of system identification methodologies are presented

- Chapter 7 states the conclusions and contribution from this work.

CHAPTER 2

LITERATURE REVIEW

2.1 INTRODUCTION

The previous chapter gave an outline of the need for monitoring construction and in particular the need to monitor the launching girder operations. This chapter discusses the previous work in the areas such as automated construction progress monitoring, the wireless sensor network, measurement system design and system identification. Section 2.2 discusses various automated construction progress monitoring techniques such as Imaging, RFID, GPS etc. while Section 2.3 discusses the need for wireless sensor network and the challenged associated implementation of a WSN in a construction site. Section 2.4 deals with the evolution of measurement system design and the need for a sensor placement methodology while designing a sensing system. Section 2.5 describes the common system identification technologies and its feasibility of application

2.2 AUTOMATED CONSTRUCTION PROGRESS MONITORING

This section discusses various automated data collection methods in construction which uses Automated Data Collection (ADC). Some of the potential ADC technologies used in construction for project monitoring are Bar Code, RFID, Distributed sensor network, GPS, Imaging, LIDAR etc. However, whether it is capable of monitoring the operations of a launching girder is a topic that has to be explored through this review.

2.2.1 Barcode

Bar codes are used in construction monitoring by evaluation and management of stock and then tracing it back to the planned schedule of dispatch and then back tracking to the construction progress (Cheng & Chen 2002). Bar code applications are implemented in three phases as shown in Figure 2.1.

- Design Phase- Each element of the design is associated with a bar code and this bar code is coded to the execution plan.

- Manufacturing phase: Each element manufactured is assigned a bar code as mentioned in the design.

- Construction phase: Before the commencement of construction, the sequence for the same is scheduled as per the plan. Installation of each and every component is as per this plan, hence scanning the bar code before the activity ensures all the previous activities in that line are completed.

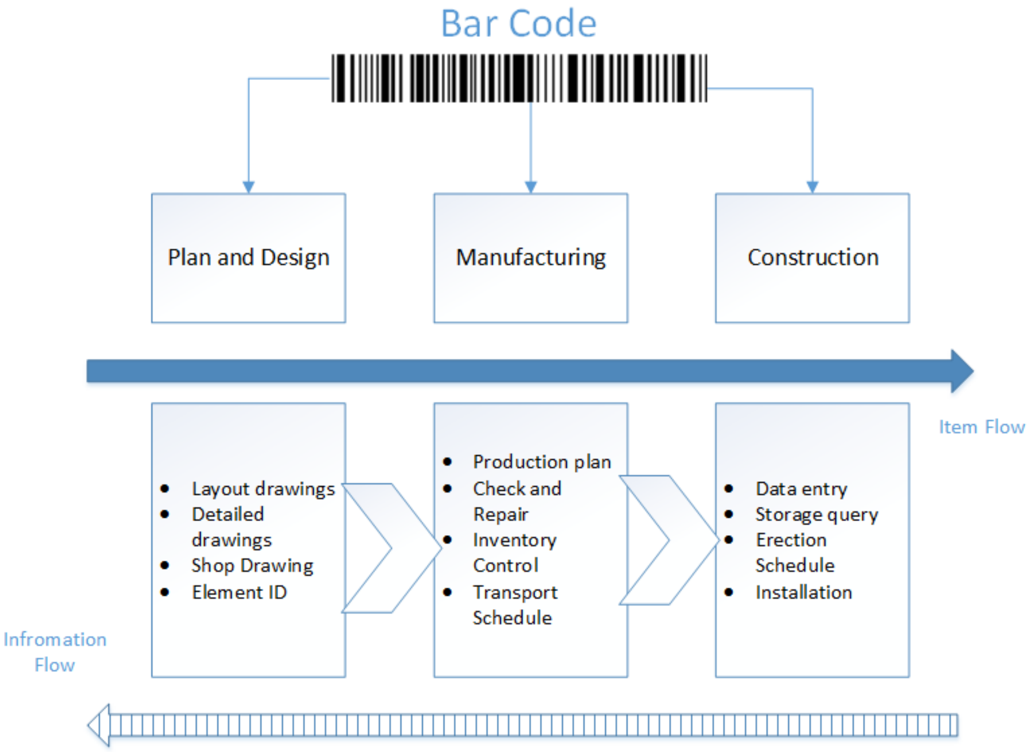

Figure 2.1 : Using bar code for construction monitoring
(Cheng & Chen 2002)

There are two points of scanning bar codes. First one being the entrance to the storage yard and second when it is lifted for the erection. Hence, the first point helps in the inventory management and second for the control center to check information such as position, sequence etc. The control center can, in turn, update the progress based on the tracked materials and components. Data collection efficiency is improved by using automated bar code scanning to gather and record the site activities.

However, there are limitations associated with the framework which is as follows.

- Barcodes have very low storage capacity, and they lack durability.
- They have low readability and can be read only when line of sight is established
- They can be read only one at a time.
- They can't be reprogrammed.

- It is difficult to attach bar code to in-situ construction components.(Bayrak 2008)

2.2.2 Radio Frequency Identification (RFID)

Yoon *et al* (2006) use RFID to track every component during ordering, production, transportation, storage, installation and inspection jobs as shown in Figure 2.2. The continuous movement of workers and materials in the construction site coupled with advances in work makes RFID technologies unable to monitor the resources effectively. This can only be overcome by integrating RFID technology with other technologies (Valero *et al*. 2015).

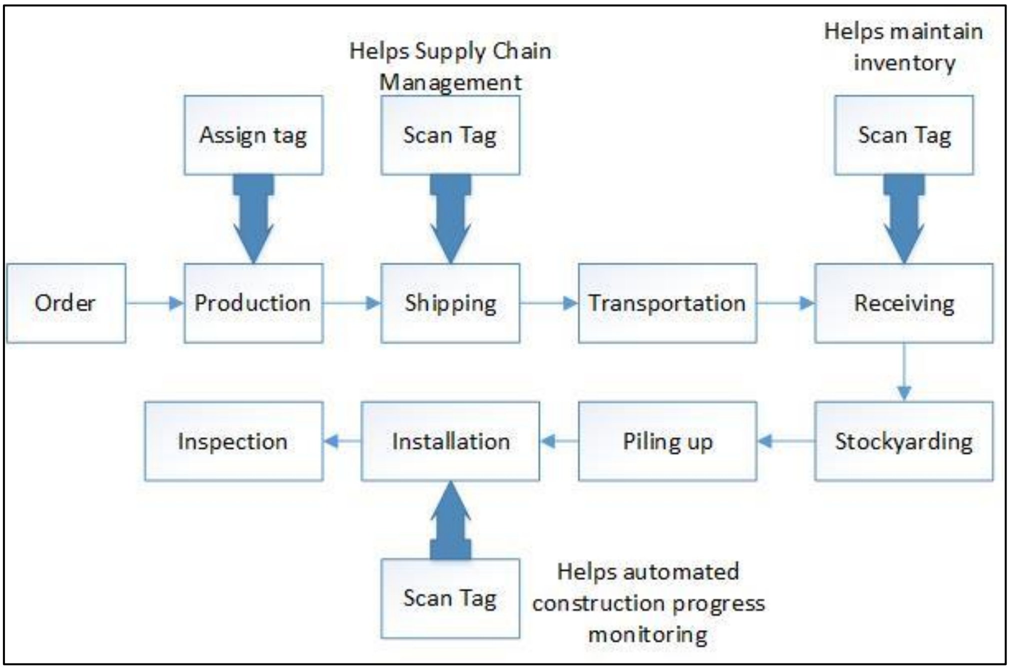

Figure 2.2: Example of a RFID system for construction progress monitoring (Yoon *et al*. 2006)

Control the material status can be used to show a 4D CAD model and compared as built with planned model and evaluate progress.(El-Omari & Moselhi 2011). RFID is used to track different components and then later used to visualize construction progress by integrating it with building information modeling (Wang *et al*. 2013). However, these methods aren't fully automated and require manual scanning of RFID tags if the object is large. In addition, rework can't be measured using this technology as it isn't modeled in the actual sequence.

2.2.3 Ultra-wide band

Similar to RFID tag, Ultra-wide band (UWB) provides real-time location tracking to resources that are equipped with a UWB tag as shown in Figure 2.3. It works on short pulse RF waveform based on time domain principles of electromagnetic theory. It has a higher range, measurement accuracy, and immunity to interference when compared with RFID (Cheng *et al*. 2010).

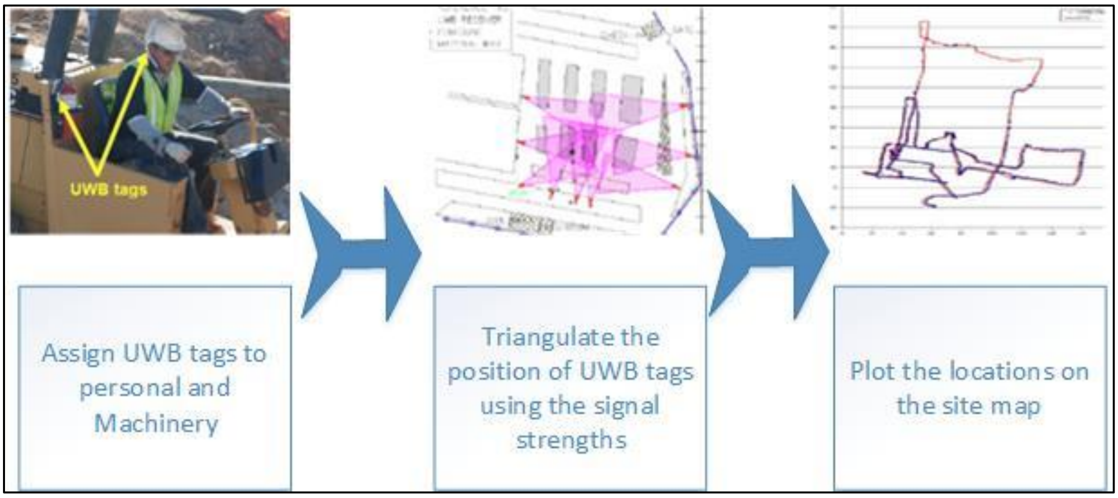

Figure 2.3: Ultra Wide Band for realtime location tracking (Cheng *et al*. 2010)

Although the ultra-wide band is accurate than RFID, it has inherent disadvantages as in RFID such as the requirement for modeling, association of tags with the equipment etc. In addition, the range of UWB is limited. Hence, it can't be used in construction such as viaduct construction which is spatially extensive.

2.2.4 Global Positioning System (GPS) and Geographical Information System (GIS)

Global Positioning System (GPS) and Geographical Information System(GIS) can be used as automatic data collection framework to enhance real-time construction progress monitoring.(Pradhananga & Teizer 2013)

Figure 2.4: A conceptual model of GPS-and-GIS-integrated Material and Equipment management system (Li *et al*. 2005)

Real time information of materials and equipment can be tracked using GPS and GIS systems as shown in Figure 2.4. This helps in obtaining the real-time vehicle locations, navigation assistance, and drive speed heading information. All these data could be integrated with real-time information management system to track the progress of construction. These data also ease the decision making in construction (Li *et al*. 2005). However, this concept can be used only when the activities have direct relation to the distinct materials used. Also, GPS is inefficient in areas where the signal reception is low. Also, these methods cannot be used indoors. In addition, GPS and GIS can be used to monitor the progress of construction based on the location. However, the updating would be span to span only (due to the resolution of GPS). In the current framework, we are able to classify span construction further into 4 major activities

2.2.5 Imaging

The actual state of the construction site is detected by photogrammetric surveys and then used this used for automated comparison with planned state for early detection of deviations in the construction process as shown in Figure 2.5 (Braun *et al*. 2015).

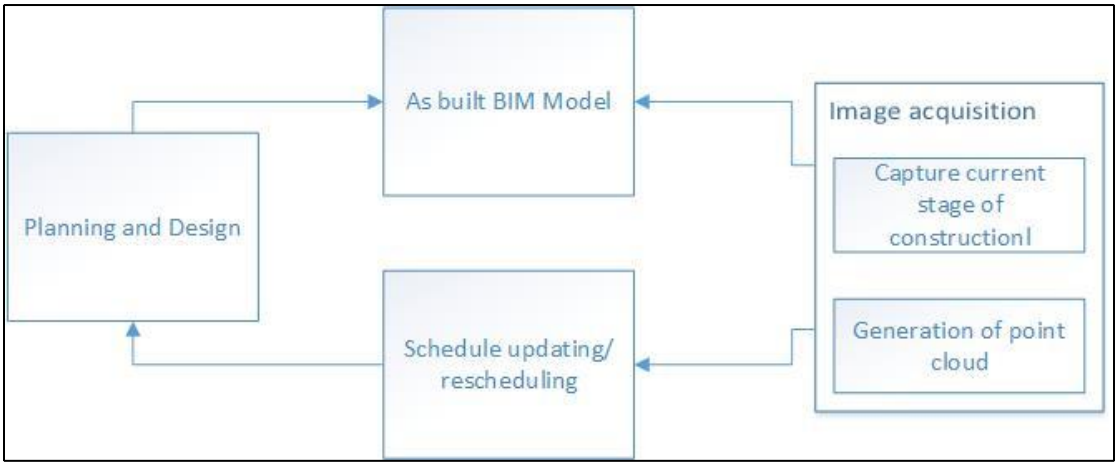

Figure 2.5: Construction progress monitoring schema (Braun *et al*. 2015)

Dense point clouds are generated from multiple photographs of the construction site and disparity maps are created from these point clouds. They are then matched with a 4D building information model to assess the progress.

Material classification is necessary to build a semantically rich as-built models. For construction progress monitoring in addition to the 3d geometric information in terms of point clouds. Dimitrov & Golparvar-Fard used vision-based method for material classification in order to monitor construction progress and generate building information models from unordered site image collections (Dimitrov & Golparvar-Fard 2014).

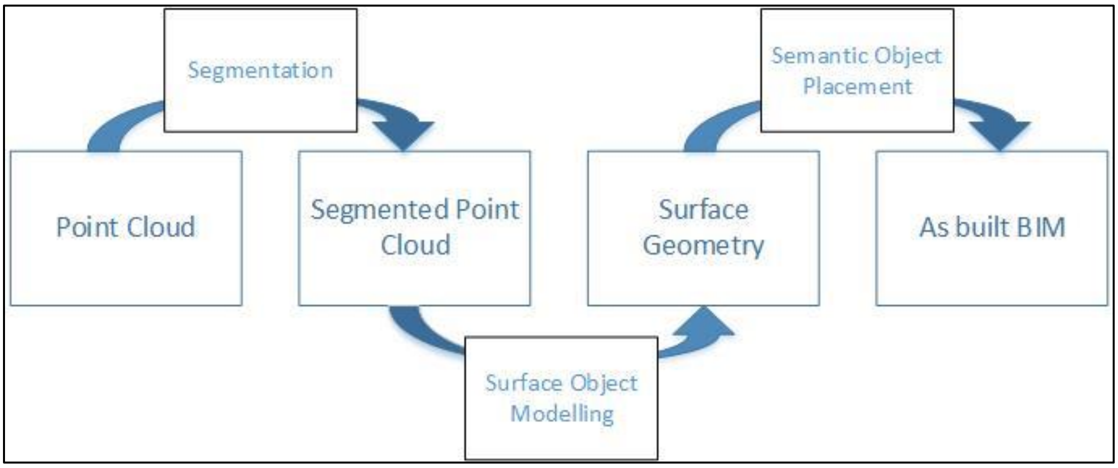

Figure 2.6: The process of generating semantically-rich SGMs from point cloud data and how material recognition can help with segmentation (Dimitrov & Golparvar-Fard 2014)

Automated material classification helps in the segmentation of the automated modeling of semantically rich as built 3d models in addition to construction progress monitoring as shown in Figure 2.6. This is achieved by segmenting point clouds using appearance information so that each subset may be used separately to extract geometric information. Semantic information can be associated with the geometry by recognizing the construction materials to label each 3d element generated as shown in Figure 2.7.

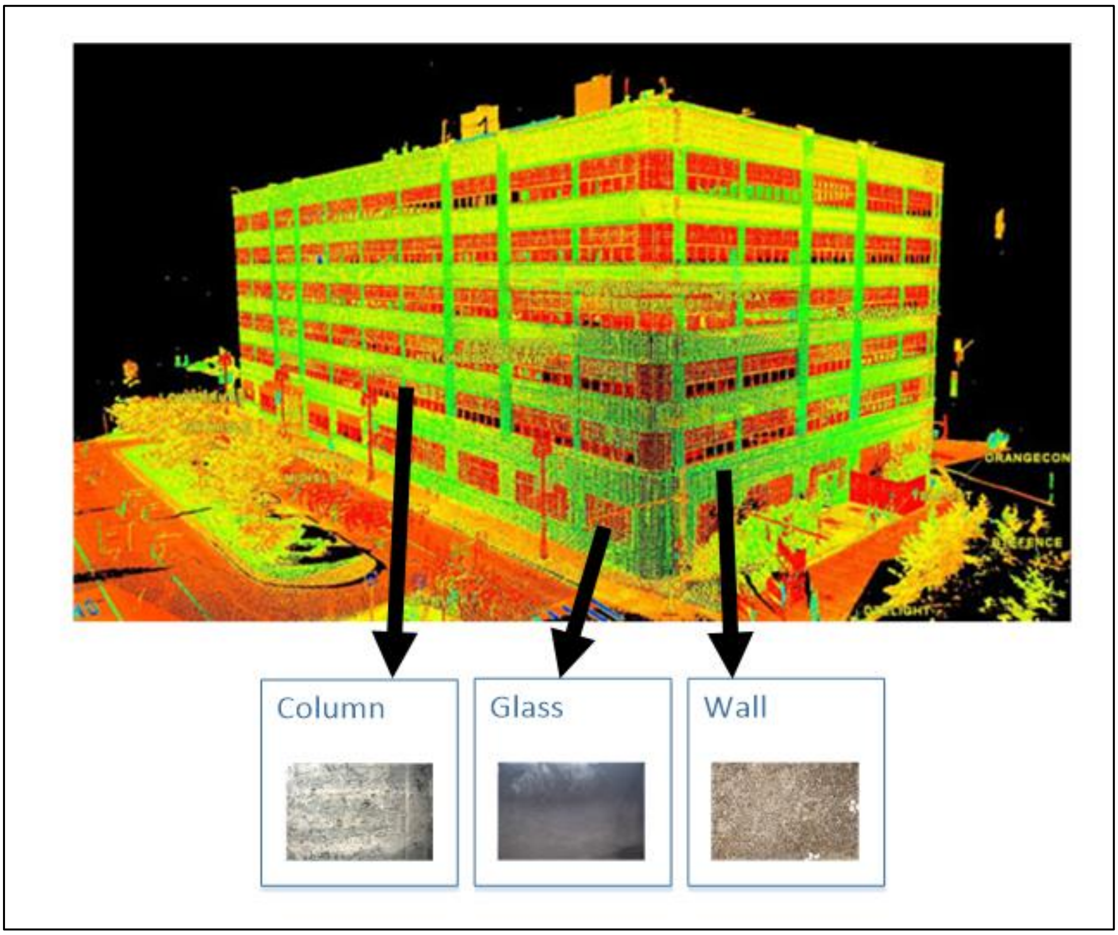

Figure 2.7: Semantically Labeling a 3D point cloud model with construction material info (Dimitrov & Golparvar-Fard 2014)

Although this method can be effectively used to monitor the progress, the method is limited to projects which are constructed at a location. In other words, it isn't applicable in construction such as viaduct construction where the location of construction changes with the progress of construction. In that case, the camera setup should be moved to the construction location manually to track the progress. Since the metro construction happens on busy streets, an ideal camera position may not be available which would give a full view on what is going on (Launching girder is 74 m long). On top of these, there may be cases of occlusions. Also, transmission of the video feed over require high bandwidth and the processing of the data require high computation power.

2.2.6 LIDAR

Laser scanning technology can be used to assess the progress control with minimal human intervention. 3D laser scanning uses light detection and ranging to produce an accurate 3D representation of objects using the principles of pulse time of flight to determine the distance to the object from transit time. A collection of points is obtained as the result of the scan which can be combined to form accurate 3D models. Turkan *et al* could obtain significant positive results for progress monitoring using 3D laser scanner and simple 3Dmodel (Turkan *et al*. 2011). Zhang and Aridity were able to develop an automated progress recording system that did not require any human intervention at the site or for processing the point clouds (Zhang & Arditi 2013). Multiple 3D scans were performed and combined to obtain point clouds. This point cloud was superimposed with a 3D model created to estimate the percentage of work completed as shown in Figure 2.8.

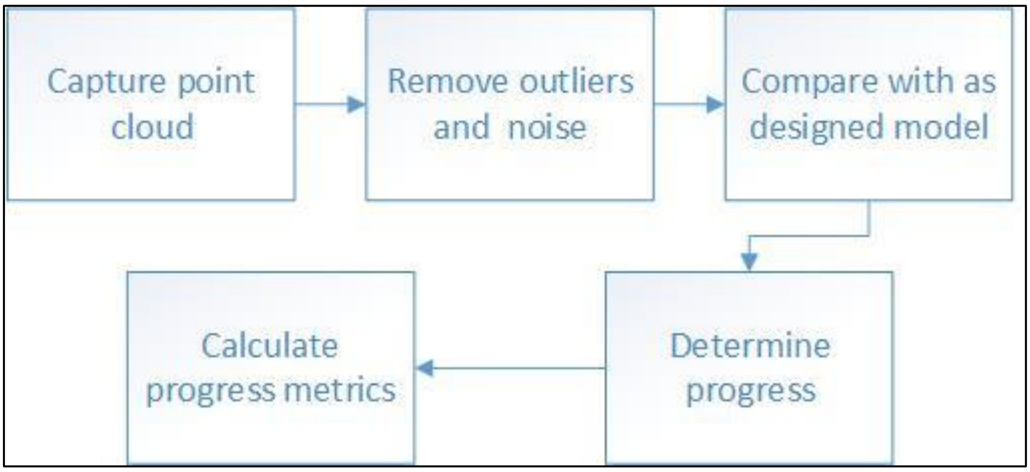

Figure 2.8: LIDAR based point cloud for construction progress monitoring by comparison with as designed 3D CAD (Zhang & Arditi 2013)

Similar to imaging techniques, this method is difficult to implement in traveling projects such as viaduct construction. In addition, 3D point clouds using Laser scanning is very dense and requires high computing power for processing which is a limitation of this method.

2.2.7 Need for Automatic Progress Monitoring using Structural Responses

All the technologies discussed in this section have inherent limitation that is the lack of mobility. For instance, an imaging technique for progress monitoring is constrained by its location and cannot be used for monitoring projects such as viaduct construction. These limitations could only be overcome if the monitoring system is integrated with the equipment or supporting structure which is central to the construction activity. Integrating ADC methods with equipment for construction progress monitoring is an area which is rarely explored. A sensing system which could measure structural responses from an equipment and infer it to the construction activity is one approach with which this issue could be addressed

2.3 WIRELESS SENSOR NETWORK (WSN)

This section describes the need for a WSN in construction site, previous application and challenges in the implementation of WSN in a construction site. This section looks into the need of a measurement system based on wireless sensor network. The survey is based on different works in which wireless sensor networks were used in construction or similar environments. This survey throws light on the technologies and approaches towards implementing a wireless sensor network on site starting with the apt wireless technology to be used.

2.3.1 Need for Wireless Sensor Network (WSN)

Traditional monitoring systems involve hardwiring sensors to a data acquisition system residing on a desktop computer. The data were then either copied from the desktop or transmitted through a wired network for analysis and decision making. These systems limited the deployment of monitoring technology, as it was difficult to connect several sensors due to the spatial constraints, sensor data distortions and losses in transmission (Chintalapudi *et al.* 2006). In addition, wired systems have higher chances of failure due to the prominence of dependent components. Further, the costs associated with implementing these systems were high and the flexibility in reconfiguring was low (Jang *et al*. 2008). In contrast, systems based on wireless technologies have increased spatial resolution, spread of the network and connect with less overhead. Additionally, maintenance of wireless sensor network is simpler since individual nodes are easier to replace in the event of a malfunction.

Wireless sensor networks have widespread applications and are an active area of research. The development of wireless sensor network was initially motivated by military applications such as battlefield surveillance, now such networks are used a wide range of industrial and consumer applications. In the built environment, wireless sensor networks have been applied to gather data for monitoring the construction as well as the operation phase of structures. Wireless sensor networks have been applied in the operation phase for monitoring structural health, energy usage, lighting control, temperature control, security monitoring, and operational safety etc. This section limits its scope to the review of previous studies on the applications of the wireless sensor network to the construction phase and structural health monitoring, as these are relevant to the current work. In addition, this section reviews past work on evaluating various wireless technologies to (or "intending to") selecting a technology appropriate for construction environment.

2.3.2 Application of WSN in Construction

Wireless Sensor Networks have been deployed in construction sites for various applications such as resource tracking, equipment monitoring, interference control, and safety monitoring. In 2008, Shen *et al* (Lu *et al*. 2007) evaluated the technical feasibility of applying wireless technologies for resource tracking at construction sites and found ZigBee based wireless network suitable for applications such as RSSI-based localization. Shin *et al*. 2011 have proposed an information framework to enable just in time resource delivery strategies using RFID and WSN based intelligent construction supply chain management. Wu *et al*. 2010 developed a WSN based on ZigBee and RFID to document near miss accident instances in real time. Naticchia *et al*. 2013 deployed WSN on site for pervasive monitoring to provide prompt support for inspectors in charge of health and safety management. Low power ZigBee protocol ensured reliability and easy installation at low cost. However, accuracy and precision limit its application to situations where the information requirement for the analysis is minimal. Technological evaluations of wireless sensor networks in building construction sites have also been carried out by (Shen *et al*. 2008) and (Jang *et al*. 2012). Shen *et al* (2008) evaluated different wireless technologies and concluded that the ZigBee wireless protocol to be the most promising technology in terms of accuracy, robustness, flexibility, and cost. Jang *et al* (2012) have done numerical simulations to study the performance of wireless sensor network for large-scale civil engineering projects. It was discovered that packet reception rates decrease with an increase in the number of nodes. It was also concluded that the practical range of transmission bit rate would be lower in the case of a dense network like that in a construction site.

Wireless sensor networks are also used in the area of structural health monitoring. In 2010, (Nagayama *et al*. 2010) has evaluated routing protocols for multi-hop communication. They proposed a modification of the AODV protocol based on analysis of application-specific characteristics pertaining to Structural Health Monitoring (SHM). (Köppe & Bartholmai 2011) developed a WSN based SHM system, including temperature compensation and RF system with high-energy efficiency. (Luo *et al*. 2014) developed a data collection and control system to control the integrated wireless network and collect the vibration data of the bridge. Their system could acquire acceleration data of four hundred meter bridge in a few seconds and successfully evaluate the bridge and determine its characteristic frequency. In 2011, (Chae *et al*. 2012) developed a ZigBee wireless sensor based bridge monitoring system. They installed 45 sensors in the bridge, which collected data from the sensors locally using ZigBee, and then transmitted wirelessly to remote server utilizing available CDMA network thereby removing expensive data loggers. Bae *et al*. 2013 studied the performance of SHM systems based on WSN using ZigBee with respect to the material characteristics. They evaluated the efficiency of WSN based on metrics such as RSSI, LQI, and PDR and predicted allowable ranges of coverage between sensor nodes. The variation of RSSI with respect to distance is as shown in Figure 2.9

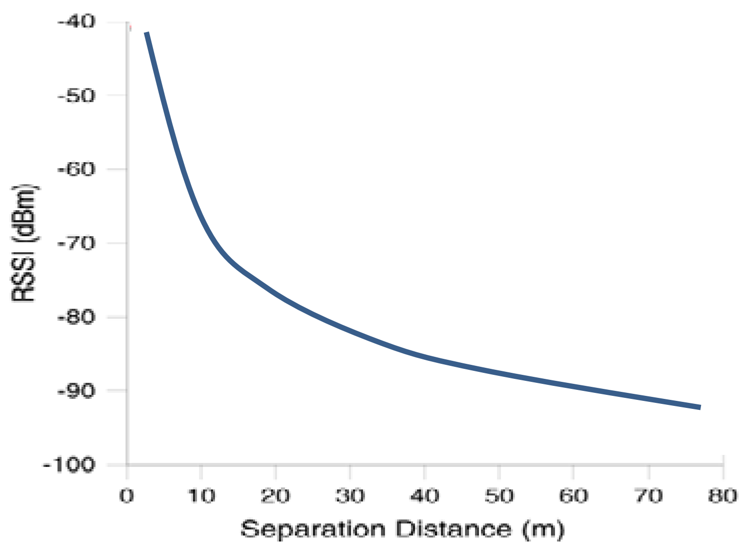

Figure 2.9: Variation of RSSI with respect to Separation between nodes (Bae *et al*. 2013)

Riaz *et al* has integrated solution based on BIM and wireless sensor technologyto reduce health and safety hazards(Riaz *et al*. 2014). The proposed system will facilitate intelligent monitoring of confined spaces to avoid time sensitive emergency situations through real time sensor data. Yi *et al* has integrated smart sensor technology, location tracking technology and information communication technology to provide early warning system to protect the well being of construction workers who have to work in hot and humid climatic conditions. (Yi *et al*. 2016). Cheng *et al* have developed a fall detection and intervention system based on WSN to facilitate a safe and proactive independent living (Cheng *et al*. 2016)This framework can be effectively used in constructions site as it was designed for cluttered environment..

Though works have been done wherein wireless sensor networks are used in construction as well as in SHM independently, very little work has been done on wireless sensor network in involving structural parameters in the area of construction engineering. SHM systems used in the construction domain for monitoring safety requirements come under this category. Long-term deformation monitoring for metro tunnel airshaft excavation during its construction stage was done by (Ran *et al*. 2012). In 2013, (Ding *et al*. 2013) presents a real-time safety early warning system to prevent accidents and improve safety management in underground construction, based on the "internet of things" (IoT) technology. However, construction-monitoring framework combining wireless sensor network and structural health parameters by applying principles of system identification on structural parameters has not been explored until now. This study brings attention to the possibilities in monitoring construction by deploying wireless sensor networks in a construction site to identify the structural state of the system.

2.3.3 Challenges in the Implementation of WSN in a Construction Site

Although implementing wireless sensor networks in unstructured environments such as construction site have many advantages, there are challenges in the deployment of wireless sensor networks in such unstructured environments. The construction site is characterized by a spatially extensive, object cluttered, fluctuating environment (Ibrahim & Moselhi 2014). The presence of moving resources, a metal dominated environment and extreme weather conditions affect wireless communication. Interference due to electromagnetic fields generated by machines and blockage of line of sight between the sender and the receiver decrease the efficiency of wireless communication (Zekavat *et al*. 2014). Therefore, selection of technologies, which can ensure accurate and robust communication, is critical to the successful deployment of the system.

2.3.4 Evaluation of WSN Technologies in a Construction Site

There are several wireless technologies available; a few common wireless technologies, which could be implemented in a sensor network, are given in Figure 2.10. Ultra-wideband has not been included due to high cost.

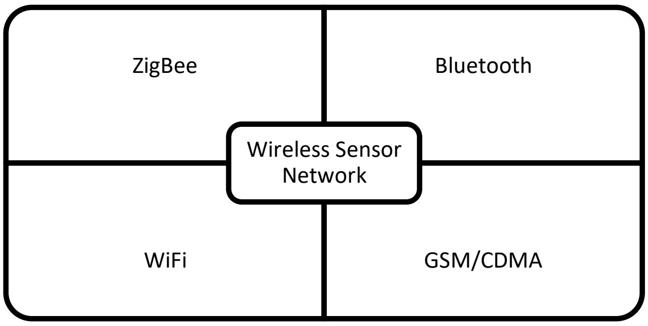

Figure 2.10: Common Wireless Technologies

Ibrahim *et al* (2014) have evaluated the performance of these networks based on received signal strength, the impact of base station distance, multipath, attenuation and antenna orientation. ZigBee networks have performed well in these tests. Effects of the separation distance between nodes and data losses through the different thickness of materials were evaluated in reliability and performance test for ZigBee-based wireless sensor network performed by Bae *et al* (2013). From the technologies shown in Figure 2.10: Common Wireless Technologies ZigBee meets the specifications of wireless sensor network based on spatial, power consumption and bandwidth criterion for deploying on a launching girder.

2.4 MEASUREMENT SYSTEM DESIGN

2.4.1 Need for Measurement System Design

It can be clearly observed that the trend towards monitoring civil engineering infrastructures for the ease of operation and maintenance is increasing as stated in section 3.1. This is made possible by incorporating a large number of sensors into the structure. However, it is also very evident that there is no proper measurement design followed while designing the measurement system and this results in over instrumentation(Brownjohn 2007). In addition to adding to the cost of sensors, over instrumentation might also make the cost of interpretation higher than the cost of sensors(Goulet & Smith 2012). Also, the unsystematic measurement system may result in a lack of sensors at critical locations. This would, in turn, lead to insufficient data and result in ambiguous interpretations(Laory *et al.* 2011). These factors necessitate a systematic measurement system design while implementing a sensing system. However, a scientific method for the design of a measurement system has its own theoretical and computational issues(Papadimitriou 2004)

2.4.2 Approaches towards Measurement System Design

Researchers have also proposed different criteria for sensor placement. Kammer and Yao(1994) proposed a method based on the maximization of the determinant of the Fischer information matrix(FIM) for optimal placement of sensors(Kammer & Yao 1994) .In addition to determinant, trace or minimum singular value of FIM is maximized to decrease the uncertainties of estimates. This method was called Effective Independence (EfI). Voon *et al* have used normalized Fisher information associated with measurement quality of sensor at a location for sensor placement (Voon *et al.* 2016). It uses normalized Fisher information in order to average out the different vibration amplitude at different locations. From their study, it is determined that variance from normalized value is better interpreted relative to the raw vibration amplitude.

Li *et al* (2008) discovered that this strategy has interdependencies with other methods such as modal kinetic energy methods, MinMac methods and QR decomposition methods etc. The MinMac algorithm was initially proposed by Carne and Dohrmann in order to have correspondence between mode shapes computed by finite element method and those measured using dynamic testing.(Carne & Dohrmann 1990).It uses Model Assurance Criteria (MAC) for evaluating the correspondence. For this both sets of mode shapes have to be differentiated to the maximum. It works as a forward sequential addition algorithm maximizing discrimination between the mode shapes of interest, with a small intuition set at the start. However Li *et al* has found instances where the objective function in the algorithm was not decreasing (Li *et al.* 2008).This happens when a newly added /removed sensor conflicts with rest of sensors in the set or maybe with the initial intuition set. This was addressed by Li *et al* by a forward-backward combinational algorithm which they call extended min mac algorithm. It computes a set of sensors with a particular no of sensors more than the min mac algorithm. Yi *et al* had modified the min mac algorithm by using selecting initial sensor assignment by using QR factorization of the structural shape (T. Yi & Li 2012). The key idea followed is to determine the best linearly independent rows of the modal matrix to minimize the off-diagonal term of MAC matrix. This is similar to the EfI method which determines QR decomposition in the column space of the modal matrix. Both EfI and QRD gave similar results when a number of modes equaled the number of sensors.

Choosing a location with very high Modal Kinetic Energy (MKE) is another criteria used in sensor placement. Locations with high amplitudes of responses are selected based on different mode shapes. MKE can be considered as a weighted EfI without iterations for structures with general mass distributions or in other words structures with a nonidentity equivalent matrix. Gu *et al* developed a combinational algorithm which integrates the advantages of MAC, EfI and MKE.(Gu *et al.* 2016) This was applied for the measurement system design on a wind turbine blade. Their study showed this combinational algorithm to perform better modal observability to distinguish dynamic features and in turn improve the accuracy of monitoring.

Some of the other algorithms for sensor placements include genetic algorithms, monkey algorithms, ant colony algorithm, particle swarm optimization algorithm etc. Genetic Algorithm (GA) assigns fitness values to sensor positions and imitates natural evolution by applying the principle of survival of fittest to arrive at the best set of sensor location. However, due to the inherent nature of the GA, iterations required for depends on the size of population space. (Buczak *et al.* 2001; Maul *et al.* 2007).Hwang and He addressed this problem by using simulated annealing and adaptive mechanisms to ensure solution quality and increase convergence speed (Hwang & He 2006). Domingo-perez *et al* used a genetic algorithm for multiobjective optimization to optimize five performance metrics derived from covariance matrix which is determinant, trace, maximum eigen value, ratio of maximum and minimum eigen value and uncertainty in a given direction (Domingo-perez *et al.* 2016).Their study concludes that a single metric may lead to sub optimal sensor placement. However, even this work has limitations that are inherent to genetic algorithms such selection of parameter values.

The particle swarm optimization (PSO) algorithm is another algorithm used in sensor placement which uses the social behavior of birds flocking. PSO algorithm is initialized with a population of solutions selected randomly and is termed particles. Each particle is then assigned random velocity value and repetitively moved inside the problem space. It is attracted towards the location of best fitness by particle and location of best fitness across the population. Each particle keeps track of its coordinates in the solution space which are associated with the best solution (fitness) that has achieved so far by that particle. This value is called personal best , pbest.Another best value that is tracked by the PSO is the best value obtained so far by any particle in the neighborhood of that particle. This value is called gbest. The basic concept of PSO lies in accelerating each particle toward its pbest and the gbest locations, with a random weighted accelaration at each time step as shown in Figure 2.11

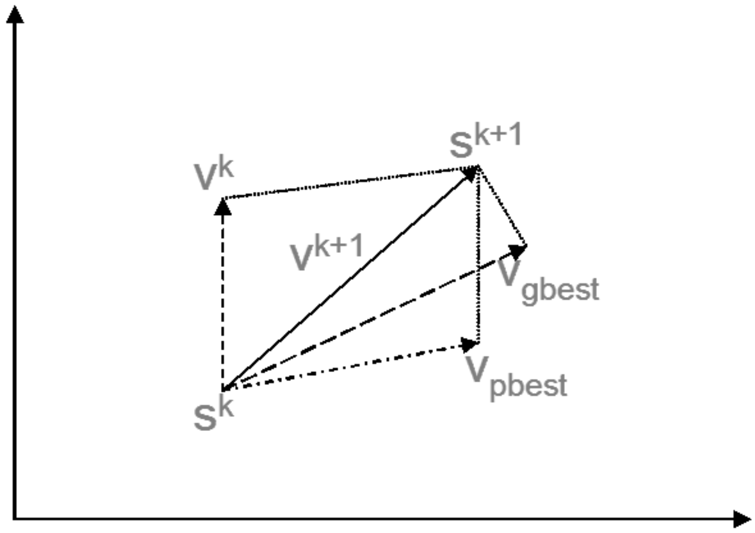

Figure 2.11: Concept of modification of a search point by particle swarm optimisation (www23.homepage.villanova.edu/varadarajan.../PSO_meander-line.ppt)

However, this method has a limitation to be applied to large solution space. Ngatchou *et al* addressed this problem using a Sequential PSO algorithm that shortened the computational run time by optimizing the objective function over random subsets (Ngatchou *et al*. 2005). This method yielded better convergence performance. Zhang and Vachtsevanos combined PSO with advanced heuristics to decide type, number and location of sensors required to effectively monitor military industrial system. It converts PSO for continuous variables to integer numbers for better performance and faster convergence (Zhang *et al*. 2007) .

Monkey algorithm (MA) is a variation of swarm intelligent algorithm which is used in solving large-scale, multimodal optimization problem. It is derived from simulation of mountain climbing processes of monkeys. It consist of three steps that are climb process, watch-jump process, and somersault process. *In the original MA, the time consumed mainly lies in using the climb process to search local optimal solutions. The essential feature of this process is the calculation of the pseudo gradient of the objective function that only requires two measurements of the objective function regardless of the dimension of the optimization problem. The purpose of the somersault process is to make monkeys find new search domains and this action primly avoids running into local search.*(Chen *et al*. 2014).Yi *et al* implemented monkey algorithm to optimal sensor placement problems by adopting integer coding to represent the solution (Yi *et al*. 2012). Results from their study showed that the modification in the monkey algorithm can enable its use in sensor placement problems. An advanced monkey algorithm termed chaotic monkey algorithm (CMA) uses chaotic searching strategy and binary coding to solve the optimal sensor placement problem. CMA is observed to be effective than the previous monkey algorithms in solving the complexities of the measurement system design (Peng *et al*. 2016).

Although there are many optimization algorithms for sensor placement problems, most of them uses modal vectors for evaluating the different models. Hence, these are effective in dynamic structural health monitoring. However, in our case the structure had different static configuration and associated dynamic configuration. Hence the above algorithms may prove insufficient to address the requirements of a sensor placement problem in a working launching girder and might require multi-model measurement design methodology.

2.4.3 Measurement System Design based on Shannon's Entropy

In 2005, (Robert-Nicoud *et al*. 2005)proposed a measurement system design methodology using multi-model approach. The iterative greedy algorithm used in that method gives maximum separation between the predictions. It uses entropy(Robert-Nicoud *et al*. 2005), from information theory (also known as Shannon's entropy) as a design criterion to identify the most optimal sensor locations. According to this method, sensors are placed at positions which offer greatest entropy reduction or in other words, the positions which separate the maximum number of candidate models. Kripakaran and Smith(Kripakaran & Smith 2009)employed this methodology on a bridge monitoring application. Their study established that increasing the number of sensors may not result in a decrease in the number of inseparable models after a threshold in the no of sensors is reached. Every other sensor added to this configuration is a redundant sensor and will not generate any useful information in an ideal configuration. Similar observations were observed in other studies as well(Papadimitriou 2004; Papadimitriou 2005; Papadimitriou *et al*. 2005; Yuen *et al*. 2001). However, you may keep some extra sensors catering to the fact that some sensors may fail due to unforeseen situations. (Papadopoulou *et al.* 2014) has proposed an improvement on entropy based measurement by using joint entropy for optimal placement of sensors to predict wind characteristics around a building(Papadopoulou *et al*. 2014).

Irrespective of the method, it is essential that sensors should be placed scientifically.Also, the measurement systems should be so designed according to the goal of measurement.In addition, the influence of epistemic errors should be considered while designing the measurement system. Papadimitriou and Lombaert(2012) has studied the effects of error dependencies on measurement design(Papadimitriou & Lombaert 2012) .Goulet and Smith (2013) has proposed a computer aided measurement system design that includes systematic bias and epistemic uncertainties. However estimating such errors is complex and requires extensive knowledge of the domain(Vernay *et al*. 2015). Hence, this study uses the sensor placement methodology built on Robert Nicoud(2005)as stated in (Soman *et al*. 2009). A similar framework was used by Raphael and Jadhav (2015) for optimal placement of sensors to monitor the behavior of transmission line towers(Raphael & Jadhav 2015)

2.5 SYSTEM IDENTIFICATION

System identification is the process of interpreting the physical characteristics of the system from the observations. Model-based system identification uses the candidate models generated by using combinations of different parameters to infer the property of the system. Model-based system identification is similar to model-based diagnosis, which uses a model structure to infer why a system is malfunctioning. The same framework can also be applied to find how the system functions too.

2.5.1 Model-Based Diagnosis

Abductive Diagnosis and consistency diagnosis are two popular theories used for model-based diagnosis. Abductive Diagnosis uses the causal model of abnormal behavior to explain observed abnormality in terms of a given causal theory (Poole 1990; Console *et al*. 1989; Lucas 1997). Two different formalizations exist for this theory, the first one regarding logic or heuristics (Console *et al*. 1989; Poole 1990) and the second one based on set theory (Peng & Reggia 1990). The one based on the logic is more powerful than the one based on the set theory. This is because of the set-theoretical formulation adopted by Peng & Reggae and not a limitation of the general set theory (Lucas 1997). Unlike abductive diagnosis, consistency-based diagnosis uses knowledge of the normal structure and the behavior of devices to infer the abnormality with a system or a device (Reiter 1987; DEKleer 1976; de Kleer *et al*. 1992).This theory can be used very well in instances where there is less prior experience on the problems. The theory is well developed on top of logic (de Kleer *et al*. 1992; Reiter 1987) and supplemented by computational environments (Riedesel 1990; de Kleer 1990). Although these theories were developed to deal abnormalities, these, especially consistency-based diagnosis can very well be applied to handle the knowledge of normal behavior as well such as finding the state of a construction equipment. Bayesian network is observed to offer a framework for both abductive (Pearl 1991) and consistency-based diagnosis (Lucas 2001).

2.5.2 Approaches towards System Identification

Bayesian inference identifies the conditional probability distribution of parameter values from the given measurement data (Box & Tiao 1992). It requires the probability distributions to be defined which represent modeling and measurement uncertainties at the sensor location, which is difficult. Incorrect parameter values may result in over conditioning of parameter values (Beven 2008). Another method, Model calibration is one of the multi-model approaches used to find an optimal model by minimizing the sum of squared difference between the observation and prediction. However, this is not acceptable method since a single answer to an inverse problem is rarely found as it is possible to get same responses at the sensor locations from many sets of parameter values (Beven 2009). In addition, it may provide values which may compensate modeling and measurement errors at sensor locations. Also, it is not suitable to use this method where model simplification is present (Goulet, Coutu, *et al*. 2013). Therefore, it is better to use methods like GLUE(Beven 2006) and error domain falsification (Goulet, Michel, *et al*. 2013; Goulet 2012; Goulet & Smith 2012) to identify the candidate model from the measurement data.

2.5.3 Model Falsification for System Identification

In 1930, Popper asserted that in science, models can only be falsified and not validated by data (Popper 1935).This concept has then been used in different studies. One of the pioneered researchers in this area, Albert Tarantola has stated "use all available a priori information to sequentially create models of the system, potentially an infinite number of them. For each model, solve the forward modeling problem, compare the predictions to the actual observations and use some criterion to decide if the fit is acceptable or unacceptable, given the uncertainties in the observations and, perhaps, in the physical theory being used. The unacceptable models have been falsified, and must be dropped. The collection of all the models that have not been falsified represents the solution" (Tarantola 2006). Multiple model approaches serve as a solution to inverse model problems that involves more than one model which explains the observed behavior. Raphael & Smith 1998 had formalized this by using evaluations of errors to segregate unlikely models from candidate models in applications for bridge diagnosis.

The system identification framework used in the present study is built upon the framework developed by Goulet *et al.* 2010. In the context of construction progress monitoring, the objective of this system identification is to identify the state of operation of an equipment/process which could be linked to the progress of whole construction. To identify the state of a system, there may be several potentially adequate model classes to represent it. Each model class takes in a number of physical parameters as inputs/parameters, which correspond to the system properties such as geometry, material characteristics, loading, boundary conditions, support conditions etc. Each combination of model class and argument set leads to a set of predictions obtained at each location. The difference between the prediction and the modeling error is the true value of a particular model instance. The true value is also equal to the difference between measured value and the measurement error. However, neither true values nor the error values are known (Goulet, Coutu, *et al.* 2013). We could only get a probability density function describing possible errors that can be estimated.

$$\text{Upper threshold bound} = \text{Predicted Value} + \text{error}\ (\delta) \quad (2.1)$$

$$\text{Lower threshold bound} = \text{Predicted Value} - \text{error}\ (\delta) \quad (2.2)$$

A model instance is falsified if the differences between its predicted and measured value are outside the threshold (Eq. 2.1 and Eq. 2.2) bounds for any comparison point as shown in Figure 2.12 . The figure shows a false acceptance of candidate models along with true acceptance of the correct model.

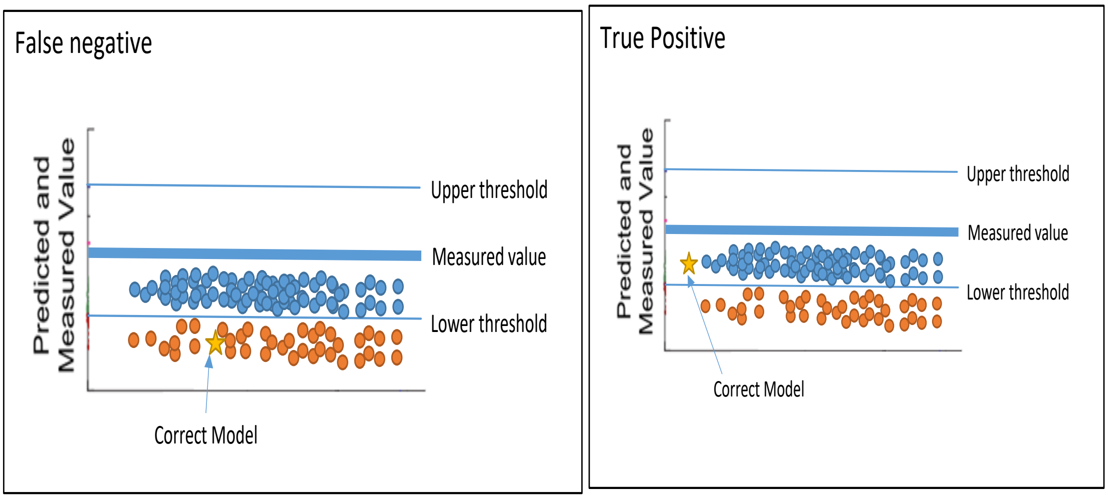

Figure 2.12 : Diagnosis-error example in the error domain.(Pasquier & Smith 2013)

2.6 SUMMARY AND RESEARCH GAPS

This chapter discussed the previous work in the areas such as automated construction progress monitoring, wireless sensor network, measurement system design, and system identification.

- Section 2.2 discusses the work done in the area of automated construction progress monitoring using different technologies such as GPS, RFID, Imaging etc. Although these technologies are effective in the applications they were employed, it may not be suitable for projects such as metro rail construction. In addition, it can be observed that construction progress monitoring using the structural response from an equipment is an area that hasn't been explored much.

- Section 2.3 gives an overview on works done which uses the wireless sensor networks in construction. However, it is observed that idea of using wireless sensor network to monitor the productivity/progress from sensor data have been explored by using RFID, Bar codes etc. and not by inferring actual state of the construction.

- Section 2.4 discusses the literature available which uses measurement system design for placing sensors in bridge monitoring and environmental monitoring, but such studies pertaining to construction progress monitoring is rarely explored.

- Section 2.5 discusses various system identification methodologies used in various fields of construction such as model calibration and Bayesian inference, but it can be observed that the system identification concept of falsification has rarely been used in construction projects.

This study tries to address the gaps mentioned above. . The following chapter describes the scope and objectives of this work and the methodology that the study follows to accomplish it.

CHAPTER 3

OBJECTIVES AND METHODOLOGY

3.1 INTRODUCTION

Previous chapters discussed the need of automated monitoring in construction and also the need to monitor launching girder. In chapter two, previous works on various studies such as automated progress monitoring, wireless sensor networks in construction and its need, sensor placement methodologies, and system identification methodologies were discussed. This chapter builds on the previous chapters and narrows down on the objectives of this work, its scope, and the methodologies.

3.2 PROBLEM STATEMENT

The need to monitor the launching girder and the challenges associated with setting up a monitoring system was discussed in the previous chapters. The common automated data collection methods used in construction may not be adequate to monitor the operations of the launching girder. Hence, it is necessary that a new method of ADC should be developed to address the issues arising from the common ADCs. This problem could be addressed by installing a structural health monitoring system on an equipment and relate the structural responses to the construction activity. Success of this method requires systematic placement of sensors. Sensors should be placed at locations which would give distinct structural responses capable of distinguishing between construction operations. Also, inferring the construction operation from the structural responses requires well designed algorithms and methodology tailored for the purpose .Therefore, this study’s focus is to develop a monitoring system that classifies the operations of the launching girder to assess the progress of the metro rail viaduct construction. This is tried out by using the strain responses from the plate girder of the launching girder and evaluating the strain pattern.

3.3 OBJECTIVES

The overall objective of this study is to develop a framework for real-time automated progress monitoring of launching girder operations.

This objective is further subdivided into three sub-objectives. They are as follows.

- To design a wireless sensor network for acquisition and transmission of data from launching girders for real-time monitoring
- To determine the optimum sensor locations for inferring launching girder operations
- To evaluate and improve existing methodologies to infer the state of launching girders from sensor data

3.4 SCOPE

Ideally, the objective of this work is to monitor the launching girder operations to monitor the productivity, progress and validate the progress. This requires monitoring the activities at a micro level. However, this study focusses on the development of the framework for the monitoring system. Hence, the monitoring system in this study concentrates on classifying the activities of launching girder into four operations using the structural responses. The four operations to which the activities are classified into are Autolaunching, segment lifting, post-tensioning, and span lowering. Validation of the design is out of the scope of this study.

3.5 METHODOLOGY

The methodology followed in this study is as shown in Figure 3.1. It is divided into 3 phases.

3.5.1 Phase 1

Phase one of the research methodology is to visit the launching girder construction site and study the structural configuration and operations of the launching girder in detail. These site visits are done presuming that it would give inputs to the wireless sensor network and sensor placement design. In addition to the site visits, phase 1 of the methodology also includes investigation of the literature for similar problems and its solutions in the construction industry.

3.5.2 Phase 2

The phase 2 of the research is split into three. The first category is the wireless sensor network design. With the inputs from the site visits, spatial and environmental conditions the wireless network sensor design is done in stages. The first stage is selecting the technology for wireless sensor network from the available technologies based on factors such as spatial and environmental performance and also cost. The second stage in wireless sensor network is to select the topology. Then, the architecture of the WSN is to be designed which caters to the spatial and environmental conditions. The next stage in WSN design is to select the hardware components which matches the wsn architecture. The final step in the wireless sensor network design is to evaluate the performance at the laboratory and subsequently at the site.

The second part of phase 3 is the measurement system design. The first stage of this part is to identify different sensor placement methodologies from literature and investigate its feasibility in the current study. Then the selected sensor placement study is evaluated for its performance by conducting a pilot. On conformance with the efficiency, it is selected. Else a better sensor placement methodology is taken.

The third part of Phase 3 is the development of System Identification Methodology. System identification methodologies from related works are critically first reviewed in this step. The compatible System Identification Methodology is chosen and then evaluated for the efficiency. If the efficiency is lower than the required, the System Identification Methodology is modified to suit the needs.

3.5.3 Phase 3

Phase 3 of the research is the validation. For this phase, the WSN is to be implemented on a working launching girder. The data from the sensors is then collected for a period. System identification is then done on this data and the inferences are recorded. Inferences are to be matched to log book data which recorded the events at the site. Percentage of the match for each methodology is recorded and the accuracies are compared based on the same.

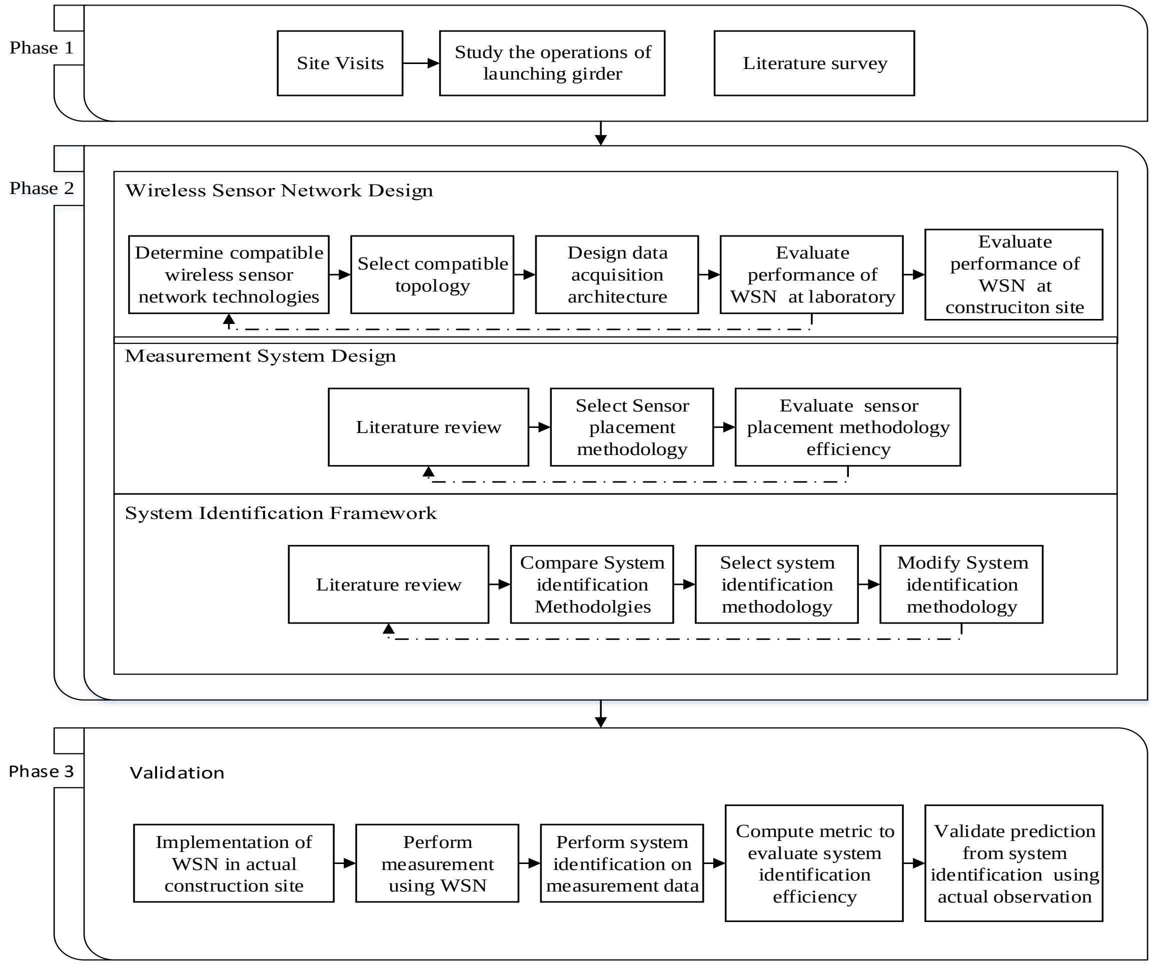

Figure 3.1: Methodology

3.6 SUMMARY

This chapter discussed the objectives of the work and the scope. The methodology followed in this work was described. Methodology essentially was subdivided into three stages. Phase one involves the site visits and literature survey. The second phase involves the design of WSN, measurement system and the development of System Identification Methodology. The third phase of the research is to evaluate the monitoring framework proposed in this research. The following chapter discusses the theoretical concepts and framework for this study.

CHAPTER 4

THEORETICAL FRAMEWORK

4.1 INTRODUCTION

This chapter presents the framework developed in this study. Section 4.1 contains the design of wireless sensor network. Section 4.2 discusses the sensor placement strategies that are used in this study. Section 4.3 describes different system identification methodologies that may be used to identify the state of construction.

4.2 WIRELESS SENSOR NETWORK

This section discusses the wireless sensor network technology (WSN) and the WSN architecture adopted in this work. This section also presents the methodology for the evaluation of the wireless sensor network both at the site and in controlled conditions.

4.2.1 Wireless Sensor Network Technology

In this study, The ZigBee protocol has been selected for local data acquisition. ZigBee was shortlisted based on different parameters such as reach quality, transmission range, bandwidth etc. as shown in Table 4.1.

Table 4.1: Comparison of wireless sensor technologies

Technology	ZigBee	GSM/GPRS/CDMA	Wi-Fi	Bluetooth
Application Focus	Monitoring and control	Wide area voice and data	The Web, Email, Video	Point to Point communication
System resources	4KB-32KB	16MB+	1MB+	250KB+
Battery Life(days)	100-1000+	1-7	5.5	1-7
Network Size	Unlimited (2^{64})	1	32	7
Bandwidth(KB/s)	20-250	64-128+	11000+	720
Transmission Range(Meters)	1-100+	1000+	1-100	1-10+
Success Metrics	Reliability, power, Cost	Reach quality	Speed, Flexibility	Cost, convenience

Previous studies have also found the ZigBee protocol to be ideal for communication in unstructured environments such as construction sites (Zekavat *et al.* 2014; Ibrahim & Moselhi 2014). Wireless modules based on ZigBee technology have lower power consumption with respect to other wireless technologies such as Wi-Fi and Bluetooth. This enables us to use power sources of lower capacity, which are cheaper. This also reduces the number of recharging required. In addition, wireless modules based on ZigBee have relatively lower costs when compared with similar technologies. It has almost 30% cost reduction over its Wi-Fi and Bluetooth counterparts. For the long range communication to the web server from the site, GSM technology is used.

4.2.2 Network Topology

The ZigBee built upon IEEE 802.15.4 supports three out of four of IEEE 802.15.4 topologies. The supported topologies being Star, Tree, and Mesh.

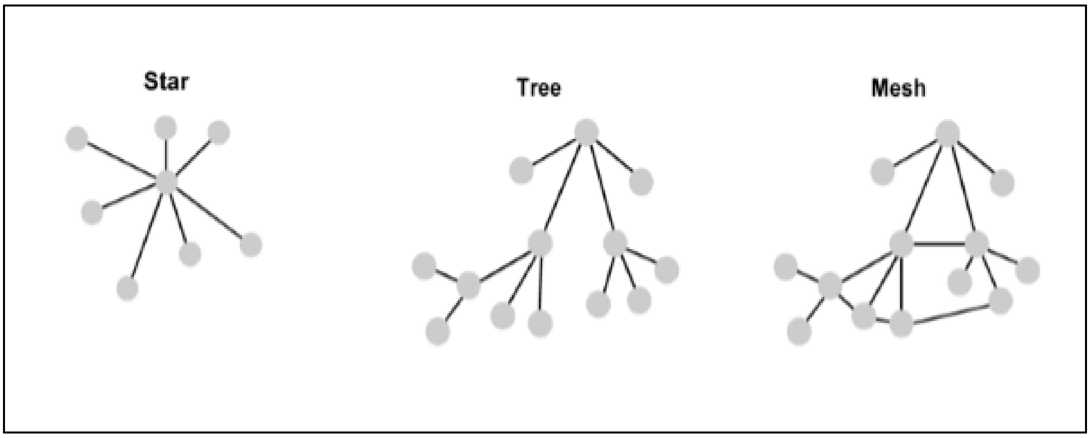

Figure 4.1: Different topologies for ZigBee Wireless Technology

The star topology consists of a central coordinator with several end device nodes (Figure 4.1). The advantage of this topology is that packets reach the destination with not more than two hops. In this topology, end device can communicate only with the coordinator. This may create a bottleneck at the coordinator. In addition to this, there are no alternative paths from the sender to the receiver.

The tree topology consists of a coordinator in the central position with routers and devices as child nodes (Figure 4.1). Routers can act as a parent and have end devices as their child node. However, a child node can have only one parent. That is if an end device has a router as a parent; it can communicate with the coordinator only through that router. The main disadvantage of this network is that if a parent fails, all the child nodes will lose connectivity. In addition, two adjacent nodes cannot communicate with each other. The information has to reach the node through the parents (Rasid & Noordin 2009). The advantages of the tree topology are that it uses less RAM and can incorporate high no of nodes with high throughput. However, it comes with high end-to-end delays.

Mesh topology is the one, which enables multi-hop networking. This topology ensures that there are alternate paths for every packet to reach its destination. The network following this topology is self-healing, i.e. if a path fails, the network would find another path by itself. In addition, every device can communicate with every other device on the network. It communicates with low end-to-end delay, but cannot be implemented for a large network(Lavric *et al.* 2012). This is because the coordinator cannot handle the data inflow from all the sensors and would finally result in major losses or even crashing the network.

For the network used in this study comprising of 64 nodes, star topology cannot be used since communication capability of an XBee is limited to connecting with a maximum of eight other XBee nodes. In addition, due to the absence of alternative paths, it is not recommended to use tree topology for WSN in unstructured environments such as a construction site. This leaves the only possibility of adopting mesh topology. However, it has higher overheads associated with it as it uses a large portion of the RAM and produces low throughput. Hence, it has to be experimentally evaluated for the current requirements.

Evaluation and performance assessment of the tree and mesh topologies have been conducted and the following findings have been reported in earlier works(Vik *et al.* 2008): Tree topology is less expensive, more efficient and can accommodate more number of nodes. Mesh topology has an advantage over tree topology in terms of reduced end-to-end delay and self-healing. However, tree topology has advantages over mesh while evaluating parameters such as throughput and efficiency, mesh topology matches the requirement for deploying a WSN on launching girder primarily due to self-healing properties and easy configuration. Hence, Mesh topology was chosen for the current network.

4.2.3 Network Architecture

This section explains the network architecture, components, and the communication technology for WSN to be deployed on a launching girder. The requirement of WSN is to monitor the structural properties of launching girder during its operations; however, the same architecture can be applied to equipment such as movable formwork, and other custom designed construction equipment, which is critical to the progress of the overall project.

The proposed network is divided into two components - local data acquisition and long range communication. Local data acquisition deals with the acquisition of data from

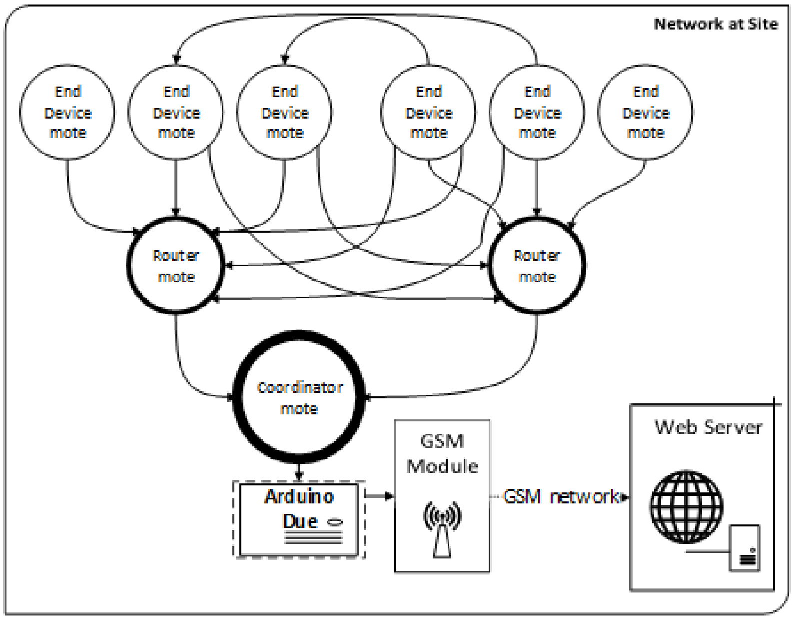

Figure 4.2: Wireless Sensor Network Architecture

different sensors on the site whereas the long-range communication are associated with long-range data communication wherein the data are transmitted to a remote server for post-processing.

ZigBee system structure consists of three different types of devices such as ZigBee Coordinator, Router, and End device. Every ZigBee network must consist of at least one coordinator which acts as a root and bridge of the network. The coordinator is responsible for handling and storing the information while performing receiving and transmitting data operations. ZigBee routers act as intermediary devices that permit data to pass to and fro through them to other devices. End device is the mote which collects the data from the sensor. Wireless sensor network architecture schema is shown in Figure 4.2.

4.3 SENSOR PLACEMENT METHODOLOGY

This section describes two sensor placement methodologies followed in this work namely intuitive sensor placement methodology and sensor placement methodology using Shannon's entropy.

4.3.1 Intuitive Sensor Placement Methodology

The traditional method of sensor placement is based on the intuitive knowledge of the behavior of the system. For example, in a laboratory experiment to calculate the stress-strain relationship, the sensor is kept at a position where the area of cross section is least. Similarly, sensors are placed at members of the maximum (Kreith & Kreider 2002; Adams *et al*. 2010; Frank *et al*. 2015; Meenatchisundaram *et al*. 2015), the maximum bending, points of contra flexure etc. based on the domain knowledge. However, often these positions based on domain-specific knowledge may lead to over instrumentation or lack of required data. Hence, it necessitates the requirement for a scientific design for a measurement system. To compare the efficiency, in this study the optimal sensor placement methodology is compared with the intuitive methods, i.e. placing the sensors at points of the maximum stress and using visualization of predicted mode shapes (T. H. Yi & Li 2012).

4.3.2 Sensor Placement Methodology based on Shannon's Entropy

The motivation behind designing a measurement system scientifically is to arrive at an optimum number of sensors and placing them at appropriate positions such that maximum information can be extracted from the sensors. This is done in two stages.

In the first stage, an initial set of locations for sensor placement is chosen by making use of the knowledge of the physical behavior of the structure and operating conditions. Sensors should be placed at the positions where physical responses vary significantly with the change in the state of the system. The initial set of locations should also satisfy the criteria such as easy installation, provisions for maintenance, minimal interference, power supply if necessary, etc. Redundancy should also be incorporated in the design, which ensures continuous data availability even in the events of a sensor or network element failure.

The second stage in measurement system design involves evaluation of the initial set of locations for their information content. This is done by making use of the Shannon's entropy(Shannon & Weaver 1949). It is one of the most significant metrics in the information theory to quantify information content. Entropy measures the uncertainty associated with the random variable. Entropy H(x) of a variable x is calculated using the Equation 4.1.

$$H(x) = -\sum_{i=0}^{n} p(x_i)\, log_2 p(x_i) \quad (4.1)$$

Where $p(x_i)$ is the probability of the occurrence of an event $x_i$in the observation distribution. The following steps describe the procedure for evaluating the Shannon's entropy to determine the optimal sensor location.

A fundamental concept in sensor placement is the use of a population of model instances that represent different possible states of the system. A model instance is defined as the instantiation of a model class that has definite values for all the model attributes. In the case of a launching girder, a model instance represents a specific set of boundary conditions, material properties, geometry, and loading. The predicted response of each model instance at every potential sensor location is determined through simulation - in the present application, through finite element analysis. The objective of sensor configuration is to find sensor locations that have maximum variations in model predictions so that after a set of measurement values are obtained, many model instances can be eliminated from the candidate set. The sensor configuration should also avoid locations that contain duplicate information content so that a minimum number of sensors are used.

A methodology for sensor placement is shown in Figure 4.3. This is a variation of the methodology developed by(Robert-Nicoud *et al*. 2005). The steps in the methodology are described below.

1. Create a list Sub_Models to store the subsets of models that cannot be separated by the current sensor configuration. For the first iteration, this set would contain one element that is Initial_Modelset.

2. Create a set Optimum_Location to store the optimum sensor locations. At the start, the set is empty.

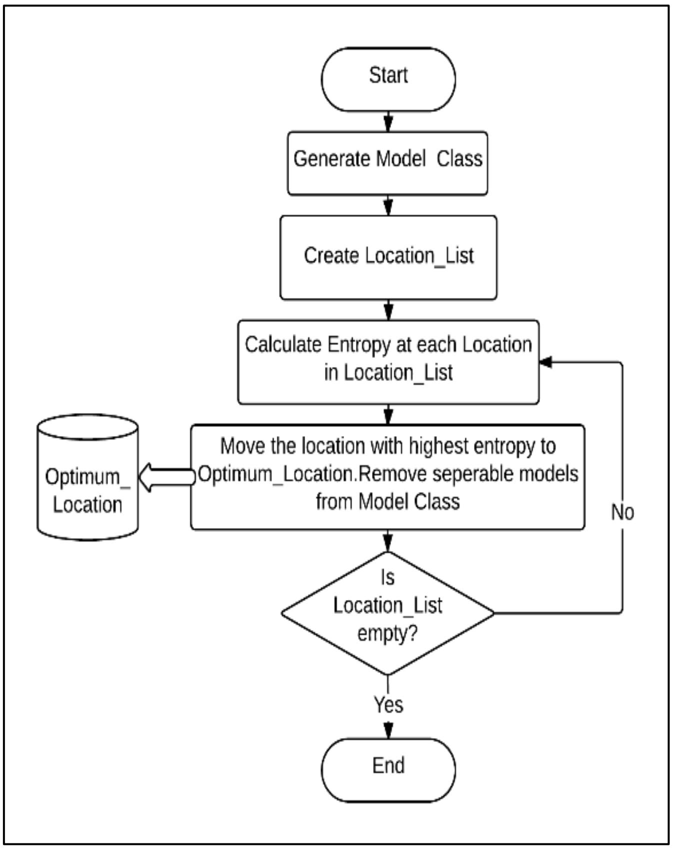

Figure 4.3: Sensor Placement Methodology using Shannon's Entropy

3. Repeat Steps 6-7 for each subset in the list Sub_Models.

4. Create a histogram for each location in Location_list by grouping the model predictions into intervals. The bounds of intervals are computed such that the width of the interval is equal to the sensor precision plus modeling uncertainty. The rationale for this is that if the measured value is at the midpoint of the interval, all the model predictions within the interval could be considered as matching the measurement within the precision of measurement and modeling. The probability of an interval is the number of model predictions in the interval divided by the total number of model instances in the model subset.

5. Calculate the Shannon's entropy for each location.

6. Find the location corresponding to the maximum entropy among all the locations and model subsets. Add the selected location to the set Optimum_Location and remove it from the set Location_list. Divide each model subset into children subsets corresponding to the intervals of the selected sensor location. Each element of Sub_Models is replaced by the children after removing children subsets that contain only one model instance.

7. Repeat steps 5 to 7 until the list Location_list is empty.

The set Optimum_Location would contain all the positions, for the placement of sensors, which would give the maximum information content. Depending on available budget and other considerations, the sensor configuration might contain only the first few sensors in the set. In any case, if the addition of new sensors does not improve the entropy, the selection process is stopped. Remaining sensors provide redundant or duplicate information that is already provided by previous sensors. However, a small level of redundancy is required for every network, hence, more sensors may be added. In case redundancy is required, the locations of the extra sensors have to be determined through a scientific sensor placement strategy.

4.4 SYSTEM IDENTIFICATION

Three approaches to system identification are used and compared in this study, which are as follows.

- The system identification methodology adopted from Goulet *et al*. (Goulet *et al*. 2010), termed as 'System Identification Methodology -A' uses raw measurement data. Modifications are made to the System Identification Methodology A in the presumption to increase the accuracy of inference.

- A modified methodology termed 'System Identification Methodology B', uses derived features for identifying candidates.

A further modified methodology termed as 'System Identification Methodology C', is an improvement of the System Identification Methodology B by using domain-specific heuristics.

Inferences made using system identification methodologies A, B and C are evaluated by comparing it with the records in the log book and their accuracies are compared.

4.4.1 System Identification Methodology A

The system identification framework used in the present study is built upon the framework developed by (Goulet *et al.* 2013) . In the context of construction progress monitoring, the objective of system identification is to identify the state of operation of equipment which could be linked to the progress of the entire construction. A typical falsification workflow is shown in Figure 4.4. The system identification process starts with defining a set of model classes representing different possible states of the system. Each model class contains a number of parameters which correspond to the system

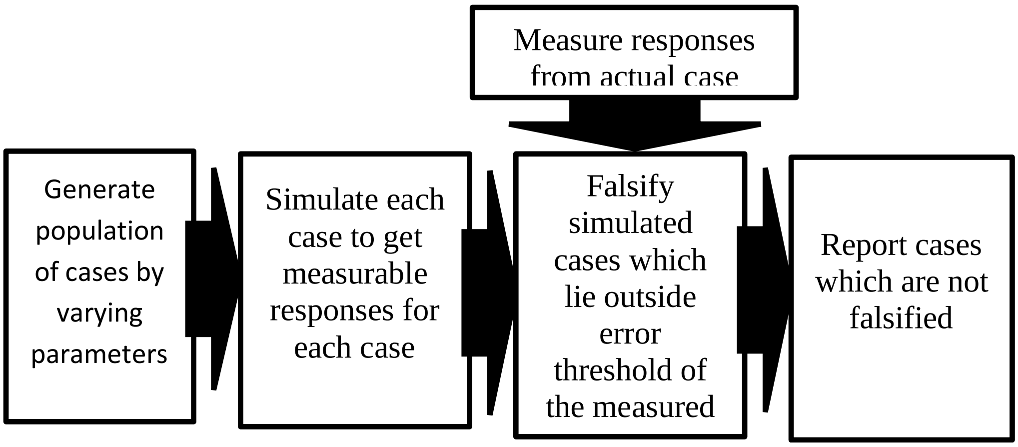

Figure 4.4: Falsification Workflow

properties such as geometry, material characteristics, loading, boundary conditions, support conditions etc. Each combination of model parameters leads to a set of predictions (which can be measured), for example, strain values at each location.

The model prediction differs from the correct structural response at a location by an amount equal to the modeling error. The measured value also differs from the actual response by the value of the measurement error. However, neither correct values nor the error values are known precisely [26]. Therefore, a probability density function describing possible errors needs to be estimated. The thresholds of possible values of actual responses are defined by the Equations 4.2 and Equation 4.3.

$$\textit{Upper threshold bound} = \textit{Predicted Value} + \textit{error}\ (\delta) \qquad (4.2)$$

$$\textit{Lower threshold bound} = \textit{Predicted Value} - \textit{error}\ (\delta) \qquad (4.3)$$

A model instance is falsified if the difference between its predicted response and the measured value is outside the threshold bounds at any sensor location. This system identification strategy based on model falsification has been proved to be accurate in various experiments (Goulet 2012; Goulet *et al.* 2013).

The System Identification Methodology A is performed as shown in Figure 4.5. The steps involved in System Identification Methodology B is as follows:-

(i.) Import the data from the server.

(ii.) Compare the reading at first location with the set of simulated readings at the same location. Block 1 of Figure 4.5 represents this step.

(iii.) If the reading lies in the threshold of the simulated readings, try the first matching simulation. Else report an anomaly. This step is represented by blocks 3,4 and 9 in Figure 4.5.

(iv.) Compare the readings at remaining locations with the simulated reading. If they match report the state of the system as that simulated case. Else try the next matching simulation. If no more matching simulations are available, report anomaly. This step is represented by blocks 5,6,7,8,9,10 in Figure 4.5.

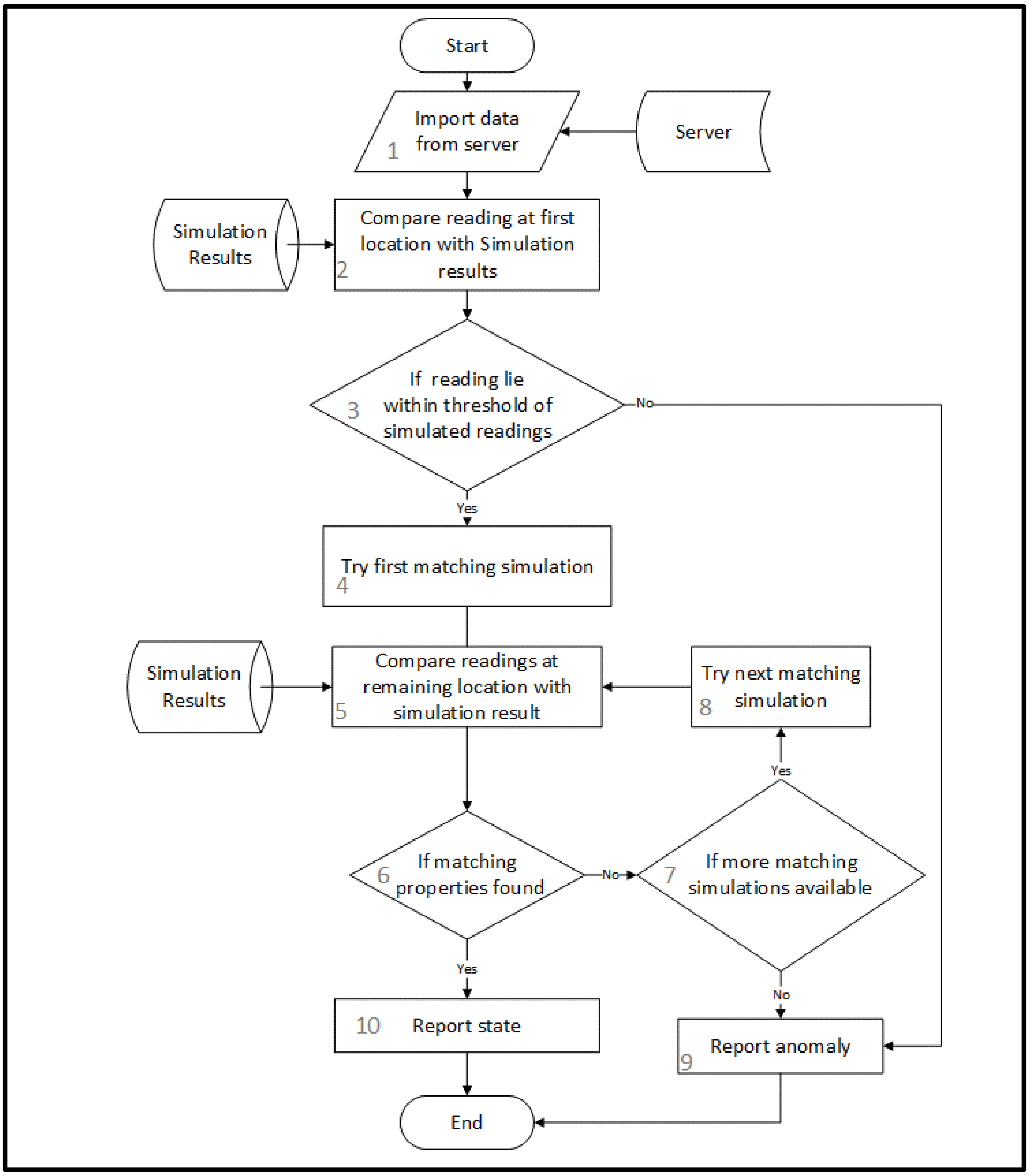

Figure 4.5: Algorithm to perform System Identification Methodology A

4.4.2 System Identification Methodology B

System Identification Methodology A with its strict limits on errors may not be suitable for an unstructured environment like construction. Uncertainties are inherent in construction processes which result in errors that cannot be modeled/simulated before the operations Strict limits on error bounds will influence the rejection of candidate models and increase chances of type 2 error Type 2 errors are the errors which fail to represent an effect that is present. For example, if auto-launching is taking place and the algorithm fails to report it, the error can be termed type 2. Even when measurement errors are present, the general trends in the structural response do not change. Hence, system identification based on identifying the trends in structural responses is likely to be more reliable.

The current work uses slopes between measurements at adjacent locations in addition to the measured readings and predictions. Even if the strain values have errors, trends such as increase or decrease in their values are likely to match the predictions of models. Therefore, in this methodology, a model is falsified if the predicted slope between the readings at adjacent locations is outside the threshold of the measured slope.

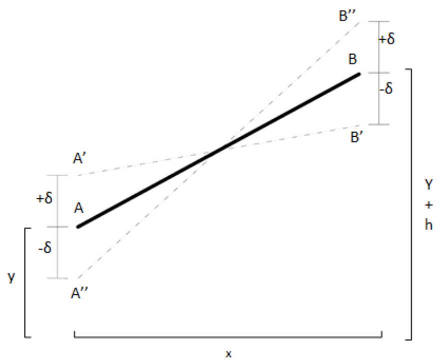

Figure 4.6: Evaluation of Slope Error

However, in this case, the threshold is computed differently. Consider Figure 4.6. Let y be the true value at a location A and δ be the combined error. Then,

$$\text{Upper threshold } (A') = y + \delta \quad (4.4)$$

$$\text{Lower threshold } (A'') = y - \delta \quad (4.5)$$

Similarly at B,

$$\text{Upper threshold } (B'') = y + h + \delta \quad (4.6)$$

$$\text{Lower threshold } (B') = y + h - \delta \quad (4.7)$$

Let the distance between A and B be of unit value. Hence, the slope of line segment AB is (h). Similarly, the slope of the line $A'B'$ is $(h-2\delta)$ and the slope of line $A''B''$ is $(h+2\delta)$. Therefore, the threshold bounds of slope in this framework is as follows,

$$\text{Upper threshold bound} = \text{Predicted Slope Value} + 2^{*}\text{error } (\delta) \qquad (4.8)$$

$$\text{Lower threshold bound} = \text{Predicted Slope Value} - 2^{*}\text{ error } (\delta) \qquad (4.9)$$

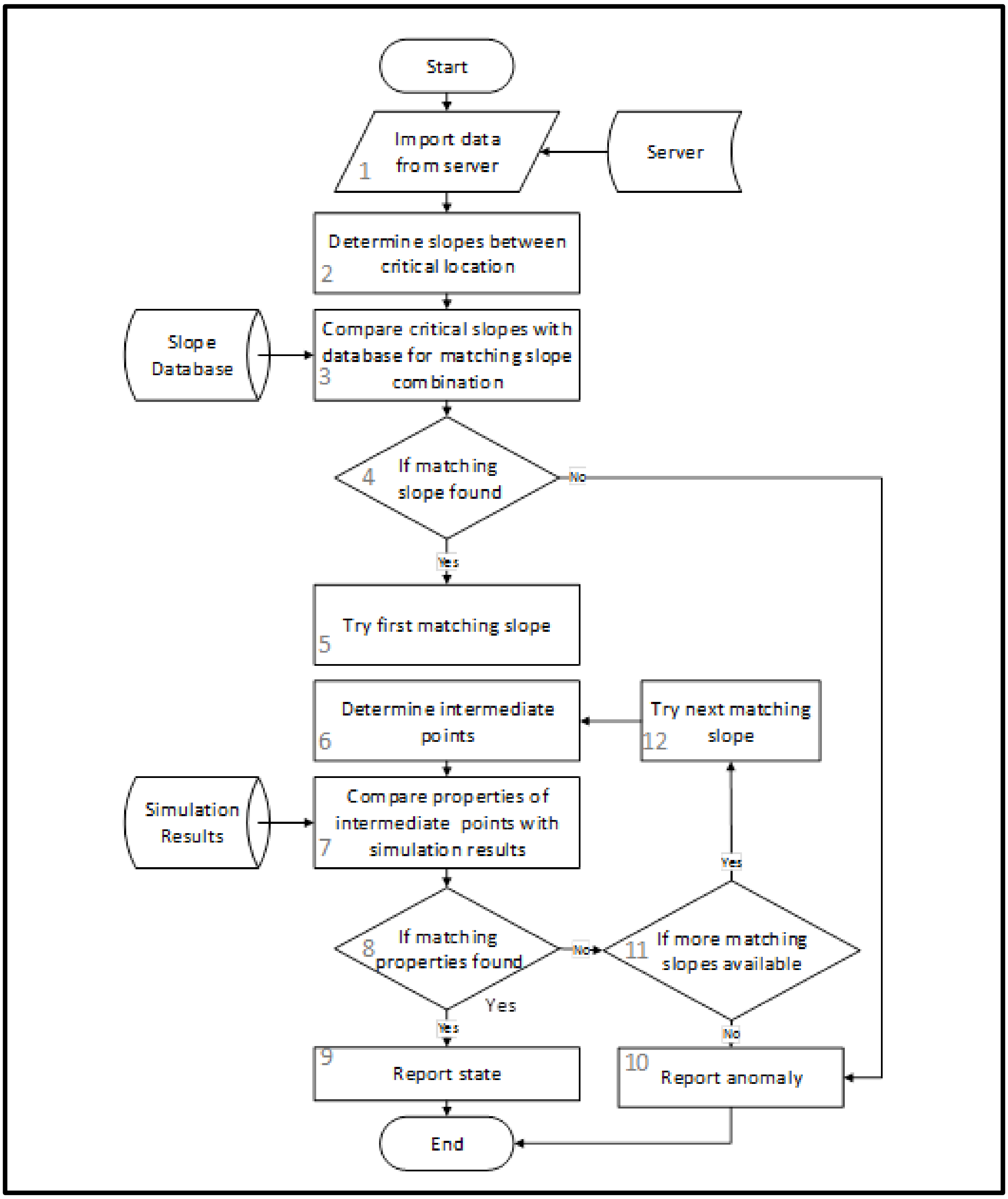

Figure 4.7: Algorithm to perform System Identification Methodology B

The steps involved in System Identification Methodology B are as shown in Figure 4.7:-

(i.) Import the data from the server. This is represented by Block 1 of Figure 4.7.

(ii.) Determine the slopes at the critical locations and compare it with slopes from simulated cases. This is represented by Blocks 2 and 3 in Figure 4.7.

(iii.) If a set of matching slopes are found, proceed to Step (iv), else report an anomaly. Blocks 4 and 10 in Figure 4.7 represent this step.

(iv.) Try the first set of matching slopes (Block 5).

(v.) Predict the intermediate readings by following the pattern from matching simulated case(Block 6).

(vi.) Compare the properties/patterns of the intermediate points with the simulated case, if it matches report the state corresponding to that case. Else try the next set of matching slopes from Step (iii) and repeat steps (v) and (vi). If no more matching slopes are available, report anomaly. This is represented by blocks 8,9,10,11 and 12 of Figure 4.7.

4.4.3 System Identification Methodology C

System Identification Methodology B is further modified by using domain-specific heuristics. The inference from System Identification Methodology B is evaluated using domain-specific knowledge, such as precedence relationships. For example, if the construction operation consists of 5 activities which should be performed sequentially, Activity 5 can only take place after activity 4, and activity 4 after activity 3. Therefore, system identification methodology evaluates the current inference with the previous inference and eliminates inferences that are impossible according to the construction sequence adopted. This heuristics, when integrated with System Identification Methodology B, has the potential to eliminate type 1 error or false positives which might arise in System Identification Methodology B. Evaluation based on heuristics are performed as a final check after the falsification based on slopes is done.

The first step in the system identification framework is to generate a population of models. The models represent different stages of operation of the equipment as well as possible faults that could happen due to human error, environmental effects, etc. The next step is to quantify the errors associated with modeling and measurement. Then, for each model instance, the slopes between readings at sensor locations is calculated and stored in the database. Upper and lower threshold bound for slopes at each location are computed and stored in the database (DB-B) as shown in Figure 4.8. Similarly, another database (DB-A) stores the slope data of the critical locations.

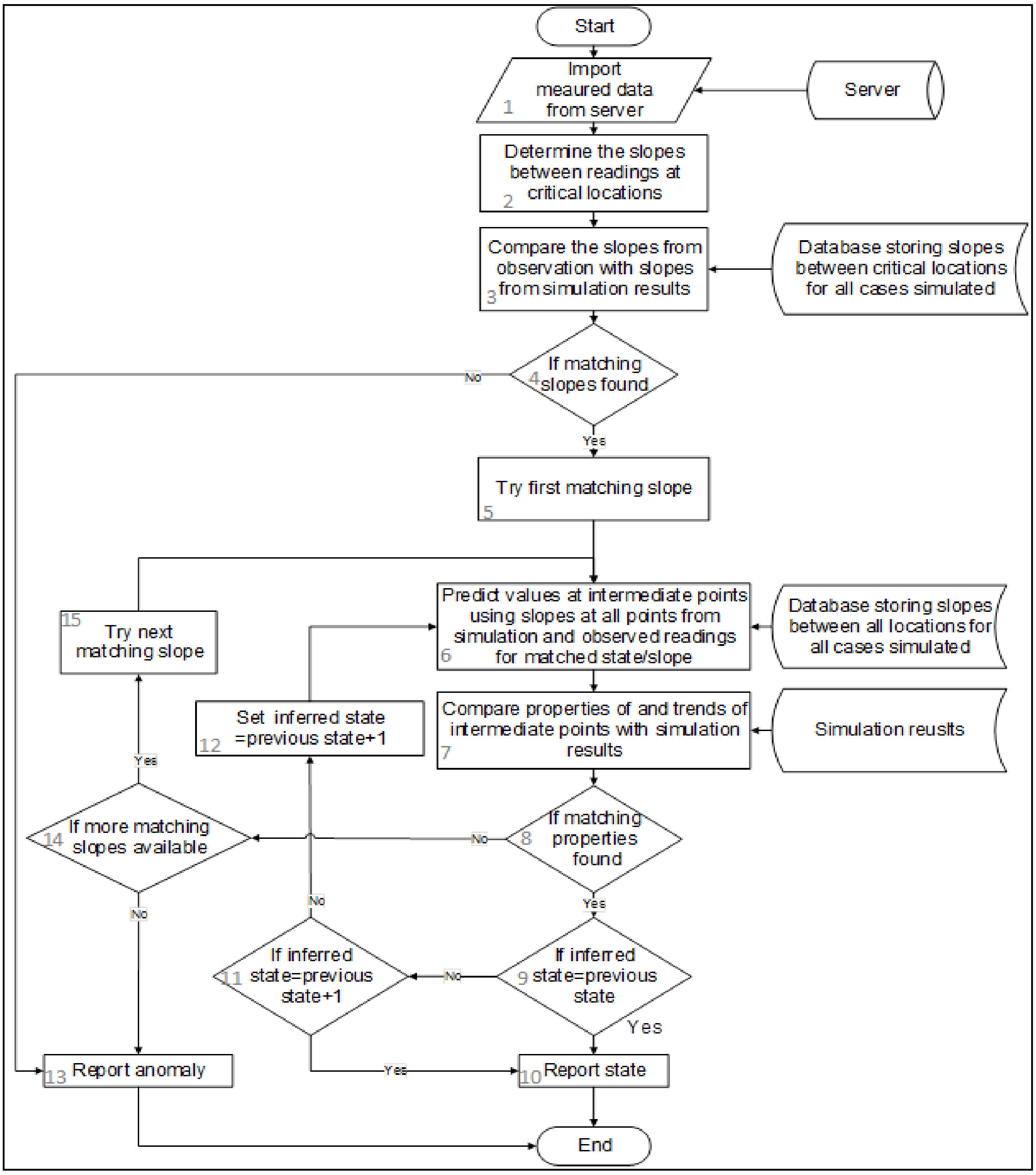

Figure 4.8: Algorithm to perform System Identification Methodology C

The process of falsification in System Identification Methodology C is shown as a sequence of blocks in Figure 4.8. The sequence is as follows:

(i.) Import the data from the server (Block 1)

(ii.) Determine the slopes at the critical locations and compare it with slopes from simulated cases. This step is represented by Blocks 2 & 3 in Figure 4.8.

(iii.) If matching slopes are found, proceed to Step (iv), else report an anomaly. Block 4 represent this step in Figure 4.8.

(iv.) Try the first matching slopes. This step is represented by Block 5 in Figure 4.8.

(v.) Predict the intermediate readings by following the pattern from matching simulated case. Block 6 represent this step in Figure 4.8.

(vi.) Compare the properties/patterns of the intermediate points with the simulated case, if it matches, proceed to step (vii). Else try the next matching slope from Step (iii) and repeat steps (v) and (vi). If no more matching slopes are available, report anomaly as shown in Blocks 7,8,14 & 15 of Figure 4.8.

(vii.) Check whether the matching property is either the previous inference or the state following the previous state. If yes, report the inference. Else proceed to step (viii). This is shown in blocks 9,10,11 of Figure 4.8.

(viii.) Set the inference to the state following the previous inference and repeat steps (v) to (vii).

4.5 SUMMARY

This chapter summarizes the methodologies used in this study for the development of the framework for real-time automated progress monitoring of launching girder operations. Different wireless technologies were compared and ZigBee based wireless senor network was found to be suitable for the deployment. Among the different topologies for the ZigBee network, Mesh topology was chosen for the current study. For deriving maximum information from the sensors, two sensor placement methodologies, intuitive methodology and methodology based on Shannon's entropy was discussed. The methodology for the systematic sensor placement using Shannon's entropy is described in this chapter in detail. To analyze the data from these sensors, three system identification methodologies were discussed. The first system identification methodology is based on model falsification is adopted from the literature, while the other two are modifications of the first methodology. The first modified methodology uses derived features while the second system identification methodology uses derived features as well as heuristics to infer the stage of construction from the sensor data. Chapter 5 discusses the actual implementation of this framework in an actual working launching girder.

.

CHAPTER 5

IMPLEMENTATION AND EVALUATION

5.1 INTRODUCTION

This chapter presents the implementation of the framework at a construction site involving the use of a launching girder for metro viaduct construction. This section is further subdivided into four parts. The first part introduces the construction project and presents relevant design details. Part two discusses the design of the wireless sensor network and part 3 the measurement system design. Part 4 talks about three system identification methodologies used to identify the state of construction.

5.2 CONSTRUCTION PROJECT CASE STUDY

Implementation was done on a launching girder in the Hyderabad Metro Rail Ltd. which was constructing spans over the Malakpet region as shown in Figure 5.1.

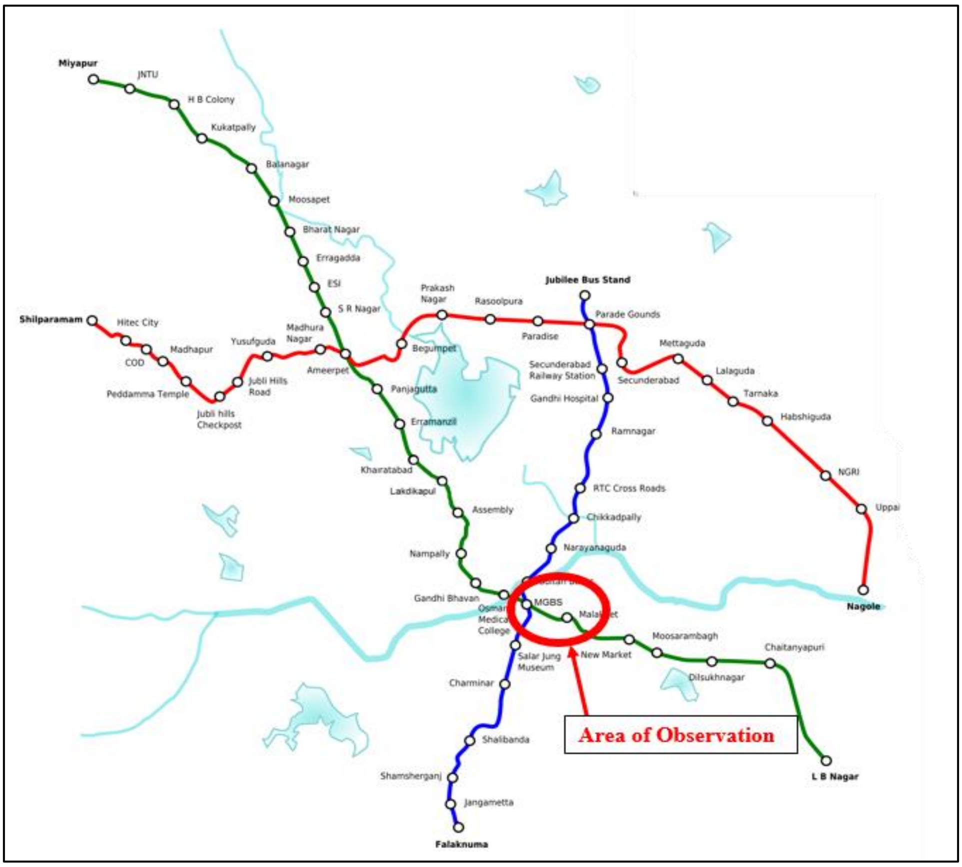

Figure 5.1: Map showing the area of implementation in Hyderabad Metro Rail Project

The Launching Girder (LG) is fabricated as a plate girder and spans continuously over four supports. It consists primarily of five parts. Steel plate girder, front support, middle support, rear support and rear trolley. The launching girder used for the study was 70m long as shown in Figure 5.2. A typical section of the launching girder box was 2m wide and 2.8m high. The flanges were 32mm thick while the webs were 16 mm thick as shown in Figure 5.3.

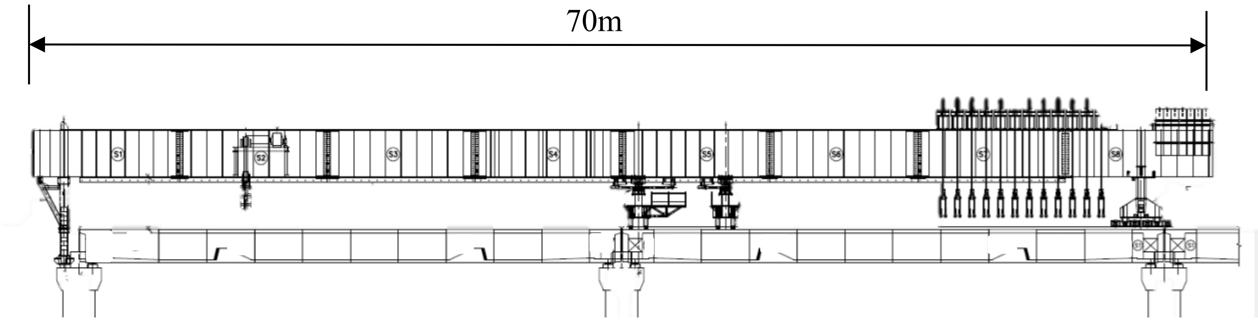

Figure 5.2: Elevation of the launching girder under study

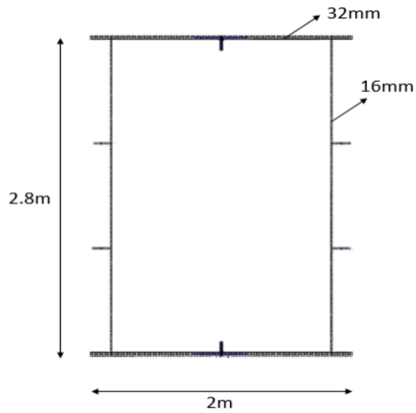

Figure 5.3: Typical box girder in the launching girder under study

5.3 WIRELESS SENSOR NETWORK

The wireless sensor technology, topology, and architecture for the WSN implementation of launching girder is as described in section 4.1. This section discusses the hardware components used for the WSN implementation on the launching girder and the methodology for the performance evaluation of the launching girder.

5.3.1 Hardware Components

The hardware components of the data acquisition system can be classified into two broad categories, the sensors, and the communication motes. Details of the sensors and communication mote are explained in detail in this section.

5.3.1.1 Sensors

Different types of sensors used for structural health monitoring are accelerometers, strain gauge, thermometer, wind gauge, inclinometer, displacement sensors, seismographs, etc.(Ding *et al*. 2013). However, for this work, only strain gauge sensor (Figure 5.4:1) is used, as it suffices to fulfill the objective of this work i.e. to identify the structural state of the system. HBM make K-LY4 120 ohm (www.hbm.com.pl/pdf/s1265.pdf <http://www.hbm.com.pl/pdf/s1265.pdf [Accessed 10 January 2015]) strain gauge is used in this setup. The 120-ohm resistance of the strain gauge was selected to minimize the drift since the sensor would be deployed for several days on the LG. The output of the strain gauge is in the form of resistance, which needs to be converted to a voltage for the end device to read it. Hence, a quarter-bridge amplifier was made specifically for this sensor. The output of the amplifier was calibrated using a standard Universal Testing Machine and clip on deflection meter as illustrated in Figure 5.4. Further, the output of amplifier was compared with output of a standard amplifier for validating the calibration data.

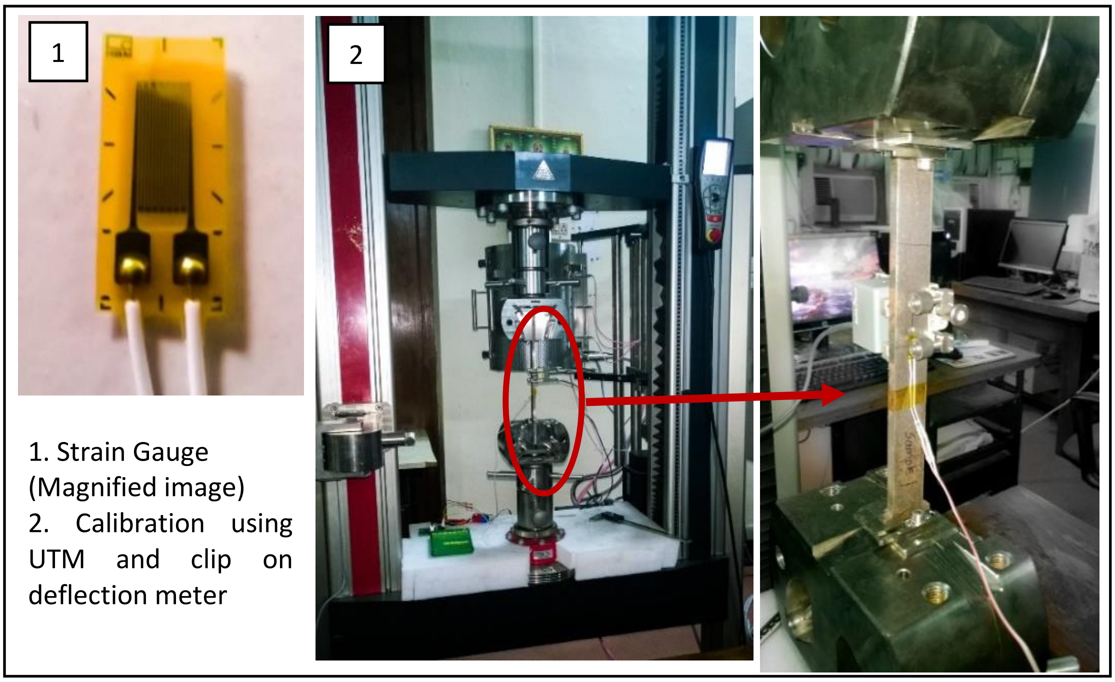

Figure 5.4: 1-Strain Gauge (Magnified Image); 2-Calibration using UTM

5.3.1.2 Communication Motes

The network consists of 3 communication motes: End Device mote, Router Mote & Gateway mote.

End device mote consists of the sensor, amplifier board and XBee (communication module) as shown in Figure 5.5. It is mounted on the surface where the response is to be recorded. The mote can be powered using a 12-volt battery. However, in this study, motes are powered using an external source. End device uses a low power 1-milliwatt antenna Series 2 XBee that has a range of 100m in open conditions and operates at 3.3 volts at 40 mills ampere for data transmission. This module delivers 250 kbps data rate and has six 10-bit analog to digital converter (ADC) input pins to which sensors could be connected. It is configured to sample every 5 seconds. The 5-second window ensures appreciable sensor data for structural identification without increasing load on the coordinator. The XBee module remains in the sleep mode for a remaining time. No of end device motes to be deployed in a launching girder was systematically determined based on the structural dependencies, communication limits, failure models, etc. 64 such motes are deployed in the test bed. The above hardware specification is ideal for the application since it delivers required bandwidth while economizing on energy consumption.

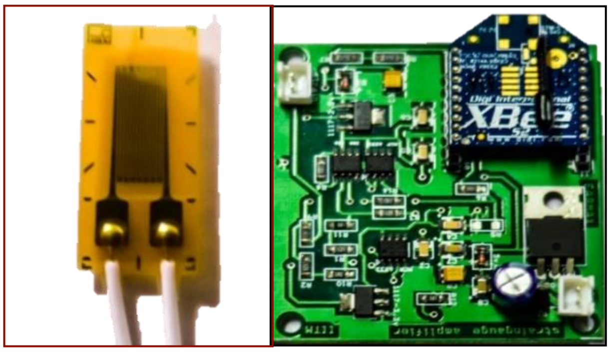

Figure 5.5: Strain Gauge (Magnified Image) and
End Device Mote

Router mote is similar to end device mote, but it does not incorporate an amplifier circuit (Area marked as a red line in Figure 5.6 shows the empty slot for the amplifier chip). It has a voltage regulator circuit with XBee module similar to end device as shown in Figure 5.6. XBee module selected is long range XBee Pro with 63-milliwatt antenna, which has a range of 1000 m in open conditions. It operates at 3.3 volts at 215 MA and delivers data at the rate of 250 kbps. It has a router firmware uploaded to it. It is placed in appropriate positions such that data packets from end devices could easily use one of these to hop over to reach the coordinator if in case the coordinator is not in range. It is kept powered on for the complete period.

Figure 5.6: Router mote

Gateway mote at the end consists of an XBee module (Figure 5.7 c), Microcontroller board (Figure 5.7 a), Real time clock and GSM Shield (Figure 5.7b) along with power supply. Microcontroller board used in the gateway mote is Arduino Due. The Arduino Due is a microcontroller board based on the Atmel SAM3X8E ARM Cortex-M3 CPU. It has a 32-Bit ARM core that allows operation on 4 bytes wide data within a single CPU, which clocks at 84 MHz the board, has an SRAM of 96 Kilobytes and 512 Kilobytes of flash memory for code. The large RAM in this module is ideal for the application since it is required to manage data from 64 sensors. The GSM module is based on SIM900A SMT chip with low power consumption. The mote uses DS1307 RTC module, which comes preprogrammed with the current time for logging the time data with the sensor data. The ZigBee module in the gateway mote is the same as that in the Router mote, however, the one in gateway mote has a coordinator firmware.

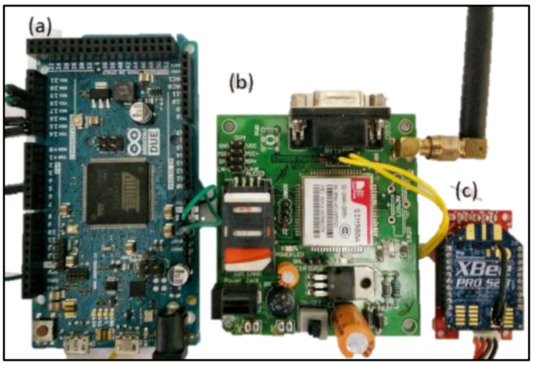

Figure 5.7: (a): Arduino due microcontroller (b)
SIM900A module (c) XBee Pro coordinator module

The Microcontroller is a channel between the coordinator and GSM Module. Programming is done on the Arduino Due using Arduino IDE to collect the data from the coordinator. Data is collected for a window of 40ms five times a minute. This data was averaged (optimal filter) , statically mapped to the sensor ID and time stamped. The data is encrypted and then send to the GSM module from the microcontroller using serial communication. Data is then transmitted to the remote server using GSM network.

5.3.2 Performance Evaluation

This section presents the experimental evaluation of the performance of mesh network topology for the current application. A series of experiments is performed to assess the performance of the WSN focusing on the spatial characteristic of a launching girder. XCTU application from Digi International (http://www.digi.com/products/wireless-wired-embedded-solutions/ZigBee-rf-modules/xctu [Accessed 10th January 2015]) is used to evaluate the performance of the network. The metrics used for evaluation are Received signal strength indication (RSSI) and Packet delivery ratio (PDR).

RSSI is a power level index used as a measurement of power present in the received signal. A Higher level of RSSI indicates stronger signal strength, which represents a strong network link. It is expressed in dBm, the power ratio in decibels (dB) of measured power over 1 milliwatt (mW)(Jang *et al*. 2008; Naticchia *et al.* 2013; Lavric *et al*. 2012; Linderman *et al.* 2010; Piyare *et al.* 2013). RSSI is proportional to the logarithm of the inverse of the distance squared. i.e. $RSSI = -K \, . \, logD + A$ where K is the slope and A the intercept when RSSI is plotted against distance. PDR is defined as the ratio of a number of error packets to the total number of packets transmitted over a certain period. It can be used to quantify the reliability of WSN(Bae *et al*. 2013).

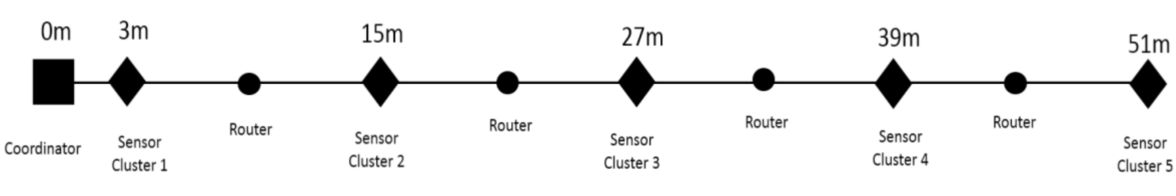

Figure 5.8: Line diagram showing spatial distribution of modules during lab test

Figure 5.8. Shows a schematic layout of the experimental set-up. The layout replicates the spatial configuration of the wireless sensor network when the system is installed on a launching girder. The original idea was to simulate 74m of length as the launching girder. However, the laboratory conditions limited it to 51 m. The sensors were spaced evenly at 12m, longest girder length of a segment the launching girder. Sensor cluster

with multiple sensors is deployed at each interval. The test was performed in order to test the communication potential of the ZigBee modules. This test was done prior to the sensor placement studies. The original idea was to simulate 74m of length as the launching girder. However, the laboratory conditions limited it to 51 m. The sensors were spaced evenly at 12m, longest girder length of a segment the launching girder.

Using XCTU software, one node is configured as the coordinator, four nodes as routers and 32 nodes as an end device / router. Routers are added for better connectivity since coordinator cannot communicate with more than eight other nodes. This setup replicates the sensor network that is deployed on a launching girder wherein coordinator

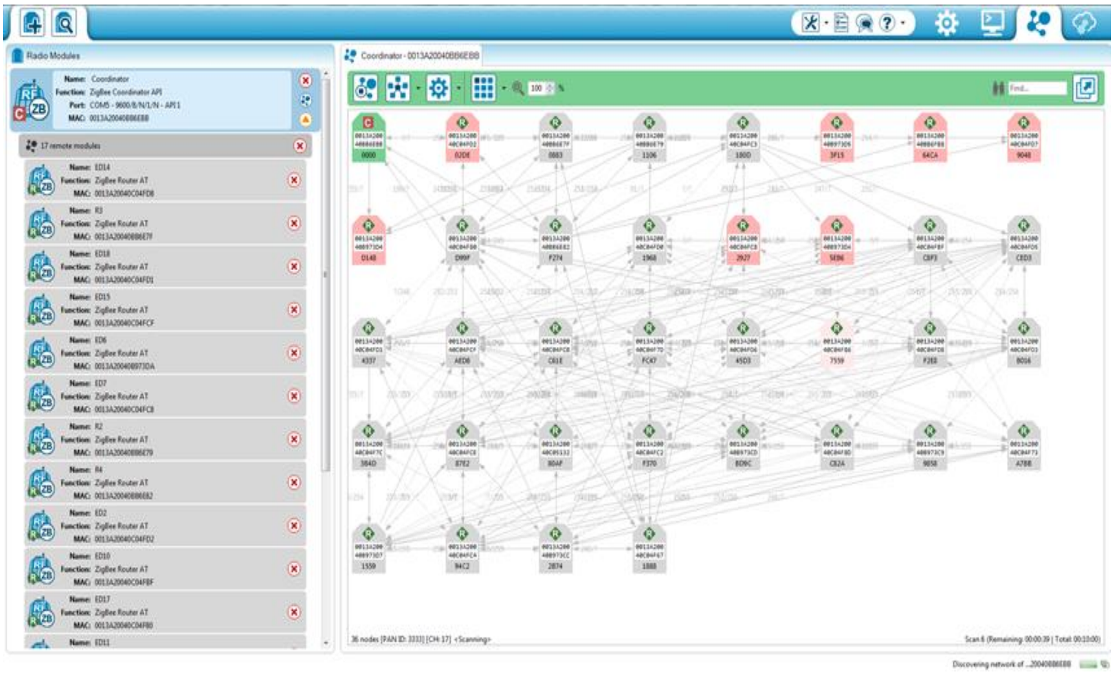

Figure 5.9: Screen shot of XCTU during the test

is placed at the rear end (0m). To reduce the load on the coordinator, another coordinator may be placed on the front end. However, it is not recommended as access to the front of the LG is constrained.

The test is started when the coordinator is connected to all nodes (Figure 5.9). End devices located at different distances from the coordinator start transmitting packets to the coordinator. To calculate RSSI, one remote node is selected at a time and the test is done. The coordinator sends a packet to the node and the packet is sent back by the node. Once the coordinator receives the data packet, it sends an acknowledgment back to the end device. RSSI is calculated from the strength of the received packet. An average of RSSI after receiving 500 packets from an end device is used as the RSSI value for that particular node. PDR is also determined for these nodes from the packets received. Four different packet sizes are transmitted to study the variation. The test is repeated for nodes at different distances from the coordinator.

The same experiment was conducted at the actual launching construction site for the 30-byte data packet size. For the experiment, one node is configured as the coordinator, eight nodes as routers and 49 nodes as an end device.

5.4 MEASUREMENT SYSTEM DESIGN

This section discusses the sensor placement methodology followed while implementing the measurement system on the launching girder. One of the methodologies is using the intuitive placement of sensor based on the domain specific knowledge. The second methodology is the systematic design of measurement system using Shannon's entropy as a metric.

5.4.1 Intuitive Sensor Placement

In this study two methodologies for intuitive sensor placement are tested. The first intuitive sensor placement methodology uses the sensors to be placed at member which gives the maximum stress (Adams *et al.* 2010; Kreith & Kreider 2002; Frank *et al.* 2015; Meenatchisundaram *et al.* 2015) . Since this position has the maximum magnitude, it is presumed that this position would give the maximum variation between the models. Positions with decreasing magnitude of strain are chosen as the order of priority for the placement. Positions and priority of the intuitive sensors placement method 1 are as shown in Figure 5.10.

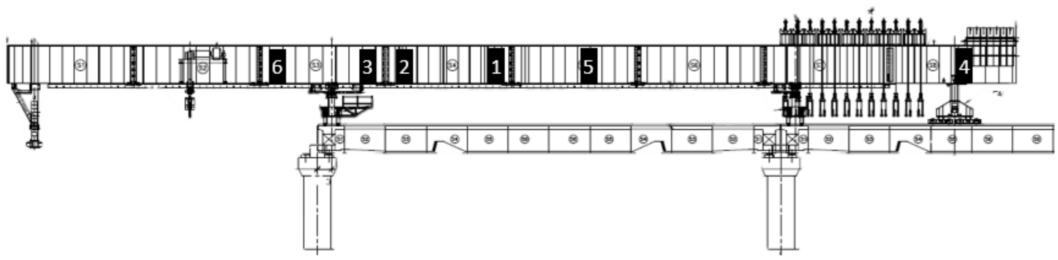

Figure 5.10: Sensor placement using intuitive sensor placement method 1

The second intuitive sensor placement methodology used in this study explores the visualization of responses such as mode shapes as stated in Yi and Li 2012 (T. H. Yi & Li 2012). Two criterion used for evaluation are the changes in BM across the span and points of contra flexure. Positions and priority of the intuitive sensors placement method 2 are as shown in Figure 5.11.

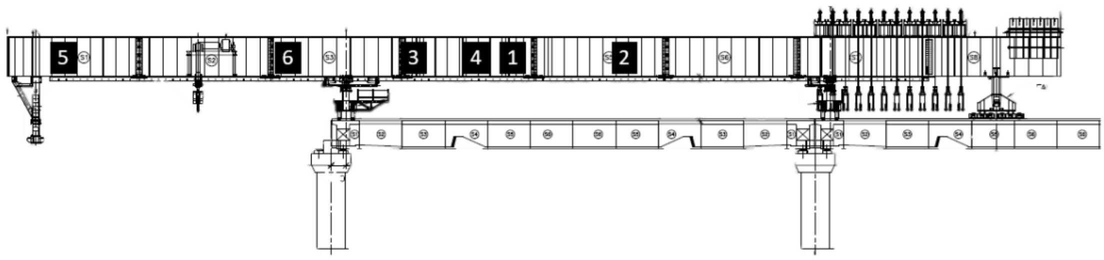

Figure 5.11:Sensor placement using intuitive sensor placement method 2

5.4.2 Systematic Sensor Placement

This section describes the sensor placement strategy using Shannon's entropy as mentioned in section 4.2.2 on an actual launching girder. A pilot study inclusive of launching at a position was conducted to decide the effect of sensor resolution and influence of the no of sensors. After the pilot study, a full scaled study including all the operations of the launching girder was done to determine the placement of sensors to monitor the operations of launching girder.

5.4.2.1 Pilot Study

As part of the pilot study, a series of structural models of the launching girder are created by varying parameters such as support settlement, counterweight, the stiffness of the member, fixity of joints, etc. Also, these structural models should be created at different positions of the auto-launching as well as segment lifting. However the current pilot study focusses on two parameters at a position of launch (22m of the cantilever), they are counter weight and support settlement. The counter weight values varied from 56 metric ton to 68 metric ton in the steps of 2 ton. These parameters were chosen based on the knowledge from the construction site visits and interaction with site personnel. Both these parameters are prone to variation from design during the construction operation. Support settlements at two locations were varied from zero to 20mm. The model class contains 3087 model instances (7 counter weight*21 support settlement * 21 support settlement). The model instances are then analyzed using a finite element analysis package Felt. Strain responses at each location are evaluated for every model instance. Strain distribution at each location is then divided into intervals where the width of the interval corresponds to the precision of the measurement. Shannon's entropy is calculated for each location and sensor positions are chosen based on the methodology discussed in the previous section. Results of the analysis are presented in the section 6.3.1.

5.4.2.2 Actual Study

A population of models was created from the model classes. Initially, 33 base cases (Table 5.1) were made which simulates the actual launching girder operations.

Table 5.1: Base cases to create model class

Case	Operation	Sub operation	Remarks
1	Autolaunching	Start	
2		Release Middle support	
3		Middle support to S7	
4		Rear Support to old Middle support position	
5		Middle support to S1	
6		launch till rear trolley reaches rear support	Launching -0m
7		launch till rear trolley reaches rear support	Launching -5m
8		launch till rear trolley reaches rear support	Launching -10m
9		launch till rear trolley reaches rear support	Launching -15m
10		launch till rear trolley reaches rear support	Launching -20m
11		launch till rear trolley reaches rear support	Launching -20.75m
12		Move the rear support	Launching -20.75m
13		Launch till next support	Launching -25m
14		Launch till next support	Launching -30m
15		Launch till next support	Launching -31m
16		Front supported on the pillar	
17	Segment lifting	Segment trolleys on to the launching part	
18		Attaching the lifting beam	
19		Lifting segment	
20		Lifting segment + transfer to segment trolley	Segment 1
21		Lifting segment + transfer to segment trolley	Segment 2
22		Lifting segment + transfer to segment trolley	Segment 3
23		Lifting segment + transfer to segment trolley	Segment 4
24		Lifting segment + transfer to segment trolley	Segment 5
25		Lifting segment + transfer to segment trolley	Segment 6
26		Lifting segment + transfer to segment trolley	Segment 7
27		Lifting segment + transfer to segment trolley	Segment 8
28		Lifting segment + transfer to segment trolley	Segment 9
29		Lifting segment + transfer to segment trolley	Segment 10
30		Lifting segment + transfer to segment trolley	Segment 11
31		Transfer to segment trolley	Segment 12
32	post tensioning		
33	Span lowering	End	

These constitute the four operations, namely, auto-launching, segment lifting, post-tensioning and span lowering. Around 1, 52,656 models were generated by varying the different parameters in Table 5.2. The variation of parameters was decided from site studies and design data these models were then analyzed using FELT, a lightweight open source finite element analysis software.

Table 5.2: Variation of Parameters

Parameter	Range		Interval
Counterweight	Min	63500Kg	500Kg
	Max	68500 Kg	
Segment weight	Min	15690 Kg	800Kg
	Max	20594 Kg	
Front support settlement-Right	Min	0 mm	7mm
	Max	28 mm	
Front support settlement-Left	Min	0 mm	7mm
	Max	28 mm	
Rear Trolley Settlement Right	Min	0 mm	7mm
	Max	28mm	
Rear Trolley Settlement Left	Min	0 mm	7mm
	Max	28 mm	

For each case, responses at 356 locations from the output of finite element analysis were tabulated. Only measurement error is considered here, as the estimation of modeling errors is challenging. Entropy at each of these points was then computed. For the sensor placement, a measurement system was designed which is based on Shannon's entropy (Shannon & Weaver 1949) as described in section 4.3.2.Results of the analysis are presented in section 6.3.2. Positions and priority of the systematic sensors placement are as shown in Figure 5.12.

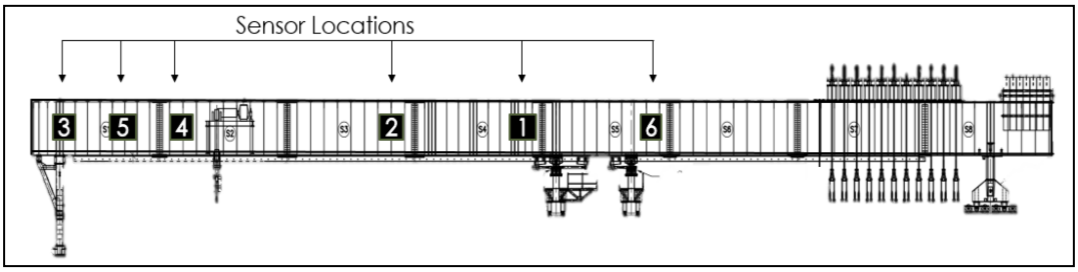

Figure 5.12 : Sensor placement using Shannon's entropy method

In addition to these sensor positions, 4 more locations were added to provide redundant information. In total, sensors are installed at 10 locations with 4 sensors each.

5.5 SYSTEM IDENTIFICATION

This section briefly discusses the duration of monitoring and the validation methodology followed.

5.5.1.1 Data from Site

The launching girder was monitored using the wireless sensor network based data acquisition setup over a period of 2 months. 19724 readings were recorded during this period. The launching girder completed the erection of 4 spans during this time period. The frequency of data capture is one per minute. Only static strains were taken. The noise is filtered partly in the hardware using single pole low pass differential configuration, common mode capacitors and low magnitude resistors, high resolution adc etc. On the software side, the signal was smoothened using optimal filtering algorithm.

5.5.1.2 Validation using logbook

The data from launching girder was analyzed using three system identification methodologies as mentioned in section 4.3. Inferences from each System Identification Methodology were compared with the site log book which recorded the activities at the site. System identification mapped the readings into one of the four operations i.e. Autolaunching, segment lifting, post-tensioning and span lowering. The inferences were compared with the readings from logbook and percentage of the match was recorded. The results from the validation are as reported in section 6.4.1.The accuracies of the different system identification methodologies are compared using the number of correct, incorrect and zero matches as a metric.

5.6 SUMMARY

This chapter discussed the implementation of a wireless sensor network on a launching girder in operation at a construction site. Hardware components of the wireless sensor network and its performance evaluation methodology were discussed. The current study uses a strain gauge and custom built amplifier for sensing. The amplifier was calibrated with a standard UTM. The calibration data was further validated using a standard amplifier. For communication, three motes were used which are end device mote, router motes and gateway motes. Different end device motes collects the data from the strain gauges and transmits it to the gateway mote. The router motes makes the data routing process efficient. The gateway mote receives the data transmitted from the end devices, encrypts it and send it to a server. This data is then downloaded from the server into a client computer. In this computer, System identification is done on the downloaded data using the three system identification methodologies mentioned in the previous chapter and inferences from each methodology is noted. These inferences are compared with the recordings on the site log book for determining the accuracies of each methodologies. Results of the implementation are discussed in chapter 6.

CHAPTER 6

RESULTS AND DISCUSSION

6.1 INTRODUCTION

This chapter presents the results from the experiments as specified in Chapter 5. Results from the performance evaluation of the wireless sensor network is presented in section 6.2. The comparison of efficiencies of the intuitive and scientific sensor placement methodologies are discussed in Section 6.3. Section 6.4 compares the accuracies three system identification methodologies.

6.2 WIRELESS SENSOR NETWORK

This section presents the results of the performance evaluation of the wireless sensor network. Two tests were conducted i.e. the performance evaluation at the laboratory and the performance evaluation at the site. Results of the analysis are as follows.

6.2.1 Performance Evaluation at Laboratory

Variation of RSSI (Received Signal Strength Indicator) with distance is shown in Figure 6.1, Consistent with the results reported in the literature(Piyare *et al*. 2013). RSSI decreases with distance from the coordinator. However, the reduction in strength if plotted logarithmically will not result in a linear relationship with distance as expected. This is in conformation with (Parameswaran *et al*. 2009)wherein it was observed that even in ideal scenarios RSSI does not give a consistent behavior. The fluctuations at distances from 40 to 60 m in 10 bytes and 30 bytes can be correlated with reflection and multipath phenomena due to end walls and presence of electromagnetic interference from equipment such as Wi-Fi routers. This is also supported by the findings of Bae *et al* (2013)10 and Piyare *et al* (2013)29. Despite the observations that RSSI fluctuated from the theoretical expectation, all the values lie above the threshold of XBee requirements, which is -102dBm (http://www.digi.com/pdf/ds_XBeemultipointmodules.pdf [Accessed 10th January 2015]) Therefore, it can be concluded that the current wireless sensor network has enough signal strength to support data transmission in the range specified.

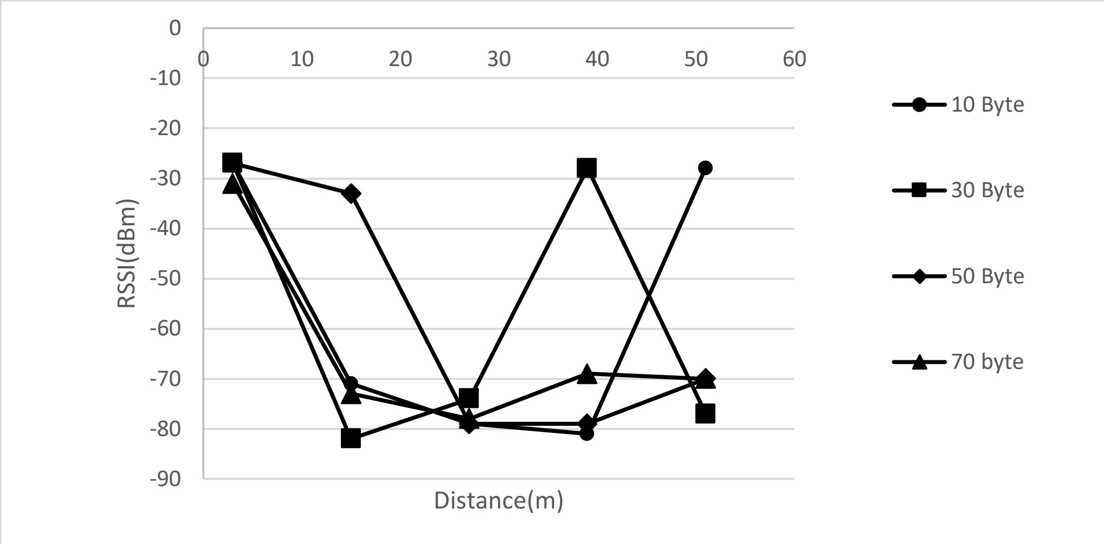

Figure 6.1: Variation of RSSI with distance

Figure 6.2 shows the PDR data. PDR of 30-byte data consistently lies at 100% for the whole range while PDR for the rest of the packets has a decline after 40m. Most of the readings lie above the 90 % range. General trend is that the PDR decreases with increases in packet size, but observations obtained do not follow the trend. 10 bytes and 50-byte packet sizes show unexpected fluctuations at 0-30 m. Further experimentation is required to explore the reason for the fluctuations. However, as all the PDR points lie above 75%, the current wireless sensor network satisfies the required reliability criteria.

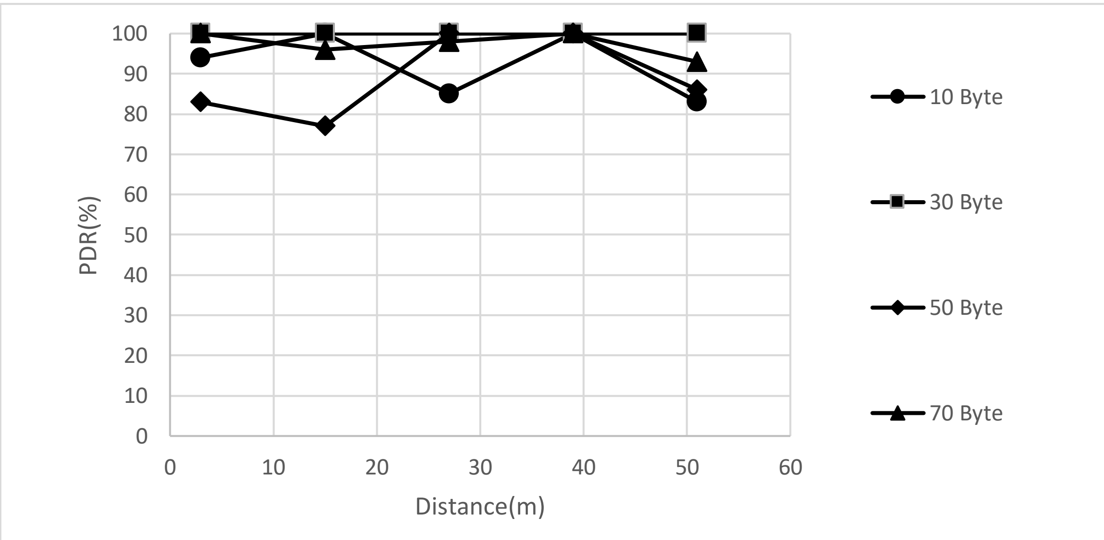

Figure 6.2: Variation of PDR with distance

6.2.2 Performance Evaluation on Launching Girder Construction Site

The results of the analysis are as shown in Figure 6.3. However, Variation of RSSI is consistent with the results reported in the literature (Piyare *et al*. 2013).Despite the fluctuations in RSSI values, all the values lie above the threshold of XBee requirements, which is -102dBm Also, the PDR values consistently lie above the 90% mark. Therefore, it can be concluded that the current wireless sensor network has enough signal strength to support data transmission in the range specified and also satisfy the reliability criteria.

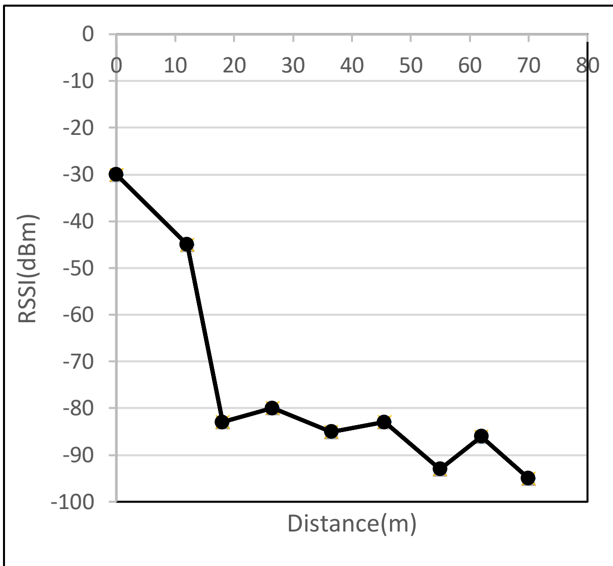

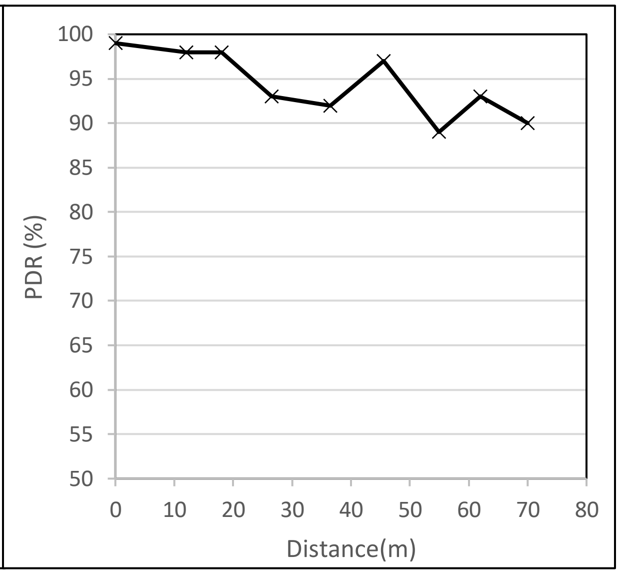

Figure 6.3: Performance of Wireless sensor network.
Variation of RSSI with Distance (Left); Variation of PDR with Distance (Right)

To test the redundancy in the network, the Routers and end devices at all the points were removed and replaced systematically to check the stability of the network in case of device failures. A network as predicted automatically routed the packets through a different device and proved efficient even in the absence of certain notes in between. The evaluation confirmed that the technologies, components & topology used for the WSN were appropriate for implementing a wireless sensor network to monitor launching girder operations.

6.3 SENSOR PLACEMENT METHODOLOGY

This section presents the results from an evaluation of the sensor placement methodology. A pilot study and a full-scale test were conducted. The pilot study discusses the influence of precision, influence of an increase in a number of sensors and also whether sensor placement study is required or not. Full-scale study compares the results from intuitive and scientific sensor placement study during the actual launching girder implementation.

6.3.1 Pilot Study

This section presents the results of evaluations done in the previous section. The objective of the evaluations is to find the optimum sensor configuration as well as to study the influence of precision of measurement in the design of measurement configuration system. Results of the analysis are given in Table 6.1.

Table 6.1: Influence of Precision

Precision	No of Sensors	Entropy of the First sensor
0.0004	6	2.52
0.00004	4	4.68
0.000004	4	7.94

It can be observed that as the precision increases, entropy increases. From this, it can be inferred that higher the precision in measurements higher the information content. The reason for this observation is that, higher the precision at a location, the number of candidate models could be separated as the interval width of the histogram is reduced.

When precision is increased from 0.0004 to 0.00004, the number of sensors with non-redundant information decreases. However, when the precision is again increased to 0.000004, the number of sensors does not decrease. This proves that even if the precision is increased, a minimum number of sensors is required for effective model separation.

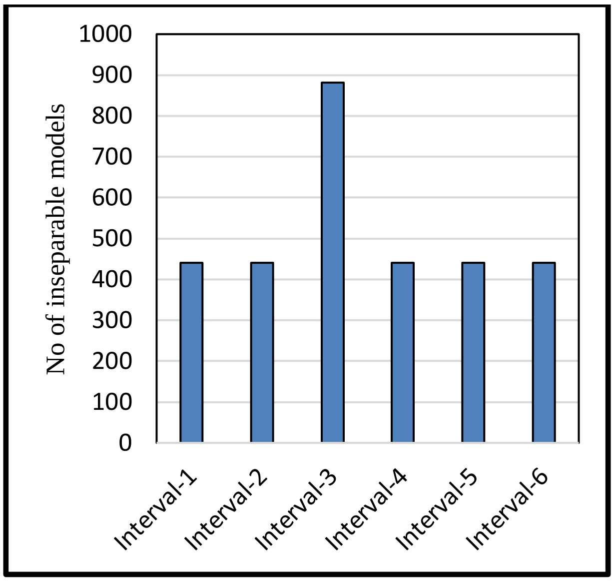

Figure 6.4: Distribution of inseparable candidate models; Precision=0.004; No of sensors =1

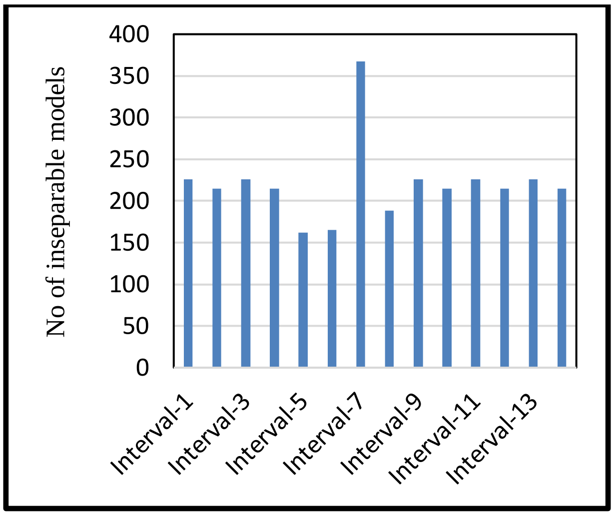

Figure 6.5: Distribution of inseparable candidate models; Precision=0.004; No of sensors =3

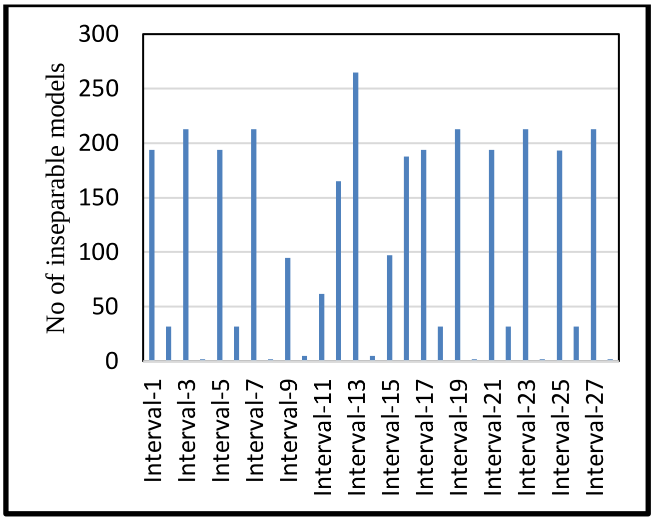

Figure 6.6: Distribution of inseparable candidate models; Precision=0.004; No of sensors =6

From the Figure 6.4, Figure 6.5, Figure 6.6 it can be seen that number of inseparable models decreases with the addition of a sensor. It is observed that inseparable models are distributed over larger intervals as the sensors are being added. Thus, an increase in the number of sensors employed has an influence on the accuracy of the measurement.

Table 6.2: Precision=0.000005
Entropy at Different locations

Location	Entropy
Element7	7.94
Element54	2.72
Element4	1.45
Element22	0.81
Element1	0

From the Table 6.2, it can be seen that element 1 has an entropy value of zero. All the subsequent elements also have entropy value zero. This means that the number of sensors has no influence on the information content after information saturation is reached. This observation reinforces the results of previous studies (Kripakaran & Smith 2009; Papadimitriou 2004; Papadimitriou 2005).

From these observations, it could be concluded that the precision of the measurement system increases the efficiency and resolution of the identifications. The increase in the precision of the measurement system reduces the number of sensors to be deployed. However, a minimum number of sensors is required for efficient identification of candidate models. In addition, it can be inferred that the increase in a number of sensors increases the efficiency of measurement system until information saturation is reached. The addition of sensors has no effect on the measurement system efficiency after this saturation point.

The conclusions from these observations contradict the current trend in designing the measurement systems based on the engineering experience alone. The locations arrived using such heuristic approaches might ignore sensor locations that contain rich information, which results in ambiguous interpretation. Also unsystematic approaches in measurement system design result in a large amount of redundant data leading to high data interpretation costs. Out of the 20 locations chosen for experimentation, only 4-6 locations (4 corresponds to 0.000004 precision and 6 correspond to 0.0004 precision) gave non-redundant information. This reinforces the fact that extensive monitoring using a large number of sensors might not be necessary to arrive at the required model separation. Therefore designing measuring system in a systematic approach is cost-effective compared to the traditional approach. Decreased cost in implementation would motivate the stakeholders to include monitoring systems in their projects resulting in safer projects. The effect of precision of measurement gives us a more comprehensive idea of the precision to be selected for a measurement system. It gives the decision maker flexibility in choosing between a precise measurement system with costlier sensors or less precise system with cost effective sensors.

6.3.2 Full-Scale Sensor Placement Study

Sensor placement methodology as mentioned in section 4.2 is evaluated by comparing it with the general intuitive methods such as, keeping sensors at the positions of maximum stress. It is a common misconception that the point of maximum stress would give more resolution(Raphael & Jadhav 2015; Adams *et al.* 2010; Kreith & Kreider 2002; Frank *et al.* 2015; Meenatchisundaram *et al.* 2015). Though it is partly correct, in many cases, even with higher resolution, we may observe low variance and hence lesser separation of models. Sensor placement methodology based on point of maximum stress is termed Intuitive Sensor Placement Method 1.This study also takes into account intuitive methods for placement using the knowledge about the behavior of the structure such as point of stress variation and contra flexures. This sensor placement methodology is termed Intuitive Sensor Placement Method 2. Sensor placement using the concept of maximum information as stated in section 4.2 is termed entropy method.

These sensor placement methods (both intuitive and entropy based) are compared based on its capability to separate models during system identification. When a sensor location is added, it could classify the models into different intervals based on the sensor resolution. Number of inseparable models in each interval gives an idea about the efficiency of the sensor placement methodology. To compare different methods, two metrics are being used in this study. These metrics compare the number of models which remains unseparated in each interval. As the no of unseparated models reduces, the efficiency of measurement system increases. The two metrics used for the comparison are as follows.

- For the first metric, the interval which contains the maximum number of inseparable models is determined, and the number of inseparable models for that interval gives the first metric –the maximum number of inseparable models in an interval set at the sensor location. Lesser the magnitude of this metric, more the efficiency of the sensor placement strategy. Variation of this metric with the number of sensors for both intuitive and entropy based sensor placement strategy is as shown in Figure 6.7.

- The second metric is the Average number of inseparable models per interval. This is obtained by calculating the arithmetic mean of number of inseparable models taking into account all the intervals at that sensor location. The efficiency of the sensor placement strategy is inversely proportional to this metric. Variation of this metric with the no of sensors added for both intuitive and entropy based sensor placement strategy is as shown in Figure 6.8.

From the Figure 6.7 and Figure 6.8, it is clearly evident that the sensor placement methodology based on entropy performs better than the intuitive method for placing sensors. It can be observed in Figure 7 that for the first sensor location the metric for both intuitive method 1 and entropy based measurement system design are equal. This is because the sensor location suggested by both methods is the same. But every other sensor added after the first one clearly shows that the intuitive methods results in the selection of locations having duplicate or redundant information. Also, Intuitive method 2 behaves more efficient than Intuitive method 1 for the sensor locations after the first sensor. Therefore, this study confirms conclusions of previous studies which state that systematic sensor placement methodology is essential for good performance (Robert-Nicoud *et al*. 2005; Goulet *et al*. 2010; Papadopoulou *et al*. 2014; Raphael & Jadhav 2015; Joshua & Varghese 2013).

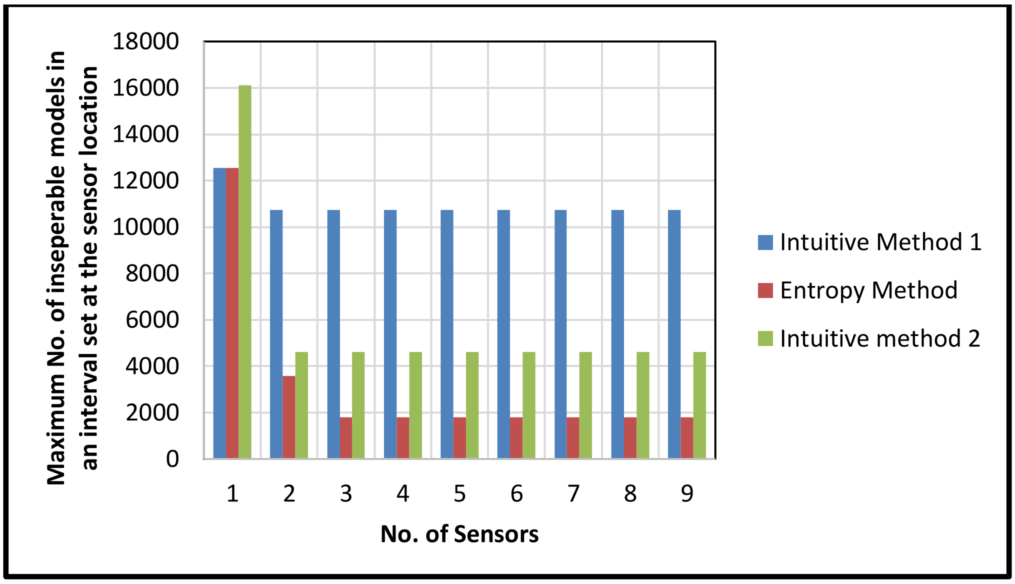

Figure 6.7: Maximum no of inseparable models in an interval set at sensor location

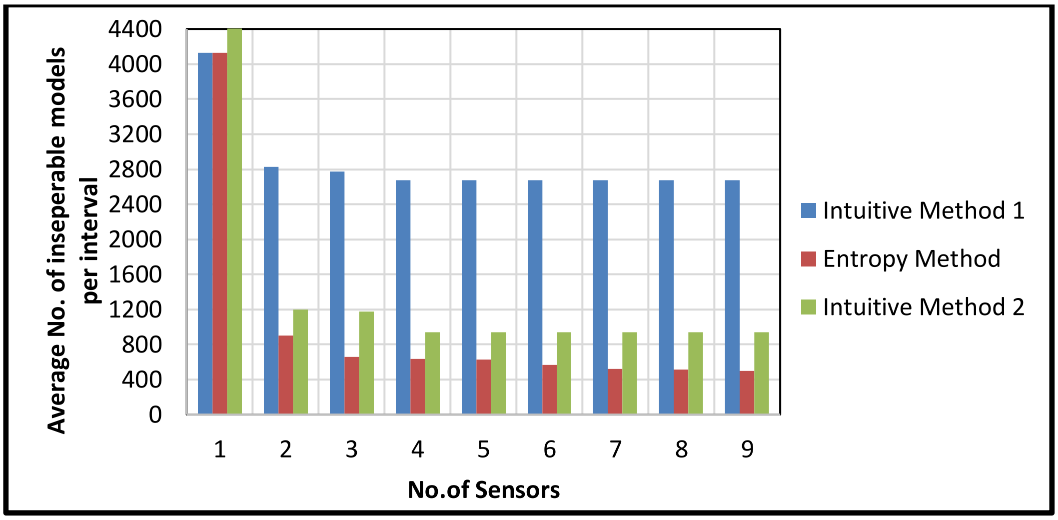

Figure 6.8: Average number of inseparable models per interval

6.4 SYSTEM IDENTIFICATION.

This section discusses the results of the implementation of the wireless sensor network on the launching girder. As mentioned in section 4, the accuracy of the system identification methodologies is evaluated by comparing the inferences with the actual recordings from the log book at the site. The model falsification algorithm outputs either the state of the system or an anomaly. An anomaly is a zero match to the model predictions. These results are compared with the log book details of that particular time and checked for consistency. 19724 readings collected over a period of 2 months were used for the comparison. Percentage of the match between the inferences and actual recorded values is used as a metric to quantify the accuracy of the System Identification Methodology.

6.4.1 Comparison between Different System Identification Methodologies

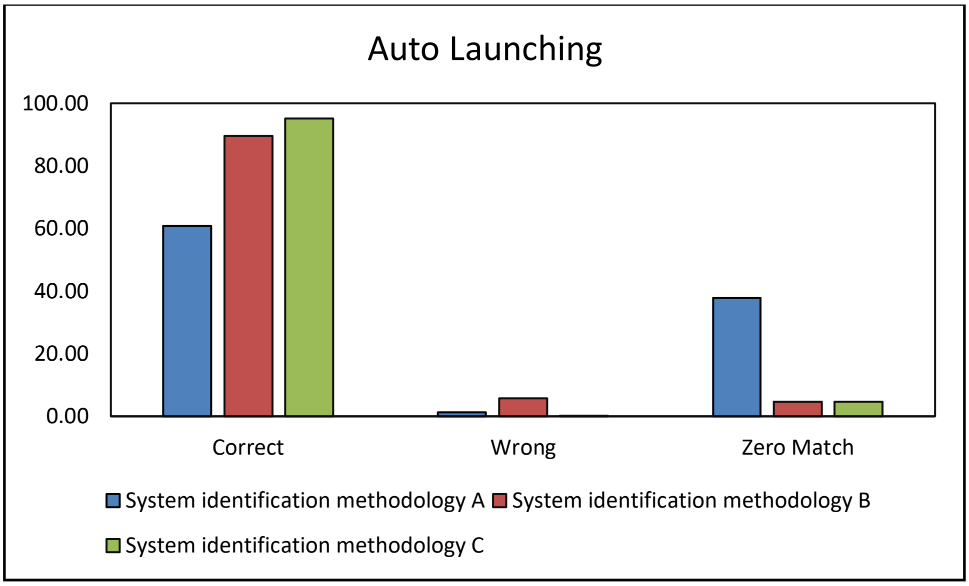

Figure 6.9: Comparison of accuracies for Auto Launching

Figure 6.9 compares the accuracies of the system identification methodologies A, B, and C for auto launching. The System Identification Methodology B methodology yielded an accuracy of 89.6% with 5.75% Type 1 error and 4.65% Type 2 error which is a significant improvement over System Identification Methodology A methodology which yielded an accuracy of 61% with 1.3% Type 1 error and 37.8% Type 2 error. This is mainly because System Identification Methodology B uses the trends instead of direct observations to falsify the models. However, it can be seen that the number of wrong interpretations is more for the methodology B. This is the consequence of slope trends matching some wrong situations due to the expanded error neighborhood. Even though the methodology A does not give better accuracy, the number of wrong interpretations is also less. In short, methodology B has higher type 1 error and methodology A has higher type 2 error. System Identification Methodology C (System identification based on derived features and heuristics) shows better performance than the others and has an accuracy of 95.1% with 0.28% Type 1 error and 4.65% Type 2 error. It could filter out the type 1 error in System Identification Methodology B by using heuristics.

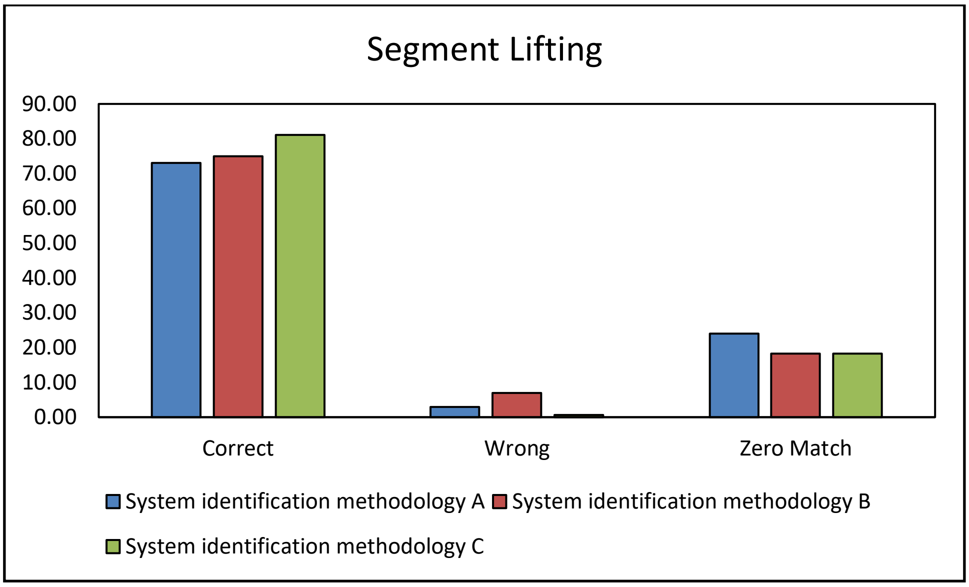

Figure 6.10: Comparison of accuracies for Segment Lifting

Figure 6.10 compares the accuracies of the system identification methodologies A, B, and C for Segment Lifting. The System Identification Methodology B methodology yielded an accuracy of 74.91% with 6.89% Type 1 error and 18.20% Type 2 error which is a slight improvement over System Identification Methodology A methodology which yielded an accuracy of 72.97% with 3% Type 1 error and 24.3% Type 2 error. Although accuracy has slight increase Type 1 error has also increased. Type 2 error in both the cases is nearly the same. Hence in this activity, it could be concluded that System Identification Methodology B doesn’t actually increase the interpretation accuracy. However, System Identification Methodology C has a considerable improvement in the accuracy yielding 81.1% correct observation combined with 0.71%Type one error and 18.2% Type 2 error. This improvement over the System Identification Methodology C clearly exhibits the relevance of heuristics in system identification methodologies.

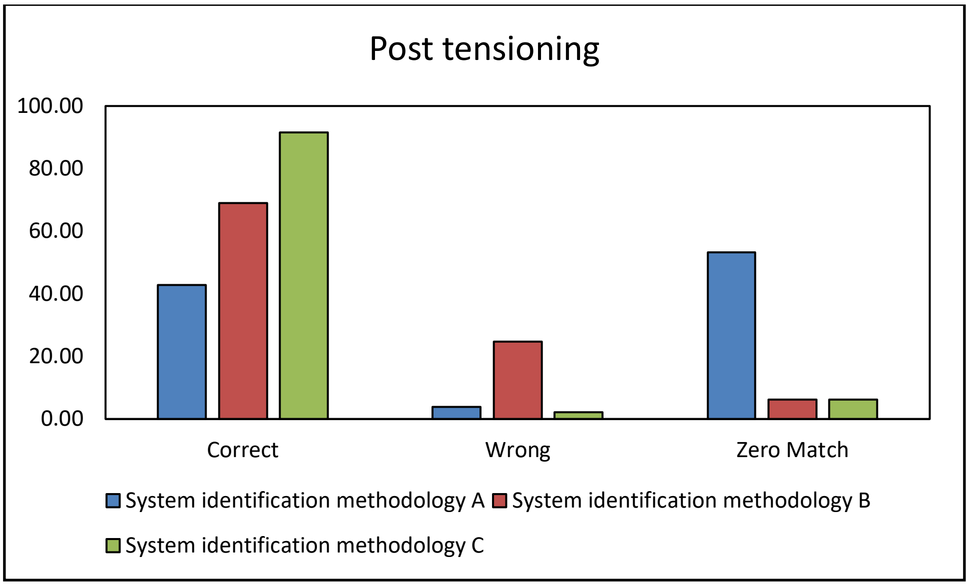

Figure 6.11: Comparison of accuracies for Post-Tensioning

Figure 6.11 compares the accuracies of the system identification methodologies A, B, and C for Post-Tensioning. The System Identification Methodology B methodology yielded an accuracy of 68.9% with 24.78% Type 1 error and 6.32% Type 2 error which is a significant improvement over System Identification Methodology A methodology which yielded an accuracy of 42.75% with 3.97% Type 1 error and 53.28% Type 2 error. Although there is a considerable increase in the accuracy for the System Identification B when compared to System Identification A, the accuracy isn't high enough for system identification since more than 24.78% of the observations are reported wrong.

System Identification Methodology C, on the other hand, shows better performance than the others and has an accuracy of 9..571% with 2.11% Type 1 error and 6.38% Type 2 error. Heuristics check in the System Identification Methodology C is the reason for this increased efficiency.Post-tensioning activity clearly demonstrated the effect of this addition.

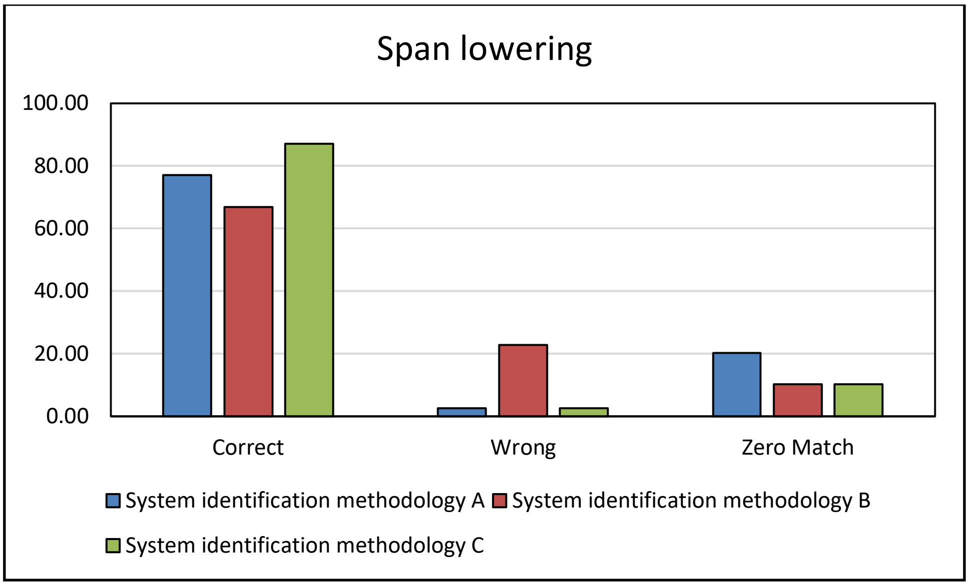

Figure 6.12: Comparison of accuracies for Span Lowering

Figure 6.12 compares the accuracies of the system identification methodologies A, B, and C for Span Lowering. The System Identification Methodology a methodology yielded an accuracy of 77.1% with 3% Type 1 error and 20.3% Type 2 error which is a slight improvement over System Identification Methodology B methodology which yielded an accuracy of 66.93% with 22.7% Type 1 error and 10.36% Type 2 error. This is one of the cases which shows the drawback of System Identification Methodology B due to its expansion in error threshold. This decrease in accuracy is primarily because the strain pattern of span lowering is quite similar to last stage of post-tensioning, the start of auto-launching and the start of segment lifting stages. Hence, many observations under span lowering were misinterpreted as the cases mentioned.

However, the heuristic check in the System Identification Methodology C could isolate these misinterpretations and map the observations to span lowering which led to an accuracy of 87.05%. However, it should also be noted that accuracy, in this case, was less than 90%. This is because, some of the readings were matched to the last stage of post-tensioning and start of auto-launching, as it satisfied both slope based trend and heuristics.

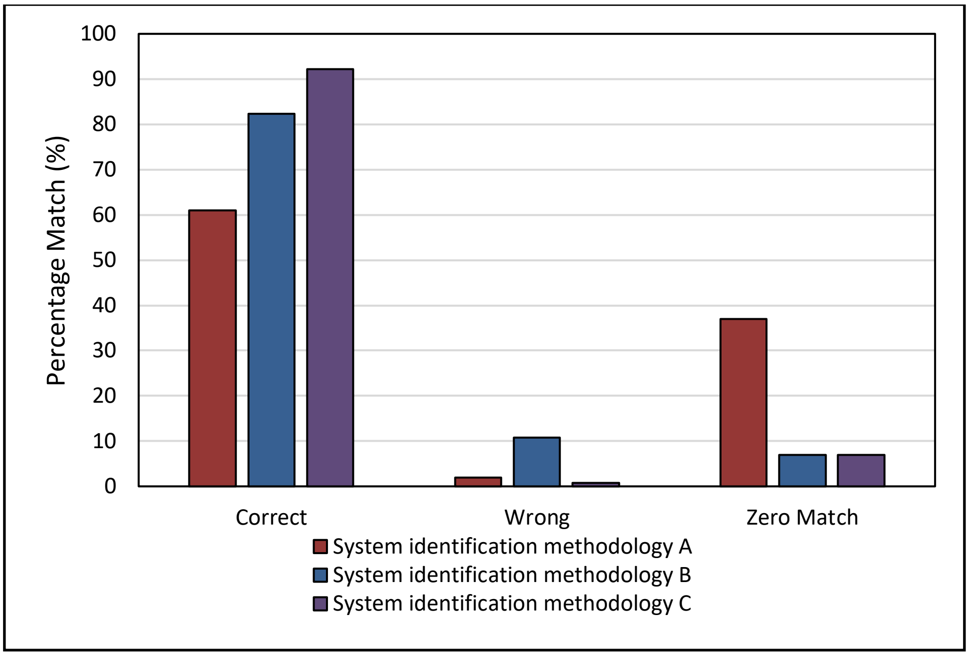

Figure 6.13: Comparison of accuracies between different system identification methodologies

Figure 6.13 compares the accuracies of the system identification methodologies A, B, and C. The System Identification Methodology B has a higher correct match of 82.3% compared to 61% for methodology A. This is mainly because System Identification Methodology B uses the trends instead of direct observations to falsify the models. However, we have seen than System Identification Methodology B has its own limitation in activities like span lowering where there are lesser accuracies. Also, it can be seen that the number of wrong interpretations is more for the methodology B. This is because slope trends happen to match even for some wrong situations. Even though the methodology A does not give better accuracy, the number of wrong interpretations is also less. In short, methodology B has higher type 1 error and methodology A has higher type 2 error. System identification based on derived features and heuristics (System Identification Methodology C) shows better performance than the others and has an accuracy of 92.2%. It could filter out the type 1 error in System Identification Methodology B by using heuristics and leading to accuracies of 90% and above for three out of four observed activities.

6.4.2 System Identification based on Derived Features and Heuristics

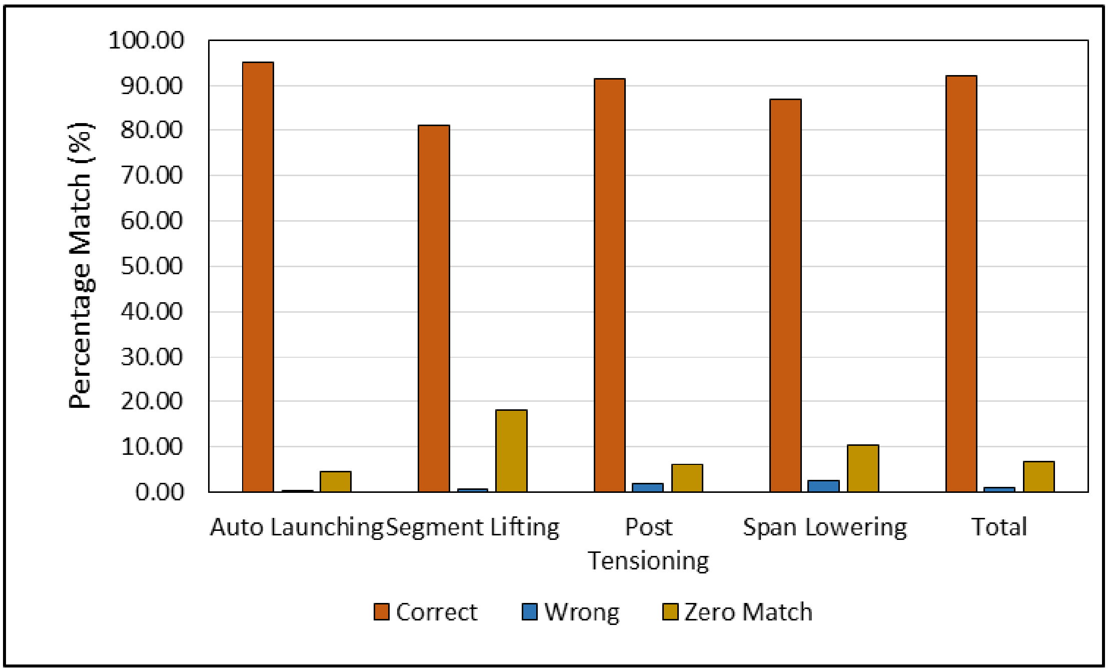

Figure 6.14: Detailed accuracy of System Identification using Derived Factors and heuristics

Figure 6.14 shows the percentage of match between the inferences with the log book entries for System Identification Methodology C. The system identification accuracy is more than 80% for all the operations. Operations such as post-tensioning and span lowering are identified correctly less than 90% of the times. This is because of the low sample size of observations. The total accuracy of identification for all the operations is 92.2%. Several factors contribute to the 7.8% error in identification. Errors in the installation of the strain gauge and the assumption of initial conditions as well as modeling errors have an influence on the final error percentage. However, it is difficult to control such errors at a construction site.

The Type 1 error (wrong match) in the System Identification Methodology is less than 1%, and it can be considered insignificant. However, the Type 2 error or in other words zero matches contribute to 6.96%. In the context of progress monitoring, the Type 2 error might not contribute to a serious misinterpretation since the effect is that the schedule doesn't get updated for that entry. Still, the frequency of updating is significantly higher than the conventional monitoring and therefore this error has the least impact. However, for productivity or safety monitoring, the presence of Type 2 error would result in ambiguous interpretations and false alarms (in cases no alarms for an actual case). From a productivity perspective, failure to update the completion may result in decreased productivity of that activity which in turn leads to incorrect decision support.

Although the sensor data was matched to one of the 33 cases (minor operations), results are classified into one of the four operations only. This is done so due to two reasons. The level of detail in which recordings were made in the log book was at a macro level and hence the evaluation of minor activities are not possible. In addition, there are uncertainties in the installation, errors in measurement, etc. which decrease the resolution of measurement which is a limitation of this study. Although the study is limited to these constraints, the System Identification Methodology has the potential to classify even the minor activities provided the perfect installation of the measurement system and reduction in interference with the measurement.

6.4.3 Statistical Analysis

The t-test was done on the readings of System Identification Methodology A & B to assess whether the means of two groups are statistically different from each other. The same was done on the readings of System Identification Methodology B & C also. Test was done on a sample of 250 readings. Correct identification was given a value 1, wrong identification was given value -1 and the zero match value 0.

The null hypothesis for the t-test between System Identification Methodologies A & B is that results of both the methodologies are same. In other words the falsification using slope has no additional effect on the inferencing when compared to falsification using raw strain data. Results of the test is as shown in Figure 6.15. The null hypothesis was rejected with 98% confidence which is well above 95% confidence used in management and scientific tests. Hence we can conclude that the Falsification methodology using derived features such as slope between readings of critical locations have significant effect on the improvement in the accuracy.

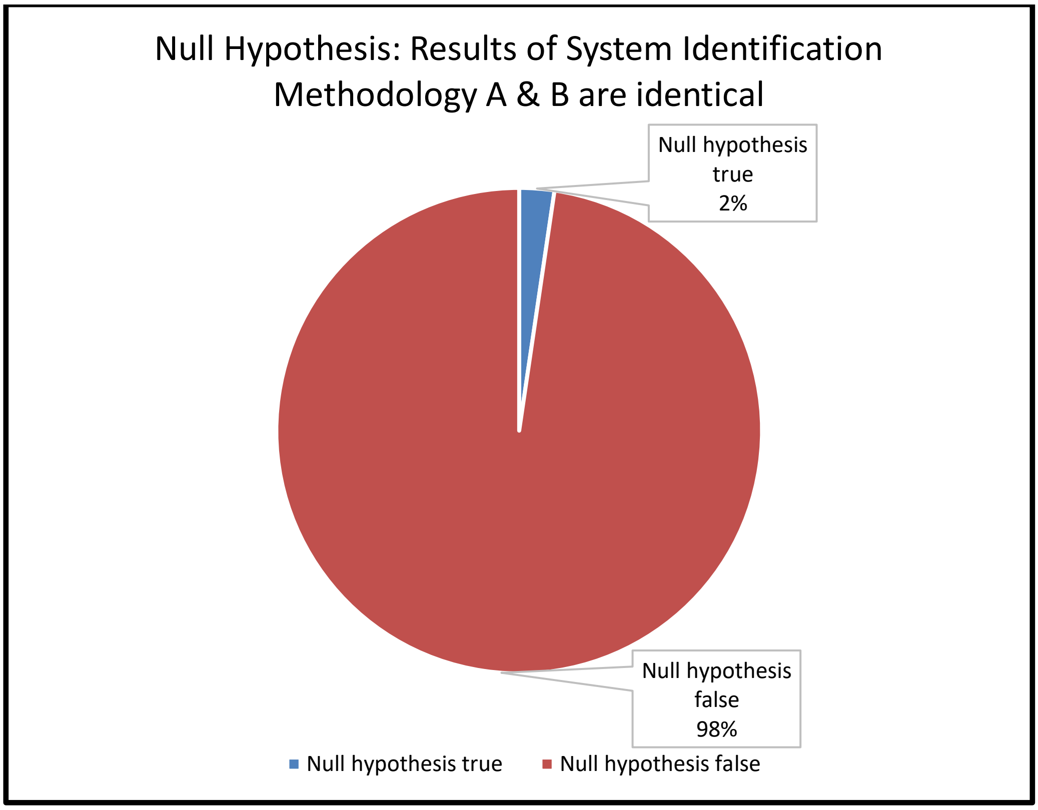

Figure 6.15: Results of T-Test between System Identification Methodology A and System Identification Methodology B

The null hypothesis for the t-test between System Identification Methodologies B & C is that results of both the methodologies are same. In other words the addition of heuristics to the System Identification Methodology B has no additional effect on the inferencing when compared to falsification using slope. Results of the test is as shown in Figure 6.16. The null hypothesis was rejected with 99.9965% confidence which is well above 95% confidence used in management and scientific tests. Hence we can conclude that the addition of heuristics to the System Identification Methodology B have significant effect on the improvement in the accuracy.

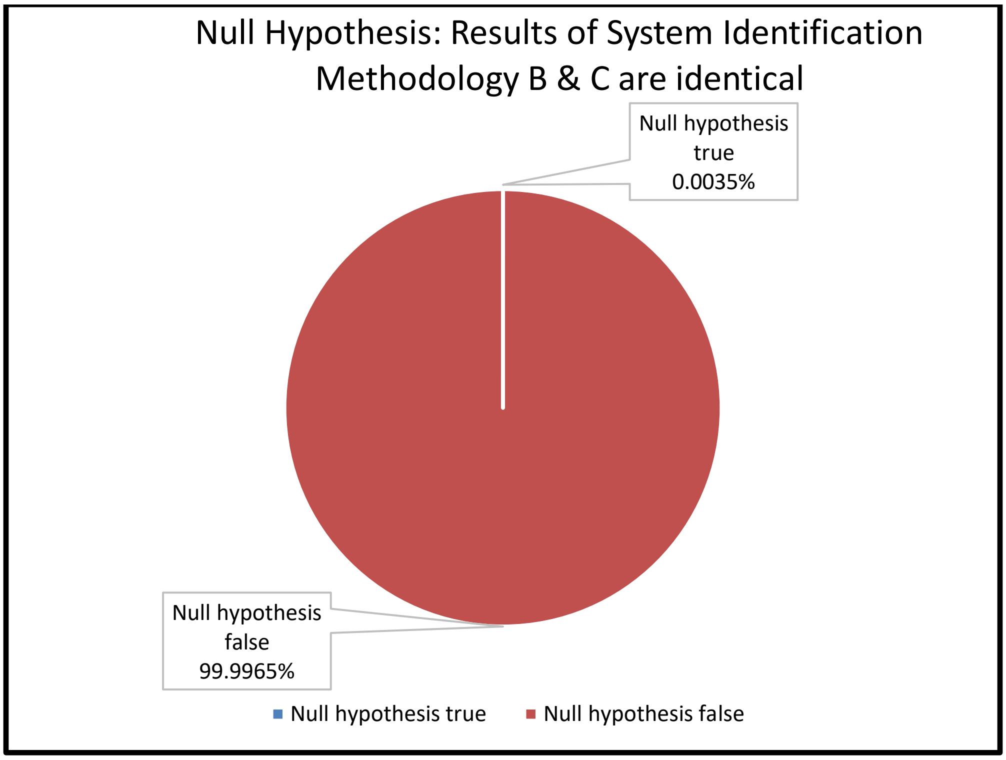

Figure 6.16: Results of T-Test between System Identification Methodology B and System Identification Methodology C

6.5 SUMMARY

This chapter presented the results from the implementation of the data acquisition system on a working launching girder. The WSN was evaluated based on RSSI and PDR and both was found above the minimum threshold in both laboratory and site conditions and hence reliable. Pilot study and a full-scale study conducted reinforces the need for a scientific sensor placement methodology. Sensor placement methodology based on Shannon's entropy is found efficient in placing the sensors at locations that would give maximum accuracy. 3system identification methodologies were used to analyze the data from the WSN. An existing System Identification Methodology from the literature was evaluated and tested on the actual data from a metro rail construction site to infer the state of operation of a launching girder. However, this methodology yielded an accuracy of 61% with 2% Type 1 error and 37% Type 2 error. To explore improvements a new system identification strategy based on derived features was developed, and this showed an accuracy of 82.3% with 10.84% Type 1 error and 6.97. This methodology was further altered by incorporating heuristics and domain knowledge which yielded an accuracy of 92.2% with 0.83% Type 1 error and 6.97% Type 2 error.

CHAPTER 7

SUMMARY AND CONCLUSION

This chapter summarizes the work done in this research. Conclusions from the work and the contributions of the work are present here. Potential for further work in this area and a brief introduction to extended applications of this framework are also presented.

7.1 SUMMARY

The overall objective of this work is to monitor the progress of the viaduct construction process in real time. An automated monitoring system was adopted over the traditional monitoring system to monitor the progress as the automated monitoring system performs better in terms of accuracy and response time. The monitoring system uses structural responses from the launching girder to identify its operations such as auto-launching, segment lifting, post-tensioning and span loading by employing a strain-based sensor network on a launching girder. Monitoring the state of the launching girder operations would give direct information related to the progress of metro rail viaduct construction.

The study was conducted in three phases. The first phase involved investigating the literature for the available methods for automated monitoring and also visiting the launching girder site to understand the operations and the potential for instrumentation in the launching girder. During the second phase, positions for the placement of the sensors was identified by using Shannon's entropy as metric for the information content. A wireless sensor network was designed for the data acquisition at the launching girder site from the sensors. Conventional system identification methodologies were altered to suit the monitoring application in construction in this phase. Finally during the phase three of the research, the monitoring system was implemented on a working launching girder and then tested for the applicability and accuracy. The monitoring system was used for the data collection for a period of two months during which four spans were erected.

For the local data acquisition at the launching girder site, a strain-based wireless sensor network was designed. Wireless sensor network was preferred over a conventional wired data acquisition systems to improve the scalability and flexibility for reconfiguration, reduce data distortion, etc. However, developing a wireless sensor network for a construction site is challenging due to the spatially extensive, object cluttered and fluctuating environment at the construction site. Hence, different wireless technologies was evaluated taking into account different parameters such as transmission range, reliability, bandwidth, reach quality, etc. ZigBee technology was found ideal for the implementation a construction site. Performance evaluations for ZigBee technology both at laboratory and at the construction site based on metrics such as Received Signal Strength Indicator (RSSI) and Packet Delivery Ratio (PDR). Results of the evaluations showed the ZigBee-based wireless sensor network to be reliable.

To ensure that each sensor in the wireless sensor network yields maximum information for the continuous monitoring of a launching girder during its operational phase, positions for the sensor placement was determined scientifically. Scientific sensor placement was done by evaluating the information generated at multiple locations of the launching girder using Shannon's entropy as a measure of information content. The idea is borrowed from the literature in the field of information theory. Sensors were placed at the locations which had the maximum entropy. The location obtained using this method was compared with locations for sensors placed by intuitive methods and the sensor placement using entropy was found more efficient.

To interpret the data from the acquisition system at the launching girder site, different system identification methodologies were evaluated. From the literature, System identification methodology using model falsification had an advantage over methods such as Model Calibration and Bayesian inference. This is because Model Calibration and Bayesian inference require a clearly defined error structure for accurate identification whereas such clear classification of error structure is challenging from a construction industry perspective. However, conventional system identification methodologies based on model falsification yielded low accuracies and was modified to increase the accuracy of inference. The modified system identification methodologies uses derived features and heuristics for improving accuracies. The system identification methodologies were tested using the sensor data from a working launching girder and the accuracies these methodologies were evaluated by comparing with the readings from log book which records activities happening at the site. The modified system identification methodologies is observed to have better accuracy when compared with the conventional system identification methodology.

7.2 CONCLUSIONS

There are three key conclusions from this study which are presented in this section.

1. The ZigBee-based wireless sensor network is observed to be reliable at the metro rail viaduct construction site to monitor launching girder operations and it satisfied the criteria based on RSSI and PDR. It is observed during the implementation of WSN at the launching girder site that the ZigBee technology can handle the interference and noises from the construction site and provide reliable communication with reasonable signal strength and reach quality.

2. During the sensor placement studies, it was found that the intuitive methods for sensor placement results in redundant and duplicate information. Hence, it is essential to design a measurement system scientifically for efficient monitoring of launching girder operations. Positions to place sensors on a launching girder for monitoring its operations were determined using a scientific method based on Shannon's entropy. Positions and priority of the sensors placement are as per the scientific methodology is as shown in Figure 7.1 for the selected case study. This optimal placement of sensors results in higher accuracy of identification compared to intuitive methods.

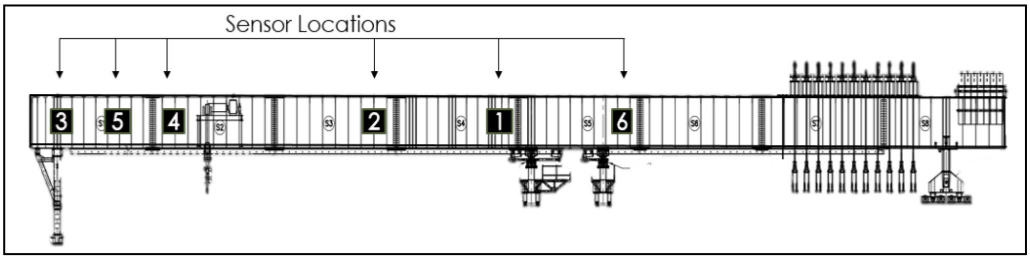

Figure 7.1: Optimal Sensor Placement on the Launching Girder

3. While evaluating different system identification methodologies with the sensor data from the launching girder, it was found that the conventional system identification methods based on model falsification do not show adequate accuracy. The conventional system identification methodology had an accuracy of 61% with 2% Type 1 and 37% Type 2 error. Hence, Conventional System

Identification based on Model Falsification was modified to develop a System identification methodology based on derived features and heuristics. The modified system identification methodology developed in this research performs better than the ones proposed in the literature with an accuracy of 92.2% with. 0.82% Type 1 error and 6.96% Type 2 error.

7.3 CONTRIBUTIONS

This study presents a framework for automated monitoring of metro rail viaduct construction process using the structural responses from a launching girder. The framework describes in detail the design of data acquisition system using ZigBee wireless sensor network, strategies for optimal sensor placement and presents a system identification methodology for classification of launching girder operations using sensor data. This study gives evidence that conventional system identification methods may not be accurate and system identification based on derived features and heuristics might be required to monitor accurately the construction operations. This was demonstrated by implementing a real-time monitoring system in a launching girder and comparing the accuracies of three system identification methodologies (one conventional and two modified).

Another contribution from this work is that this study demonstrates the use of construction progress monitoring with the aid of structural responses. This method was able to infer the construction activities with reasonable accuracies. This is a field in construction monitoring which is not adequately explored and has a great potential especially in the areas of productivity monitoring, safety monitoring, and automation.

7.4 FURTHER WORK

The further works which can be done in this area are presented in this section. It is subdivided into two sections which discusses further improvements in launching girder monitoring and the application of framework in different areas of construction.

7.4.1 Improvements in Launching Girder monitoring

The real-time monitoring system developed in study broadly classifies the launching girder operations into four operations which are auto launching, segment lifting, post-tensioning, and span lowering. Precise installation of sensors and an improved resolution of the data acquisition setup can make further sub-classification of these operations into great possible. This improvement would enable the system to perform productivity monitoring in addition to progress monitoring.

In the current study, the system identification is done either on a client computer or in the cloud. It is possible to run the system identification algorithm at the site itself using embedded computers which would significantly reduce the response time and overhead costs. This can be achieved either by optimization of the code for system identification which reduce the computing requirements and enable the system identification right at the site or by using small form factor high performance embedded computers which can be installed at the site.

In the current study, the number of scenarios to which system identification maps the model into is limited to cases that have been observed at the site. More scenarios such as different stages of failures, predictable anomalies etc. could be further added which would enable this system to contribute to the validation of the design, safety monitoring of launching girder etc. in addition to the progress monitoring.

7.4.2 Extended Applications of the framework

The current study is aimed at monitoring the operations of a launching girder in real time. However, the same framework may be used in monitoring other construction activities as well. Two examples of the activities which could use the framework are given below.

- Using strain based sensors on temporary structures such as scaffolding can be used to analyze the productivity
- Installing strain gauges on formwork would help the construction engineers to understand the concrete pour details and the productivity of the same.

In general, this framework can be applied to all the processes which involve the reuse of equipment, temporary structures etc. using different stages of the construction. Although the framework remains the same, choice of sensors, suitability of system identification methodology etc. should test for the specific construction processes.

The system identification algorithms developed in this study provides guidelines for inferring the state of the construction activity from structural responses of temporary structure/ equipment for these applications. Overall, the framework proposed can be a sub- system within a larger Internet of Things (IoT) based construction automation system which can monitor, analyze and control different aspects of construction in real-time.

REFERENCES

1. Adams, T.M., Layton, R.A. & Siahmakoun, A., 2010. *Introductory MEMS Fabrication and Applications*, New York: Springer-Verlag New York Inc.

2. Bae, S.C. *et al.*, 2013. Prediction of WSN placement for bridge health monitoring based on material characteristics. *Automation in Construction*, 35, pp.18–27. Available at: http://dx.doi.org/10.1016/j.autcon.2013.02.002.

3. Bayrak, T., 2008. Semi Automatic Construction Progress Measurement Using a Combination of CAD Modelling , Photogrammetry and Construction Knowledge. *(Thesis)Heriot-Watt University SCHOOL OF THE BUILT ENVIRONMENT*.

4. Braun, A. *et al.*, 2015. A concept for automated construction progress monitoring using BIM-based geometric constraints and photogrammetric point clouds. *Journal of Information Technology in Construction*, 20(November 2014), pp.68–79.

5. Brownjohn, J.M.W., 2007. Structural health monitoring of civil infrastructure. *Philosophical Transactions of the Royal Society of London, Series A, Mathematical and Physical Sciences*, 365(1851), pp.589–622. Available at: ISI:000243842300014\nhttp://vibration.shef.ac.uk/doc/10176117.pdf.

6. Buczak, A.L. *et al.*, 2001. Genetic algorithm convergence study for sensor network optimization. *Information Sciences*, 133(3-4), pp.267–282.

7. Carne, T.G. & Dohrmann, C.R., 1990. A MODAL TEST DESIGN STRATEGY FOR MODEL CORRELATION Thomas. *System*, (February).

8. Chen, X., Zhou, Y. & Luo, Q., 2014. A Hybrid Monkey Search Algorithm for Clustering Analysis. ,*The Scientefic World Journal, 2014*.

9. Cheng, A.L., Georgoulas, C. & Bock, T., 2016. Fall Detection and Intervention based on Wireless Sensor Network Technologies. *Automation in Construction*, p.-. Available at: http://www.sciencedirect.com/science/article/pii/S0926580516300437.

10. Cheng, M.Y. & Chen, J.C., 2002. Integrating barcode and GIS for monitoring construction progress. *Automation in Construction*, 11(1), pp.23–33.

11. Cheng, T. *et al.*, 2010. Automated construction resource location tracking to support the analysis of lean principles. *Challenging Lean Construction Thinking: What Do We Think and What Do We Know? - 18th Annual Conference of the International Group for Lean Construction, IGLC 18*, pp.643–653. Available at: http://www.scopus.com/inward/record.url?eid=2-s2.0-4866071498&partnerID=tZOtx3y1.

12. Cheok, G.S. *et al.*, 2000. Ladars for construction assessment and update , *Automation in Construction*. , 9(5), pp.463–477.

13. Davidson, I.N. & Skibniewski, M.J., 1995. Simulation of Automated Data Collection in Buildings. *Journal of Computing in Civil Engineering*, 9(1), pp.9–20.

14. Dimitrov, A. & Golparvar-Fard, M., 2014. Vision-based material recognition for automated monitoring of construction progress and generating building information modeling from unordered site image collections. *Advanced Engineering Informatics*, 28(1), pp.37–49. Available at: http://www.sciencedirect.com/science/article/pii/S1474034613000943.

15. Ding, L.Y. *et al.*, 2013. Real-time safety early warning system for cross passage construction in Yangtze Riverbed Metro Tunnel based on the internet of things. *Automation in Construction*, 36, pp.25–37. Available at: http://linkinghub.elsevier.com/retrieve/pii/S0926580513001313.

16. Domingo-perez, F. *et al.*, 2016. Sensor placement determination for range-difference positioning using evolutionary multi-objective optimization. *Expert Systems With Applications*, 47, pp.95–105. Available at: http://dx.doi.org/10.1016/j.eswa.2015.11.008.

17. El-Omari, S. & Moselhi, O., 2011. Integrating automated data acquisition technologies for progress reporting of construction projects. *Automation in Construction*, 20(6), pp.699–705. Available at: http://dx.doi.org/10.1016/j.autcon.2010.12.001.

18. Frank, T. *et al.*, 2015. Miniaturized silicon strain gauge elements to accurately measure mechanical quantities. *Proceedings SENSOR 2015*, pp.61–65.

19. Goldratt, E.M. & Cox, J., 2004. *The Goal: A Process of Ongoing Improvement*, Available at: http://www.amazon.com/Goal-Process-Ongoing-Improvement/dp/0884271781.

20. Golparvar-Fard, M. *et al.*, 2011. Evaluation of image-based modeling and laser scanning accuracy for emerging automated performance monitoring techniques. *Automation in Construction*, 20(8), pp.1143–1155. Available at: http://dx.doi.org/10.1016/j.autcon.2011.04.016.

21. Goulet, J. *et al.*, 2010. Multimodel Structural Performance Monitoring. , *Journal of Structural Engineering*,136(October), pp.1309–1318.

22. Goulet, J. & Smith, I., 2012. Performance-driven measurement-system design for structural identification. *Journal of Computing in Civil Engineering*, (August), pp.427–436. Available at: http://ascelibrary.org/doi/full/10.1061/(ASCE)CP.1943-5487.0000250.

23. Goulet, J.-A., 2012. Probabilistic model falsification for infrastructure diagnosis. *Thesis submitted to EPFL*, 5417, pp.1–218.

24. Goulet, J.-A., Coutu, S. & Smith, I.F.C., 2013. Model falsification diagnosis and sensor placement for leak detection in pressurized pipe networks. *Advanced Engineering Informatics*, 27(2), pp.261–269. Available at: http://linkinghub.elsevier.com/retrieve/pii/S1474034613000141.

25. Gu, G., Zhao, Y. & Zhang, X., 2016. Optimal Layout of Sensors on Wind Turbine Blade Based on Combinational Algorithm. ,*International journal of Distributed Sensor Networks,* 2016.

26. Hwang, S.F. & He, R.S., 2006. A hybrid real-parameter genetic algorithm for function optimization. *Advanced Engineering Informatics*, 20(1), pp.7–21.

27. Ibrahim, M. & Moselhi, O., 2014. Experimental study of wireless sensor networks for indoor construction operations. *31st International Symposium on Automation and Robotics in Construction and Mining, ISARC*, (Isarc), pp.805–812.

28. Jang, W.-S., Healy, W.M. & Skibniewski, M.J., 2008. Wireless sensor networks as part of a web-based building environmental monitoring system. *Automation in Construction*, 17(6), pp.729–736. Available at: http://linkinghub .elsevier.com/retrieve/pii/ S0926580508000174.

29. Jang, W.-S. & Skibniewski, M.J., 2009. Cost-Benefit Analysis of Embedded Sensor System for Construction Materials Tracking. *Journal of Construction Engineering and Management*, 135(5), pp.378–386.

30. Jaselskis, E.J. & El-Misalami, T., 2003. Implementing Radio Frequency Identification in the Construction Process. *Journal of Construction Engineering and Management*, 129(6), pp.680–688.

31. Joshua, L. & Varghese, K., 2014. Automated recognition of construction labour activity using accelerometers in field situations. *International Journal of Productivity and Performance Management*, 63(7), pp.841–862.

32. Joshua, L. & Varghese, K., 2013. Selection of Accelerometer Location on Bricklayers Using Decision Trees. *Computer-Aided Civil and Infrastructure Engineering*, 28(5), pp.372–388. Available at: http://doi.wiley.com /10.1111/mice.12002.

33. Kammer, D.C. & Yao, L., 1994. Enhancement of On-Orbit Modal Identification of Large Space Structures Through Sensor Placement. *Journal of Sound and Vibration*, 171(1), pp.119–139.

34. Kijewski-correa, T. *et al.*, 2013. SmartSync : An Integrated Real-Time Structural Health Monitoring and Structural Identification System for Tall Buildings. , *Journal of Structural Engineering* (October), pp.1675–1687.

35. Kiziltas *et al.*, 2008. Technological Assessment and Process Implications of Field Data Capture Technologies for Construction and Facility / Infrastructure

Management. *Journal of information technology in construction*, 13(April), pp.134–154.

36. Kreith, F. & Kreider, J.F., 2002. *The MEMS Handbook*, CRC Press.

37. Kripakaran, P. & Smith, I.F.C., 2009. Configuring and enhancing measurement systems for damage identification. *Advanced Engineering Informatics*, 23(4), pp.424–432. Available at: http://linkinghub.elsevier.com/retrieve/pii/S1474034609000299.

38. Laory, I. *et al.*, 2011. Designing measurement systems for continuous monitoring of structures. *EG-ICE Workshop*, (2), pp.1–8.

39. Lavric, A. *et al.*, 2012. A performance study of ZigBee wireless sensors network topologies for street lighting control systems. *2012 International Conference on Selected Topics in Mobile and Wireless Networking*, pp.130–133. Available at: http://ieeexplore.ieee.org/lpdocs/epic03/wrapper.htm?arnumber=6271280.

40. Li, D.-S., Fritzen, C.-P. & Li, H.-N., 2008. Extended MinMAC algorithm and comparison of sensor placement methods. *Proceedings of the IMAC-XXVI, Florida, USA.*

41. Li, H. *et al.*, 2005. Application of integrated GPS and GIS technology for reducing construction waste and improving construction efficiency. *Automation in Construction*, 14(3), pp.323–331.

42. Linderman, L.E. *et al.*, 2010. Characterization of Wireless Smart Sensor Performance. *Journal of Engineering Mechanics*, 136(12), pp.1435–1443.

43. Maul, W.A. *et al.*, 2007. Sensor Selection and Optimization for Health Assessment of Aerospace Systems. *Nasa/Tm-2007-214822*, (July), p.pp 1–23.

44. Meenatchisundaram, S., Kulkarni, S.M. & Bhat, S., 2015. Design Analysis and Sensitivity Enhancement of Piezoresistive Micro Pressure Sensors., *Proceedings of 2015 International Conference on Future Computational Technologies (ICFCT'2015)*, pp.104–110.

45. Naticchia, B., Vaccarini, M. & Carbonari, A., 2013. A monitoring system for real-time interference control on large construction sites. *Automation in Construction*, 29, pp.148–160. Available at: http://dx.doi.org/10.1016/j.autcon.2012.09.016.

46. Navon, R., 2005. Automated project performance control of construction projects. *Automation in Construction*, 14(4), pp.467–476.

47. Ngatchou, P.N., Fox, W.L.J. & El-Sharkawi, M. a., 2005. Distributed sensor placement with sequential particle swarm optimization. *Proceedings 2005 IEEE Swarm Intelligence Symposium, 2005. SIS 2005.*, pp.385–388. Available at: http://ieeexplore.ieee.org/lpdocs/epic03/wrapper.htm?arnumber=1501647.

48. Papadimitriou, C., 2004. Optimal sensor placement methodology for parametric identification of structural systems. *Journal of Sound and Vibration*, 278(4-5), pp.923–947. Available at: http://linkinghub.elsevier.com/retrieve/pii/S0022460X04000355.

49. Papadimitriou, C., 2005. Pareto optimal sensor locations for structural identification. *Computer Methods in Applied Mechanics and Engineering*, 194(12-16), pp.1655–1673. Available at: http://linkinghub.elsevier.com/retrieve/pii/S0045782504004104.

50. Papadimitriou, C., Haralampidis, Y. & Sobczyk, K., 2005. Optimal experimental design in stochastic structural dynamics. *Probabilistic Engineering Mechanics*, 20(1), pp.67–78.

51. Papadimitriou, C. & Lombaert, G., 2012. The effect of prediction error correlation on optimal sensor placement in structural dynamics. *Mechanical Systems and Signal Processing*, 28, pp.105–127. Available at: http://dx.doi.org/10.1016/j.ymssp.2011.05.019.

52. Papadopoulou, M. *et al.*, 2014. Hierarchical Sensor Placement Using Joint Entropy and the Effect of Modeling Error. *Entropy*, 16(9), pp.5078–5101. Available at: http://www.mdpi.com/1099-4300/16/9/5078/.

53. Parameswaran, A.T., Husain, M.I. & Upadhyaya, S., 2009. Is RSSI a reliable parameter in sensor localization algorithms - an experimental study. *IEEE International Symposium on Reliable Distributed Systems*, pp.1–5.

54. Pasquier, R. & Smith, I.F.C., 2013. Model-based data interpretation and diagnosis robustness., *Proceedings of 11th International Conference on Structural Safety & Reliability (ICOSSAR), New York, USA* , pp.2497–2504.

55. Peng, Z. *et al.*, 2016. Chaotic Monkey Algorithm Based Optimal Sensor Placement. , 9(1), *International Journal of Control and Automation* ,Vol.9, No.1 (2016), pp.423–434.

56. Piyare, R., Lee, S. & Korea, S., 2013. Performance Analysis of XBee ZB Module Based Wireless Sensor Networks. ,*International Journal of Scientific & Engineering Research*, 4(4), pp.1615–1621.

57. Popper, K.R., 1935. *The Logic of Scientific Discovery*, Routledge.

58. Pradhananga, N. & Teizer, J., 2013. Automatic spatio-temporal analysis of construction site equipment operations using GPS data. *Automation in Construction*, 29, pp.107–122. Available at: http://dx.doi.org/10.1016/j.autcon.2012.09.004.

59. Ramos, L.F. *et al.*, 2013. Dynamic structural health monitoring of Saint Torcato church. *Mechanical Systems and Signal Processing*, 35(1-2), pp.1–15. Available at: http://linkinghub.elsevier.com/retrieve/pii/S0888327012003652.

60. Ran, L. *et al*., 2012. Long-Term Deformation Monitoring of Metro-Tunnel Airshaft Excavation during Construction Stage. *International Journal of Distributed Sensor Networks*, 2012, pp.1–11. Available at: http://www.hindawi.com/journals/ijdsn/2012/972893/.

61. Raphael, B. & Jadhav, K.S., 2015. Sensor Placement for Structural Monitoring of Transmission Line Towers. *Frontiers in Built Environment*, 1(November), pp.1–10. Available at: http://journal.frontiersin.org/Article/10.3389/fbuil.2015.00024/abstract.

62. Rasid, M.F.A. & Noordin, N.K., 2009. Improved Tree Routing (ImpTR) Protocol for ZigBee Network. *Journal of Computer Science*, 9(10), pp.146–152.

63. Rebolj, D. *et al*., 2008. Automated construction activity monitoring system. *Advanced Engineering Informatics*, 22(4), pp.493–503. Available at: http://www.sciencedirect.com/science/article/pii/S1474034608000487.

64. Riaz, Z. *et al*., 2014. CoSMoS: A BIM and wireless sensor based integrated solution for worker safety in confined spaces. *Automation in Construction*, 45, pp.96–106. Available at: http://dx.doi.org/10.1016/j.autcon.2014.05.010.

65. Robert-Nicoud, Y., Raphael, B. & Smith, I.F.C., 2005. Configuration of measurement systems using Shannon's entropy function. *Computers and Structures*, 83(8-9), pp.599–612.

66. Shannon, C.E. & Weaver, W., 1949. The Mathematical Theory of Communication. *The mathematical theory of communication*, 27(4), p.117.

67. Turkan, Y. *et al*., 2011. Towards Automated Progress Tracking of Erection of Concrete Structures, *Automation in Construction*,22. , pp.1–11.

68. Valero, E., Adán, A. & Cerrada, C., 2015. Evolution of RFID Applications in Construction: A Literature Review. *Sensors*, 15(7), pp.15988–16008. Available at: http://www.mdpi.com/1424-8220/15/7/15988/.

69. Vernay, D.G., Raphael, B. & Smith, I.F.C., 2015. A model-based data-interpretation framework for improving wind predictions around buildings. *Journal of Wind Engineering and Industrial Aerodynamics*, 145, pp.219–228. Available at: http://dx.doi.org/10.1016/j.jweia.2015.06.016.

70. Vik, K.H., Griwodz, C. & Halvorsen, P., 2008. Constructing low-latency overlay networks: Tree vs. mesh algorithms. *Proceedings - Conference on Local Computer Networks, LCN*, pp.36–43.

71. Voon, P., Sing, C. & Kiong, K., 2016. Approach towards sensor placement , selection and fusion for real-time condition monitoring of precision machines. *Mechanical Systems and Signal Processing*, 68-69, pp.105–124. Available at: http://dx.doi.org/10.1016/j.ymssp.2015.07.008.

72. Wang, X. *et al.*, 2013. A conceptual framework for integrating building information modeling with augmented reality. *Automation in Construction*, 34, pp.37–44. Available at: http://www.sciencedirect.com/science/article/pii/S0926580512001793.

73. Ye, X.W., Ni, Y.Q. & Xia, Y.X., 2012. Distributed Strain Sensor Networks for In-Construction Monitoring and Safety Evaluation of a High-Rise Building. *International Journal of Distributed Sensor Networks*, 2012, pp.1–13. Available at: http://www.hindawi.com/journals/ijdsn/2012/685054/.

74. Yi, T. & Li, H., 2012. Methodology Developments in Sensor Placement for Health Monitoring of Civil Infrastructures., *International Journal of Distributed Sensor Networks* , 2012.

75. Yi, T.H. & Li, H.N., 2012. Methodology developments in sensor placement for health monitoring of civil infrastructures. *International Journal of Distributed Sensor Networks*, 2012.

76. Yi, T.H., Zhang, X.D. & Li, H.N., 2012. Modified Monkey Algorithm and its Application to the Optimal Sensor Placement. *Applied Mechanics and Materials*, 178-181, pp.2699–2702. Available at: http://www.scientific.net/AMM.178-181.2699.

77. Yi, W. *et al.*, 2016. Development of an early-warning system for site work in hot and humid environments: A case study. *Automation in Construction*, 62, pp.101–113. Available at: http://dx.doi.org/10.1016/j.autcon.2015.11.003.

78. Yoon, S.-W. *et al.*, 2006. An application model of RFID technology on progress measurement and management of construction works. *23rd International Symposium on Automation and Robotics in Construction*, pp.779–783.

79. Yuen, K.-V. *et al.*, 2001. Optimal Sensor Placement Methodology for Identification with Unmeasured Excitation. *Journal of Dynamic Systems, Measurement, and Control*, 123(December), p.677.

80. Zekavat, P.R., Moon, S. & Bernold, L.E., 2014. Performance Assessment of Wireless Data Capture in Construction. , *Proceedings of Internation Symposium on Automation and Robotics in Construction and Mining 2015*.

81. Zhang, C. & Arditi, D., 2013. Automated progress control using laser scanning technology. *Automation in Construction*, 36, pp.108–116. Available at: http://linkinghub.elsevier.com/retrieve/pii/S092658051300126X.

82. Zhang, G., Drive, C. & Vachtsevanos, G., 2007. A Methodology for Optimum Sensor Localization / Selection in Fault Diagnosis. *Proceedings of Aerospace Conference, 2007 IEEE*,

APPENDIX A

Arduino code for data acquisition and transmission

et al

```
#include <XBee.h>
#define ARRAYSIZE 1024



int encrypt(String text, int keyln, char *key, int *ciphercode) ;
char *key = "98765abcd";
int keyln = 9;
uint32_t reqid;
char *clientid = "test01";
String timestamp = "";
String remarks = "";
int onModulePin = 2;
String str = "";
String Split_str[9];
int data_analog[64];
uint32_t addrss[65] = {0, 0x40C04FD7, 0x40C04FD2, 0x40B973D4, 0x40B973D5, 0x40C04FC3, 0x40B973DA, 0x40C04FC8, 0x40C04FD0, 0x40C04F86, 0x40C04FBF, 0x40C04FD5, 0x40C04FD6, 0x40B0E8B4, 0x40BB6EBB, 0x40C04FCF, 0x40C04FCB, 0x40C04F80, 0x40C04FD1, 0x40C04FD3, 0x40C04F7C, 0x40C04FCE, 0x40C05132, 0x40C04FC2, 0x40C04FD9, 0x40C04F73, 0x40C04F8D, 0x40B973C9, 0x40B973CD, 0x40B973CC, 0x40C04F6740C04FC4, 0x40B973D7, 0x40B973CF, 0x40C04F62, 0x40C04FCA, 0x40C04FCD, 0x40B973D8, 0x40B973D1, 0x40B973D9, 0x40B973D2, 0x40C04FC0, 0x40B973D6, 0x40B973CE, 0x40B973CA, 0x40C04FC1, 0x40C04FC9, 0x40B973D3, 0x40C04FCC, 0x40C04F75, 0x40C04FC7, 0x40B7A060, 0x40B79E60, 0x40B7A05E, 0x40B79E5C, 0x40B79B42, 0x40B79E5D, 0x40B79E59, 0x40B79E5A, 0x40B79E50, 0x40B7A034, 0x40B7A063, 0x40B79E54, 0x40B79E61, 0x40B79E55};
int No = 6;
int count = 0;


int encrypt(int textln, char *text, int keyln, char *key, int *ciphercode);
void acquire_data();
void getrequestid();
```

```
XBee xbee = XBee();
XBeeResponse response = XBeeResponse();
ZBRxResponse rx = ZBRxResponse();
ZBRxIoSampleResponse ioSample = ZBRxIoSampleResponse();
char ch;

void setup()
{
  pinMode(onModulePin, OUTPUT);
  Serial.begin(9600);
  Serial1.begin(115200);
  Serial2.begin(9600);
  Serial3.begin(9600);
  xbee.setSerial(Serial3);
  initialisegprs();
}
void loop()
{
  int textln;
  int i;
  int x = 0;
  int answer = 0;
  String output;
  int cipher[ARRAYSIZE];
  String tempstr;

  for (int p = 1; p <= 64; p++)
  {
    data_analog[p] = 0;
    if (p <= 8)
      Split_str[p] = "";
  }

  //Time data : Start
  String str = "";
  while (Serial2.available())
    Serial.write("Cleaning input buffer");
  Serial2.write(No);
  Serial.println(No);
  delay(250);
  if (Serial2.available())
  {
    while (Serial2.available())
    {
      ch = Serial2.read();
      if (ch == '\n');
```

```
      else
        str = str + ch;
    }
  }
  //Time data : End

  acquire_data();//Get xbee data into dataanalog[]
OptimalFilter()
  //Splits XBee data into 8 parts and stores in 8 strings :Start
  for (int p = 1; p <= 64; p++)
  {

    if (p <= 8)
      Split_str[1] = Split_str[1] + data_analog[p] + ",";
    else if (p <= 16)
      Split_str[2] = Split_str[2] + data_analog[p] + ",";
    else if (p <= 24)
      Split_str[3] = Split_str[3] + data_analog[p] + ",";
    else if (p <= 32)
      Split_str[4] = Split_str[4] + data_analog[p] + ",";
    else if (p <= 40)
      Split_str[5] = Split_str[5] + data_analog[p] + ",";
    else if (p <= 48)
      Split_str[6] = Split_str[6] + data_analog[p] + ",";
    else if (p <= 56)
      Split_str[7] = Split_str[7] + data_analog[p] + ",";
    else if (p <= 64)
      Split_str[8] = Split_str[8] + data_analog[p] + ",";

  }
  //Splits XBee data into 8 parts and stores in 8 strings :End

  //tempstr = Split_str [7];

  for (int p = 1; p <= 8; p++)
  {
    reqid++;
    remarks = "";
    remarks = remarks + reqid;
    remarks = remarks + ",";
    remarks = remarks + p;

    String text = "#test01#" + str;
    text = reqid + text;
    text = text + "#";
    //if (p == 7)
```

```
  //text = text + tempstr;
  //else
  text = text + Split_str[p];
  text = text + "#";
  text = text + remarks;
  textln = text.length();

Serial.println("______________________________________________________________________________________________________________________________________________");
  Serial.println(str);
  Serial.println(remarks);
  Serial.println(text);

  encrypt(text, keyln, key, cipher);

  output = "data=";
  for (i = 0; i < textln; i ++)// Print the entire encrypted data into a string separated by space
  {
    output = output + cipher[i] + ",";
  }
  output = "http://sensors.bennyraphael.in/cgi-bin/update.cgi?" + output; //Adding the URL to string
  output = "AT+HTTPPARA=\"URL\",\"" + output;
  output = output + "\"";
  answer = sendATcommand2("AT+HTTPINIT", "OK", "ERROR", 1000);
  Serial.print("\n Answer ="); Serial.print(answer); Serial.println("\n");
  if (answer == 1)
  {
    answer = sendATcommand("AT+HTTPPARA=\"CID\",1", "OK", 5000);
    Serial.print("\n Answer ="); Serial.print(answer); Serial.println("\n");
    if (answer == 1)
    {
      while ( Serial1.available() > 0) Serial.println(Serial1.read());
      Serial.println(output);
      Serial1.println(output); Serial.println("\n");
      char response[100];
      unsigned long previous;

      memset(response, '\0', 100);    // Initialize the string
      delay(100);
      do {
        if (Serial1.available() != 0)
        {
          response[x] = Serial1.read();
          x++;
          // check if the desired answer is in the response of the module
```

```
          if (strstr(response, "OK") != NULL)
          {
            answer = 1;
          }
        }
        // Waits for the asnwer with time out
      }
      while ((answer == 0) && ((millis() - previous) < 5000));
      Serial.println(response);
      Serial.print("\n Answer ="); Serial.print(answer); Serial.println("\n");
      delay(5000);
      memset(response, '\0', 100);
      answer = sendATcommand("AT+HTTPACTION=0", "+HTTPACTION:0,200", 5000);
      Serial.print("\n Answer ="); Serial.print(answer);
      answer = 0;
      while (answer == 0)
      {
        answer = sendATcommand("AT+HTTPTERM", "OK", 5000);
        Serial.print("\n Answer ="); Serial.print(answer);
        Serial.println("\n");
        count++;
        if (count > 20)
        {
          initialisegprs();
          goto end_pgm;
        }
      }


    }
  }
end_pgm:
  text = "";
  remarks = "";
  count = 0;
 }


}
int encrypt(String text, int keyln, char * key, int * ciphercode)
{

 int textln;
 int i ;
 int ind1 ;
 int prev ;
```

```
  int val2 ;
  int ch1 ;
  int ch2 ;

  textln = text.length();

  prev = 0;
  for (i = 0; i < textln; i++) {
    ch1 = text.charAt(i);
    ind1 = i % keyln;
    ch2 = key[ind1];
    val2 = prev % 16;
    ciphercode[i] = i + ch1 + ch2 + val2;
    prev = (prev + ch1) % 1024;
  }
  return 1;
}

void initialisegprs()
{
  Serial.println("Initialising the GSM Module");
  power_on();
  //delay(3000);
  while (sendATcommand2("AT+CREG?", "+CREG: 1,1", "+CREG: 1,5", 2000) == 0 );
  //delay(2000);
  sendATcommand("AT+SAPBR=3,1,\"CONTYPE\",\"GPRS\"", "OK", 2000);
  sendATcommand("AT+SAPBR=3,1,\"APN\",\"bsnlnet\"", "OK", 2000);
  while ( sendATcommand("AT+SAPBR=1,1", "OK", 3000) == 0);
  sendATcommand("AT+SAPBR=2,1", "OK", 2000);
  getrequestid();


}
void power_on()
{

  uint8_t answer = 0;

  // checks if the module is started
  answer = sendATcommand("AT", "OK", 2000);
  Serial.println("AT");
  if (answer == 0)
  {
    // power on pulse
    digitalWrite(onModulePin, HIGH);
    delay(3000);
```

```
    digitalWrite(onModulePin, LOW);

    // waits for an answer from the module
    while (answer == 0) {
      // Send AT every two seconds and wait for the answer
      answer = sendATcommand("AT", "OK", 2000);
      Serial.println("AT");
      Serial.println(answer);
    }
  }
}
int8_t sendATcommand(char * ATcommand, char * expected_answer1, unsigned int timeout)
{


  uint8_t x = 0,  answer = 0;
  char responsea[100];
  unsigned long previous;
  memset(responsea, '\0', 100);    // Initialize the string
  delay(100);
  while ( Serial1.available() > 0) Serial1.read();   // Clean the input buffer
  Serial1.println(ATcommand);    // Send the AT command
  x = 0;
  previous = millis();
  // this loop waits for the answer
  do {
    if (Serial1.available() != 0)
    {

      responsea[x] = Serial1.read();
      x++;
      // check if the desired answer is in the response of the module
      if (strstr(responsea, expected_answer1) != NULL)
      {
        answer = 1;
      }
    }
    // Waits for the asnwer with time out
  }
  while ((answer == 0) && ((millis() - previous) < timeout));
  Serial.println(responsea);
  //Serial.println("Flow of control :Left sendATcommand");
  return answer;
}
int8_t sendATcommand2(char * ATcommand, char * expected_answer1, char * expected_answer2, unsigned int timeout)
```

```
{
  //Serial.println("Flow of control :Entered sendATcommand2");
  uint8_t x = 0,  answer = 0;
  char responseb[100];
  unsigned long previous;

  memset(responseb, '\0', 100);    // Initialize the string

  delay(100);

  while ( Serial1.available() > 0) Serial1.read();   // Clean the input buffer

  Serial1.println(ATcommand);    // Send the AT command


  x = 0;
  previous = millis();

  // this loop waits for the answer
  do {
    if (Serial1.available() != 0) {
      responseb[x] = Serial1.read();
      x++;
      // check if the desired answer is in the response of the module
      if (strstr(responseb, expected_answer1) != NULL)
      {
        answer = 1;
      }
      if (strstr(responseb, expected_answer2) != NULL)
      {
        answer = 2;
      }
    }
    // Waits for the asnwer with time out
  }
  while ((answer == 0) && ((millis() - previous) < timeout));
  Serial.println(responseb);
  //  Serial.println("Flow of control :Left sendATcommand 2");
  return answer;
}
void getrequestid()
{
  int i = 0;
  int answer = 0;
  char data[512];
  int data_size;
```

```
  char aux_str[100];
  char aux;
  String instring = "";
  int x = 0;
  answer = sendATcommand2("AT+HTTPINIT", "OK", "ERROR", 1000);
  Serial.print("\n Answer ="); Serial.print(answer); Serial.println("\n");
  if (answer == 1)
  {
   answer = sendATcommand("AT+HTTPPARA=\"CID\",1", "OK", 5000);
   Serial.print("\n Answer ="); Serial.print(answer); Serial.println("\n");
   if (answer == 1)
   {
    while ( Serial1.available() > 0) Serial.println(Serial1.read());
    Serial.println("AT+HTTPPARA=\"URL\",\"http://sensors.bennyraphael.in/cgi-
bin/getsession.cgi?client=test01\"");
    Serial1.println("AT+HTTPPARA=\"URL\",\"http://sensors.bennyraphael.in/cgi-
bin/getsession.cgi?client=test01\""); Serial.println("\n");
    char response[100];
    unsigned long previous;

    memset(response, '\0', 100);    // Initialize the string
    delay(100);
    do {
     if (Serial1.available() != 0)
     {
      response[x] = Serial1.read();
      x++;
      // check if the desired answer is in the response of the module
      if (strstr(response, "OK") != NULL)
      {
       answer = 1;
      }
     }
     // Waits for the asnwer with time out
    }
    while ((answer == 0) && ((millis() - previous) < 5000));
    Serial.println(response);
    Serial.print("\n Answer ="); Serial.print(answer); Serial.println("\n");
    delay(5000);
    memset(response, '\0', 100);
    answer = sendATcommand("AT+HTTPACTION=0", "+HTTPACTION:0,200", 5000);
    Serial.print("\n Answer ="); Serial.print(answer);
    if (answer == 1)
    {
     x = 0;
     do {
```

```
  sprintf(aux_str, "AT+HTTPREAD=%d,100", x);
  if (sendATcommand2(aux_str, "+HTTPREAD:", "ERROR", 30000) == 1)
  {
    data_size = 0;
    while (Serial1.available() == 0);
    aux = Serial1.read();
    do {
      data_size *= 10;
      data_size += (aux - 0x30);
      while (Serial1.available() == 0);
      aux = Serial1.read();
    } while (aux != 0x0D);

    Serial.print("Data received: ");
    Serial.println(data_size);

    if (data_size > 0)
    {
      while (Serial1.available() < data_size);
      Serial1.read();

      for (int y = 0; y < data_size; y++)
      {
        data[x] = Serial1.read();
        x++;
      }
      data[x] = '\0';
    }
    else
    {
      Serial.println("Download finished");
    }
  }
  else if (answer == 2)
  {
    Serial.println("Error from HTTP");
  }
  else
  {
    Serial.println("Error getting the url");
    data_size = 0;
  }

  sendATcommand("", "+HTTPACTION:0,200", 20000);
} while (data_size > 0);
```

```
        Serial.print("Data received: ");
        i = 0;
        while (data[i] != '\0')
        {
          Serial.print(data[i]);
          i++;
        }
      }
      else
      {
        //Serial.println("Error getting the url");
      }

      answer = 0;
      while (answer == 0)
      {
        answer = sendATcommand("AT+HTTPTERM", "OK", 5000);
        Serial.print("\n Answer ="); Serial.print(answer);
        Serial.println("\n");
        count++;

      }

    }
  }
  i = 0;
  Serial.print("\n");
  //while (data[i] != '\0')
  // Serial.print(data[i]);
  Serial.println();
  i = 7;
  while (data[i] != '\0')
  {
    if (isDigit(data[i]))
      instring = instring + data[i];
    i++;
  }
  Serial.println(instring);
  reqid = instring.toInt();
}


//Handles XBEE communication
void acquire_data()
{
  Serial.println("Flow of control :Entered Acquiredata");
```

```
  int xtimeout = 5000;
  int start = millis();
  do
  {
    // delay(5000);
    xbee.readPacket();
    if (xbee.getResponse().isAvailable()) //Check whether there is an xbee response
    {
      if (xbee.getResponse().getApiId() == ZB_IO_SAMPLE_RESPONSE) //Check whether
response is an IO sample
      {
        xbee.getResponse().getZBRxIoSampleResponse(ioSample);
        uint32_t deviceID = senderLongAddress.getLsb();//Getting the 16 bit address of the
transmitting module
        Serial.print("\nDevice ID:"); Serial.println(deviceID);
        int flag = 0;
        for (int p = 1; p <= 64; p++)
        {
          if (deviceID == addrss[p]) //Mapping the address to the correct module
          {
            flag = 1;
            if (ioSample.containsAnalog())
            {
              data_analog[p] = ioSample.getAnalog(1);
              Serial.println("Recieved from:ED");
              Serial.print(p); Serial.print("\n");
            }
            else
              Serial.println("Error: No analog data");
          }
        }
        if (flag == 0)
          Serial.println("Error: Device not recognised/found");
      }
      else
        Serial.println("Error: Not an IO response");
    }
    //else
    //Serial.println("No XBee response");
  } while ((millis() - start) <= xtimeout);
  Serial.println("Flow of control :Left Acquiredata");
}
```

APPENDIX B

Shannon's Entropy Computation

This section shows the computation of Shannon's entropy through an illustrative example and also through a case from launching girder monitoring. A methodology for sensor placement is shown in Figure B.1.

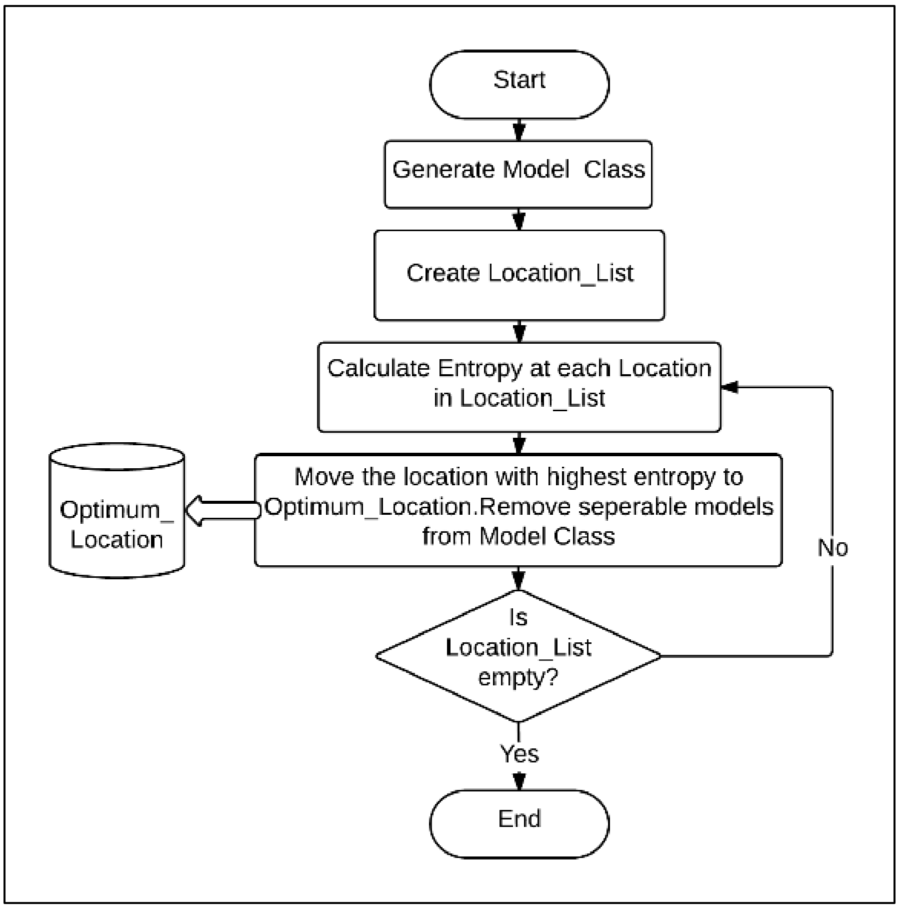

Figure B.1 Methodology for Systematic Sensor Placement

The steps in the methodology are described below.

1. Create a list Sub_Models to store the subsets of models that cannot be separated by the current sensor configuration. For the first iteration, this set would contain one element that is Initial_Modelset

2. Create a set Optimum_Location to store the optimum sensor locations. At the start, the set is empty.
3. Repeat Steps 6-7 for each subset in the list Sub_Models
4. Create a classification for each location in Location_list by grouping the model predictions into intervals. The bounds of intervals are computed such that the width of the interval is equal to the sensor precision plus modelling uncertainty. The probability of an interval is the number of model predictions in the interval divided by the total number of model instances in the model subset.
5. Calculate the Shannon's entropy for each location.
6. Find the location corresponding to the maximum entropy among all the locations and model subsets. Add the selected location to the set Optimum_Location and remove it from the set Location_list. Divide each model subset into children subsets corresponding to the intervals of the selected sensor location. Each element of Sub_Models is replaced by the children after removing children subsets that contain only one model instance.
7. Repeat steps 5 to 7 until the list Location_list is empty.

B.1 Illustrative Example

Brezta motor company has 8 cars in its lineup. Automated painting system in their company requires to identify the car automatically based on length for self-configuration. The system can measure either length of the car or height of the car to identify the car as shown in Figure B.2. In other words there are two positions in which sensor can be mounted either in direction B or in direction A.

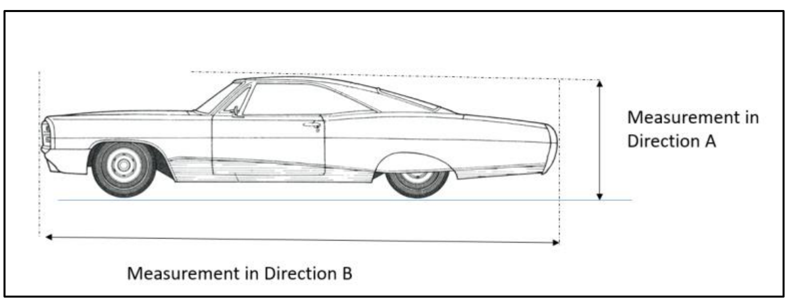

Figure B.2: Measurement directions

Hence we have 2 locations in the Location_List. i.e

- Sensor orientation 1: To measure length in direction A

- Sensor orientation 2: To measure length in direction B.

8 cars in the Brezta company's lineup would constitute to the set Sub_Models. Therefore Sub_ Models consist of Car1, Car 2, car 3, Car 4, Car 5, Car 6, Car 7, Car 8.

The precision of the sensor in 20mm. Hence, the sensors would have intervals of 20mm as precision. Therefore we can classify model prediction (car models) into each interval of the measurement as shown in Table B.1.

Table B.1 Classification of car models into intervals of measurement

Interval(mm)		Sensor Orientation 1	Interval(mm)		Sensor Orientation 2
Min	Max		Min	Max	
1500	1520	Car 1, Car 2 , Car 3	3800	3820	Car 1
1520	1540	Car 4, Car 5 , Car 6, Car 7	3820	3840	Car2
1550	1560	Nil	3840	3860	Car 3 , Car 4
1570	1580	Nil	3860	3880	Car 5
1590	1600	Car 8	3880	3900	Car 6
1610	1620	Nil	3900	3920	Car 7, Car 8

Calculating the probability of occurrence of a car in each interval is shown in Table B.2.

Table B.2: Probability of identifying a car in a measurement interval

Sensor Orientation 1			Sensor Orientation 2		
Interval(mm)		Probability of finding a car in the interval	Interval(mm)		Probability of finding a car in the interval
Min	Max		Min	Max	
1500	1520	0.375	3800	3820	0.125
1520	1540	0.500	3820	3840	0.125
1550	1560	0.000	3840	3860	0.25
1570	1580	0.000	3860	3880	0.125
1590	1600	0.125	3880	3900	0.125
1610	1620	0.000	3900	3920	0.25

Now we have the data to calculate Shannons entropy. Entropy H(x) of a variable x is calculated using the following equation.

$$H(x) = -\sum_{i=0}^{n} p(x_i)\, log_2 p(x_i)$$

Where $p(x_i)$ is the probability of the occurrence of an event $x_i$in the observation distribution. The following steps describe the procedure for evaluating the Shannon's entropy to determine the optimal sensor location. Table B.3 shows the $-p(x_i)log_2 p(x_i)$ for each interval. Sum of $-p(x_i)log_2 p(x_i)$ is the Shannon's Entropy.

Table B.3: Shannon's Entropy Computation

<table>
<tr><td rowspan="9">Shannon's Entropy</td><td colspan="3">Sensor Orientation 1</td><td colspan="3">Sensor Orientation 2</td></tr>
<tr><td colspan="2">Interval(mm)</td><td rowspan="2">-p(x)logp(x)</td><td colspan="2">Interval(mm)</td><td rowspan="2">-p(x)logp(x)</td></tr>
<tr><td>Min</td><td>Max</td><td>Min</td><td>Max</td></tr>
<tr><td>1500</td><td>1520</td><td>0.530639062</td><td>3800</td><td>3820</td><td>0.375</td></tr>
<tr><td>1520</td><td>1540</td><td>0.5</td><td>3820</td><td>3840</td><td>0.375</td></tr>
<tr><td>1550</td><td>1560</td><td>NA</td><td>3840</td><td>3860</td><td>0.5</td></tr>
<tr><td>1570</td><td>1580</td><td>NA</td><td>3860</td><td>3880</td><td>0.375</td></tr>
<tr><td>1590</td><td>1600</td><td>0.375</td><td>3880</td><td>3900</td><td>0.375</td></tr>
<tr><td>1610</td><td>1620</td><td>NA</td><td>3900</td><td>3920</td><td>0.5</td></tr>
<tr><td>$-\sum_{i=0}^{n} p(x_i)\, log_2 p(x_i)$</td><td colspan="3">1.405639062</td><td colspan="3">2.5</td></tr>
</table>

Sensor Orientation 2 has a higher entropy. Hence the sensor should be aligned in orientation 2 to classify more number of cars. This illustration demonstrates how shannon's entropy can be used to quantify information content from data. The data size is small for this example, hence we can identify the best sensor orientation as sensor orientation 2without using any metric. However, it would be difficult to identify the best sensor location when the data size is higher. Shannon's entropy is an ideal metric in these situations to identify the best sensor location

B.2 Shannon's Entropy Sample Calculation for Launching Girder Data

Table B.4 shows the strain data at 18 locations for the 33 base cases. The precision of the sensor used is 2.75E-5 micro strains. Therefore the set ModelClass has 33 cases as its contents. There are 18 contents in the location list.

Table B.4 : Strain data at 18 location for 33 base cases

Location		1	2	3	4	5	6	7	8	9	10	11	12	13	14	15	16	17	18
Cases	1	1.37E-06	1.69E-05	2.98E-05	5.30E-05	5.48E-05	5.37E-05	5.04E-05	4.67E-05	3.68E-05	2.06E-05	1.06E-06	2.00E-05	0.0001307	0.0003308	0.0003316	0.0003799	0.000253	0.000114
	2	4.91E-07	7.95E-06	1.81E-05	6.75E-05	0.000109	0.000125	0.0001501	0.0001699	0.0002101	0.0002611	0.0003123	0.0003618	0.0004035	0.0004505	0.0004507	0.0003799	0.000253	0.000114
	3	2.71E-06	3.46E-05	6.40E-05	0.000137	6.58E-05	3.91E-05	2.38E-06	3.36E-05	9.54E-05	0.0001712	0.0002451	0.0003148	0.0003726	0.000437	0.0004373	0.0003799	0.000253	0.000114
	4	3.43E-06	4.42E-05	8.24E-05	0.000183	4.99E-05	1.79E-06	7.17E-05	0.0001261	0.0002316	0.0003573	0.000477	0.0005875	0.0005953	0.0005348	0.0005345	0.0003799	0.000253	0.000114
	5	1.39E-05	0.000183	0.000198	3.07E-05	7.43E-05	0.000113	0.0001715	0.0002152	0.0003008	0.0004036	0.0005023	0.0005941	0.0005952	0.0005347	0.0005345	0.0003799	0.000253	0.000114
	6	8.66E-09	1.53E-06	2.39E-05	0.000135	0.000209	0.000237	0.0002797	0.000312	0.0003758	0.0004538	0.0005298	0.0006013	0.0005952	0.0005347	0.0005344	0.0003799	0.000253	0.000114
	7	8.66E-09	1.53E-06	5.71E-06	3.66E-05	6.76E-05	8.02E-05	0.0001006	0.0001166	0.0001497	0.0001925	0.0002364	0.0002792	0.0003156	0.000357	0.0003572	0.0003799	0.000253	0.000114
	8	8.66E-09	1.53E-06	5.71E-06	3.66E-05	4.65E-05	4.93E-05	5.51E-05	6.06E-05	7.39E-05	9.39E-05	0.000117	0.0001412	0.0001629	0.0001884	0.0001885	0.0002714	0.000253	0.000114
	9	8.66E-09	1.53E-06	5.71E-06	3.66E-05	6.75E-05	8.01E-05	7.56E-05	7.05E-05	6.36E-05	6.07E-05	6.28E-05	6.82E-05	7.49E-05	8.44E-05	8.44E-05	0.0001231	0.000175	0.000114
	10	8.66E-09	1.53E-06	5.71E-06	3.66E-05	6.75E-05	8.01E-05	0.0001004	0.0001164	0.0001216	9.85E-05	8.22E-05	7.10E-05	6.45E-05	5.99E-05	5.98E-05	5.95E-05	7.57E-05	0.000114
	11	8.66E-09	1.53E-06	5.71E-06	3.66E-05	6.75E-05	8.01E-05	0.0001004	0.0001164	0.0001349	0.0001093	9.06E-05	7.74E-05	6.93E-05	6.29E-05	6.29E-05	5.77E-05	6.94E-05	0.000114
	12	8.66E-09	1.53E-06	5.71E-06	3.66E-05	6.75E-05	8.01E-05	0.0001004	0.0001164	0.0002204	0.0005952	0.0007305	0.0006539	0.0005953	0.0005348	0.0005345	0.00038	0.000253	0.000114
	13	8.66E-09	1.53E-06	5.71E-06	3.66E-05	6.75E-05	8.01E-05	0.0001005	0.0001164	0.0001495	0.0001923	0.0004272	0.0006538	0.0005952	0.0005347	0.0005344	0.0003799	0.000253	0.000114
	14	8.66E-09	1.53E-06	5.71E-06	3.66E-05	6.75E-05	8.01E-05	0.0001005	0.0001164	0.0001495	0.0001923	0.0002362	0.0003063	0.0004081	0.0005197	0.0005202	0.0003799	0.000253	0.000114
	15	8.66E-09	1.53E-06	5.71E-06	3.66E-05	6.75E-05	8.01E-05	0.0001005	0.0001165	0.0001495	0.0001923	0.0002362	0.000279	0.0003533	0.0004431	0.0004435	0.0003799	0.000253	0.000114
	16	1.47E-06	1.82E-05	3.23E-05	5.84E-05	5.83E-05	5.65E-05	5.22E-05	4.78E-05	3.65E-05	1.88E-05	2.23E-06	2.45E-05	0.0001804	0.0003777	0.0003786	0.0003799	0.000253	0.000114
	17	1.90E-06	2.39E-05	4.15E-05	6.63E-05	6.24E-05	5.91E-05	5.26E-05	4.66E-05	3.23E-05	1.11E-05	1.30E-05	3.81E-05	0.0001636	0.0003216	0.0003223	0.0003209	0.000219	0.000108
	18	1.90E-06	2.39E-05	4.15E-05	6.63E-05	6.24E-05	5.91E-05	5.26E-05	4.66E-05	3.23E-05	1.11E-05	1.30E-05	3.81E-05	0.0001636	0.0003216	0.0003223	0.0003209	0.000219	0.000108
	19	1.90E-06	2.39E-05	4.15E-05	6.63E-05	6.24E-05	5.91E-05	5.26E-05	4.66E-05	3.23E-05	1.11E-05	1.30E-05	3.81E-05	0.0001636	0.0003216	0.0003223	0.0003209	0.000219	0.000108

	20	1.88E-06	2.36E-05	4.09E-05	6.48E-05	6.15E-05	5.85E-05	5.25E-05	4.68E-05	3.33E-05	1.28E-05	1.06E-05	4.07E-05	0.0001662	0.0003226	0.0003233	0.0003209	0.000219	0.000108
	21	1.87E-06	2.35E-05	4.08E-05	6.46E-05	6.26E-05	6.01E-05	5.48E-05	4.96E-05	3.70E-05	1.77E-05	9.93E-06	5.06E-05	0.0001739	0.0003255	0.0003262	0.0003209	0.000219	0.000108
	22	1.90E-06	2.38E-05	4.15E-05	6.65E-05	6.64E-05	6.46E-05	6.02E-05	5.58E-05	4.46E-05	2.43E-05	1.48E-05	6.58E-05	0.000185	0.0003297	0.0003303	0.0003209	0.000219	0.000108
	23	1.96E-06	2.47E-05	4.32E-05	7.15E-05	7.42E-05	7.34E-05	7.05E-05	6.71E-05	5.79E-05	2.57E-05	2.42E-05	8.48E-05	0.0001986	0.0003349	0.0003355	0.0003209	0.000219	0.000108
	24	2.08E-06	2.62E-05	4.60E-05	7.99E-05	8.64E-05	8.69E-05	8.59E-05	8.39E-05	6.72E-05	2.39E-05	3.61E-05	0.0001059	0.0002135	0.0003405	0.0003411	0.0003209	0.000219	0.000108
	25	2.24E-06	2.84E-05	5.03E-05	9.21E-05	0.000104	0.000106	0.0001054	9.87E-05	7.31E-05	1.97E-05	4.96E-05	0.0001277	0.0002289	0.0003464	0.0003469	0.0003209	0.000219	0.000108
	26	2.47E-06	3.14E-05	5.61E-05	0.000108	0.000126	0.000127	0.0001212	0.0001103	7.66E-05	1.40E-05	6.37E-05	0.0001492	0.0002441	0.0003521	0.0003526	0.0003209	0.000219	0.000108
	27	2.75E-06	3.52E-05	6.34E-05	0.000129	0.000147	0.000145	0.0001338	0.0001192	7.84E-05	7.68E-06	7.74E-05	0.0001697	0.0002584	0.0003575	0.0003579	0.0003209	0.000219	0.000108
	28	3.11E-06	0.00004	7.26E-05	0.000155	0.000164	0.000159	0.0001436	0.0001257	7.89E-05	1.29E-06	9.01E-05	0.000188	0.0002712	0.0003624	0.0003627	0.0003209	0.000219	0.000108
	29	3.53E-06	4.56E-05	8.37E-05	0.000176	0.000179	0.000171	0.0001513	0.0001308	7.88E-05	4.69E-06	0.0001015	0.0002042	0.0002825	0.0003666	0.000367	0.0003209	0.000219	0.000108
	30	4.03E-06	5.22E-05	9.72E-05	0.000192	0.000189	0.000179	0.0001569	0.0001342	7.83E-05	9.72E-06	0.0001107	0.000217	0.0002915	0.00037	0.0003704	0.0003209	0.000219	0.000108
	31	4.63E-06	6.02E-05	0.000113	0.000202	0.000195	0.000184	0.0001601	0.0001362	7.78E-05	1.31E-05	0.0001166	0.0002253	0.0002972	0.0003722	0.0003725	0.0003209	0.000219	0.000108
	32	4.63E-06	6.02E-05	0.000113	0.000202	0.000195	0.000184	0.0001601	0.0001362	7.78E-05	1.31E-05	0.0001166	0.0002253	0.0002972	0.0003722	0.0003725	0.0003209	0.000219	0.000108
	33	4.63E-06	6.02E-05	0.000113	0.000202	0.000195	0.000184	0.0001601	0.0001362	7.78E-05	1.31E-05	0.0001166	0.0002253	0.0002972	0.0003722	0.0003725	0.0003209	0.000219	0.000108

As the precision of the sensor is 2.75e-5 , we divide the range into intervals of 2.75e-5. Table B.5 shows the frequency of occurrence of model instances in each interval at a location.

Table B.5: Frequency of occurrence of model instances at intervals

Interval		Location																	
Lower	Upper	1	2	3	4	5	6	7	8	9	10	11	12	13	14	15	16	17	18
0	2.75E-05	33	21	11	0	0	1	1	0	0	19	9	2	0	0	0	0	0	0
2.75E-05	5.50E-05	0	8	11	11	3	3	7	8	8	0	2	5	0	0	0	0	0	0
5.50E-05	8.25E-05	0	3	5	10	18	16	5	4	13	1	4	4	3	2	2	2	2	0
8.25E-05	1.10E-04	0	0	2	2	3	2	9	2	1	3	3	2	0	1	1	0	0	17
1.10E-04	1.38E-04	0	0	3	3	1	3	2	16	2	0	5	1	1	0	0	1	0	16

1.38E-04	1.65E-04	0	0	0	1	2	2	7	0	4	0	0	2	4	0	0	0	0	0
1.65E-04	1.93E-04	0	1	0	3	2	5	1	1	0	4	0	2	4	1	1	0	1	0
1.93E-04	2.20E-04	0	0	1	3	4	0	0	1	1	1	0	2	2	0	0	0	17	0
2.20E-04	2.48E-04	0	0	0	0	0	1	0	0	2	0	4	3	2	0	0	0	0	0
2.48E-04	2.75E-04	0	0	0	0	0	0	0	0	0	1	0	0	2	0	0	1	13	0
2.75E-04	3.03E-04	0	0	0	0	0	0	1	0	1	0	0	2	5	0	0	0	0	0
3.03E-04	3.30E-04	0	0	0	0	0	0	0	1	0	0	1	2	1	6	5	17	0	0
3.30E-04	3.58E-04	0	0	0	0	0	0	0	0	0	1	0	0	1	7	7	0	0	0
3.58E-04	3.85E-04	0	0	0	0	0	0	0	0	1	0	0	1	1	7	8	12	0	0
3.85E-04	4.13E-04	0	0	0	0	0	0	0	0	0	1	0	0	2	0	0	0	0	0
4.13E-04	4.40E-04	0	0	0	0	0	0	0	0	0	0	1	0	0	1	1	0	0	0
4.40E-04	4.68E-04	0	0	0	0	0	0	0	0	0	1	0	0	0	2	2	0	0	0
4.68E-04	4.95E-04	0	0	0	0	0	0	0	0	0	0	1	0	0	0	0	0	0	0
4.95E-04	5.23E-04	0	0	0	0	0	0	0	0	0	0	1	0	0	1	1	0	0	0
5.23E-04	5.50E-04	0	0	0	0	0	0	0	0	0	0	1	0	0	5	5	0	0	0
5.50E-04	5.78E-04	0	0	0	0	0	0	0	0	0	0	0	0	0	0	0	0	0	0
5.78E-04	6.05E-04	0	0	0	0	0	0	0	0	0	1	0	3	5	0	0	0	0	0
6.05E-04	6.33E-04	0	0	0	0	0	0	0	0	0	0	0	0	0	0	0	0	0	0
6.33E-04	6.60E-04	0	0	0	0	0	0	0	0	0	0	0	2	0	0	0	0	0	0
6.60E-04	6.88E-04	0	0	0	0	0	0	0	0	0	0	0	0	0	0	0	0	0	0
6.88E-04	7.15E-04	0	0	0	0	0	0	0	0	0	0	0	0	0	0	0	0	0	0
7.15E-04	7.43E-04	0	0	0	0	0	0	0	0	0	0	1	0	0	0	0	0	0	0
7.43E-04	7.70E-04	0	0	0	0	0	0	0	0	0	0	0	0	0	0	0	0	0	0
7.70E-04	7.98E-04	0	0	0	0	0	0	0	0	0	0	0	0	0	0	0	0	0	0
7.98E-04	8.25E-04	0	0	0	0	0	0	0	0	0	0	0	0	0	0	0	0	0	0

Probability of occurrence of model instances in each interval at different locations are given in Table B.6

Table B.6: Probability of occurrence of modal instances in each interval at a location

Interval		Location																	
Lower	Upper	1	2	3	4	5	6	7	8	9	10	11	12	13	14	15	16	17	18
0.0E+00	2.8E-05	1.00	0.64	0.33	0.00	0.00	0.03	0.03	0.00	0.00	0.58	0.27	0.06	0.00	0.00	0.00	0.00	0.00	0.00
2.8E-05	5.5E-05	0.00	0.24	0.33	0.33	0.09	0.09	0.21	0.24	0.24	0.00	0.06	0.15	0.00	0.00	0.00	0.00	0.00	0.00
5.5E-05	8.3E-05	0.00	0.09	0.15	0.30	0.55	0.48	0.15	0.12	0.39	0.03	0.12	0.12	0.09	0.06	0.06	0.06	0.06	0.00
8.3E-05	1.1E-04	0.00	0.00	0.06	0.06	0.09	0.06	0.27	0.06	0.03	0.09	0.09	0.06	0.00	0.03	0.03	0.00	0.00	0.52
1.1E-04	1.4E-04	0.00	0.00	0.09	0.09	0.03	0.09	0.06	0.48	0.06	0.00	0.15	0.03	0.03	0.00	0.00	0.03	0.00	0.48
1.4E-04	1.7E-04	0.00	0.00	0.00	0.03	0.06	0.06	0.21	0.00	0.12	0.00	0.00	0.06	0.12	0.00	0.00	0.00	0.00	0.00
1.7E-04	1.9E-04	0.00	0.03	0.00	0.09	0.06	0.15	0.03	0.03	0.00	0.12	0.00	0.06	0.12	0.03	0.03	0.00	0.03	0.00
1.9E-04	2.2E-04	0.00	0.00	0.03	0.09	0.12	0.00	0.00	0.03	0.03	0.03	0.00	0.06	0.06	0.00	0.00	0.00	0.52	0.00
2.2E-04	2.5E-04	0.00	0.00	0.00	0.00	0.00	0.03	0.00	0.00	0.06	0.00	0.12	0.09	0.06	0.00	0.00	0.00	0.00	0.00
2.5E-04	2.8E-04	0.00	0.00	0.00	0.00	0.00	0.00	0.00	0.00	0.00	0.03	0.00	0.00	0.06	0.00	0.00	0.03	0.39	0.00
2.8E-04	3.0E-04	0.00	0.00	0.00	0.00	0.00	0.00	0.03	0.00	0.03	0.00	0.00	0.06	0.15	0.00	0.00	0.00	0.00	0.00
3.0E-04	3.3E-04	0.00	0.00	0.00	0.00	0.00	0.00	0.00	0.03	0.00	0.00	0.03	0.06	0.03	0.18	0.15	0.52	0.00	0.00
3.3E-04	3.6E-04	0.00	0.00	0.00	0.00	0.00	0.00	0.00	0.00	0.00	0.03	0.00	0.00	0.03	0.21	0.21	0.00	0.00	0.00
3.6E-04	3.9E-04	0.00	0.00	0.00	0.00	0.00	0.00	0.00	0.00	0.03	0.00	0.00	0.03	0.03	0.21	0.24	0.36	0.00	0.00
3.9E-04	4.1E-04	0.00	0.00	0.00	0.00	0.00	0.00	0.00	0.00	0.00	0.03	0.00	0.00	0.06	0.00	0.00	0.00	0.00	0.00
4.1E-04	4.4E-04	0.00	0.00	0.00	0.00	0.00	0.00	0.00	0.00	0.00	0.00	0.03	0.00	0.00	0.03	0.03	0.00	0.00	0.00
4.4E-04	4.7E-04	0.00	0.00	0.00	0.00	0.00	0.00	0.00	0.00	0.00	0.03	0.00	0.00	0.00	0.06	0.06	0.00	0.00	0.00
4.7E-04	5.0E-04	0.00	0.00	0.00	0.00	0.00	0.00	0.00	0.00	0.00	0.00	0.03	0.00	0.00	0.00	0.00	0.00	0.00	0.00
5.0E-04	5.2E-04	0.00	0.00	0.00	0.00	0.00	0.00	0.00	0.00	0.00	0.00	0.03	0.00	0.00	0.03	0.03	0.00	0.00	0.00
5.2E-04	5.5E-04	0.00	0.00	0.00	0.00	0.00	0.00	0.00	0.00	0.00	0.00	0.03	0.00	0.00	0.15	0.15	0.00	0.00	0.00
5.5E-04	5.8E-04	0.00	0.00	0.00	0.00	0.00	0.00	0.00	0.00	0.00	0.00	0.00	0.00	0.00	0.00	0.00	0.00	0.00	0.00
5.8E-04	6.1E-04	0.00	0.00	0.00	0.00	0.00	0.00	0.00	0.00	0.00	0.03	0.00	0.09	0.15	0.00	0.00	0.00	0.00	0.00
6.1E-04	6.3E-04	0.00	0.00	0.00	0.00	0.00	0.00	0.00	0.00	0.00	0.00	0.00	0.00	0.00	0.00	0.00	0.00	0.00	0.00
6.3E-04	6.6E-04	0.00	0.00	0.00	0.00	0.00	0.00	0.00	0.00	0.00	0.00	0.00	0.06	0.00	0.00	0.00	0.00	0.00	0.00
6.6E-04	6.9E-04	0.00	0.00	0.00	0.00	0.00	0.00	0.00	0.00	0.00	0.00	0.00	0.00	0.00	0.00	0.00	0.00	0.00	0.00
6.9E-04	7.2E-04	0.00	0.00	0.00	0.00	0.00	0.00	0.00	0.00	0.00	0.00	0.00	0.00	0.00	0.00	0.00	0.00	0.00	0.00
7.2E-04	7.4E-04	0.00	0.00	0.00	0.00	0.00	0.00	0.00	0.00	0.00	0.00	0.03	0.00	0.00	0.00	0.00	0.00	0.00	0.00
7.4E-04	7.7E-04	0.00	0.00	0.00	0.00	0.00	0.00	0.00	0.00	0.00	0.00	0.00	0.00	0.00	0.00	0.00	0.00	0.00	0.00
7.7E-04	8.0E-04	0.00	0.00	0.00	0.00	0.00	0.00	0.00	0.00	0.00	0.00	0.00	0.00	0.00	0.00	0.00	0.00	0.00	0.00
8.0E-04	8.3E-04	0.00	0.00	0.00	0.00	0.00	0.00	0.00	0.00	0.00	0.00	0.00	0.00	0.00	0.00	0.00	0.00	0.00	0.00

To find the Shannon's entropy, p(x)log (p(x)) needs to be calculated for each interval at location. Sum of the negatives of p(x)log (p(x)) at a location gives the Shannon's entropy at that location. Table B.7 represent this data.

Table B.7 p(x)log (p(x)) values for each interval at a location

Interval		Location																	
Lower	Upper	1	2	3	4	5	6	7	8	9	10	11	12	13	14	15	16	17	18
0	2.75E-05	0.00	-0.41	-0.53	NA	NA	-0.15	-0.15	NA	NA	-0.46	-0.51	-0.25	NA	NA	NA	NA	NA	NA
2.75E-05	0.000055	NA	-0.50	-0.53	-0.53	-0.31	-0.31	-0.47	-0.50	-0.50	NA	-0.25	-0.41	NA	NA	NA	NA	NA	NA
0.000055	8.25E-05	NA	-0.31	-0.41	-0.52	-0.48	-0.51	-0.41	-0.37	-0.53	-0.15	-0.37	-0.37	-0.31	-0.25	-0.25	-0.25	-0.25	NA
8.25E-05	0.00011	NA	NA	-0.25	-0.25	-0.31	-0.25	-0.51	-0.25	-0.15	-0.31	-0.31	-0.25	NA	-0.15	-0.15	NA	NA	-0.49
0.00011	0.000138	NA	NA	-0.31	-0.31	-0.15	-0.31	-0.25	-0.51	-0.25	NA	-0.41	-0.15	-0.15	NA	NA	-0.15	NA	-0.51
0.000138	0.000165	NA	NA	NA	-0.15	-0.25	-0.25	-0.47	NA	-0.37	NA	NA	-0.25	-0.37	NA	NA	NA	NA	NA
0.000165	0.000193	NA	-0.15	NA	-0.31	-0.25	-0.41	-0.15	-0.15	NA	-0.37	NA	-0.25	-0.37	-0.15	-0.15	NA	-0.15	NA
0.000193	0.00022	NA	NA	-0.15	-0.31	-0.37	NA	NA	-0.15	-0.15	-0.15	NA	-0.25	-0.25	NA	NA	NA	-0.49	NA
0.00022	0.000248	NA	NA	NA	NA	NA	-0.15	NA	NA	-0.25	NA	-0.37	-0.31	-0.25	NA	NA	NA	NA	NA
0.000248	0.000275	NA	NA	NA	NA	NA	NA	NA	NA	NA	-0.15	NA	NA	-0.25	NA	NA	-0.15	-0.53	NA
0.000275	0.000303	NA	NA	NA	NA	NA	NA	-0.15	NA	-0.15	NA	NA	-0.25	-0.41	NA	NA	NA	NA	NA
0.000303	0.00033	NA	NA	NA	NA	NA	NA	NA	-0.15	NA	NA	-0.15	-0.25	-0.15	-0.45	-0.41	-0.49	NA	NA
0.00033	0.000358	NA	NA	NA	NA	NA	NA	NA	NA	NA	-0.15	NA	NA	-0.15	-0.47	-0.47	NA	NA	NA
0.000358	0.000385	NA	NA	NA	NA	NA	NA	NA	NA	-0.15	NA	NA	-0.15	-0.15	-0.47	-0.50	-0.53	NA	NA
0.000385	0.000413	NA	NA	NA	NA	NA	NA	NA	NA	NA	-0.15	NA	NA	-0.25	NA	NA	NA	NA	NA
0.000413	0.00044	NA	NA	NA	NA	NA	NA	NA	NA	NA	NA	-0.15	NA	NA	-0.15	-0.15	NA	NA	NA
0.00044	0.000468	NA	NA	NA	NA	NA	NA	NA	NA	NA	-0.15	NA	NA	NA	-0.25	-0.25	NA	NA	NA
0.000468	0.000495	NA	NA	NA	NA	NA	NA	NA	NA	NA	NA	-0.15	NA	NA	NA	NA	NA	NA	NA
0.000495	0.000523	NA	NA	NA	NA	NA	NA	NA	NA	NA	NA	-0.15	NA	NA	-0.15	-0.15	NA	NA	NA
0.000523	0.00055	NA	NA	NA	NA	NA	NA	NA	NA	NA	NA	-0.15	NA	NA	-0.41	-0.41	NA	NA	NA
0.00055	0.000578	NA	NA	NA	NA	NA	NA	NA	NA	NA	NA	NA	NA	NA	NA	NA	NA	NA	NA
0.000578	0.000605	NA	NA	NA	NA	NA	NA	NA	NA	NA	-0.15	NA	-0.31	-0.41	NA	NA	NA	NA	NA
0.000605	0.000633	NA	NA	NA	NA	NA	NA	NA	NA	NA	NA	NA	NA	NA	NA	NA	NA	NA	NA

0.000633	0.00066	NA	NA	NA	NA	NA	NA	NA	NA	NA	NA	NA	-0.25	NA	NA	NA	NA	NA	NA
0.00066	0.000688	NA	NA	NA	NA	NA	NA	NA	NA	NA	NA	NA	NA	NA	NA	NA	NA	NA	NA
0.000688	0.000715	NA	NA	NA	NA	NA	NA	NA	NA	NA	NA	NA	NA	NA	NA	NA	NA	NA	NA
0.000715	0.000743	NA	NA	NA	NA	NA	NA	NA	NA	NA	NA	-0.15	NA	NA	NA	NA	NA	NA	NA
0.000743	0.00077	NA	NA	NA	NA	NA	NA	NA	NA	NA	NA	NA	NA	NA	NA	NA	NA	NA	NA
0.00077	0.000798	NA	NA	NA	NA	NA	NA	NA	NA	NA	NA	NA	NA	NA	NA	NA	NA	NA	NA
0.000798	0.000825	NA	NA	NA	NA	NA	NA	NA	NA	NA	NA	NA	NA	NA	NA	NA	NA	NA	NA
Entropy		**0.00**	**1.38**	**2.18**	**2.39**	**2.12**	**2.34**	**2.58**	**2.07**	**2.50**	**2.21**	**3.14**	**3.68**	**3.47**	**2.91**	**2.90**	**1.57**	**1.42**	**1.00**

Maximum entropy is obtained at Location 12. Hence the first sensor should be placed at Location 12. Therefore, Location 12 is the first element in the set Optimum_Location. Location 12 should be removed from the set Location_List. Also, there are two model instances completely distinguished through measurement at location 12. Hence, those two model instances should be removed from the set Sub_Models. Currently, Location_list has 17 elements, Sub_Models have 31 elements and Optimum_Locations has 1 element. Therefore remove the column corresponding location 12 and the rows corresponding to Model instances 2 and 25 which is separated by location 12. The Table B.8 shows the strain data for remaining 17 location and 31 undistinguished model instances.

Table B.8 Strain data at 17 locations for 31 cases

Location		1	2	3	4	5	6	7	8	9	10	11	13	14	15	16	17	18
Cases	1	1.4E-06	1.7E-05	3.0E-05	5.3E-05	5.5E-05	5.4E-05	5.0E-05	4.7E-05	3.7E-05	2.1E-05	1.1E-06	1.3E-04	3.3E-04	3.3E-04	3.8E-04	2.5E-04	1.1E-04
	3	2.7E-06	3.5E-05	6.4E-05	1.4E-04	6.6E-05	3.9E-05	2.4E-06	3.4E-05	9.5E-05	1.7E-04	2.5E-04	3.7E-04	4.4E-04	4.4E-04	3.8E-04	2.5E-04	1.1E-04
	4	3.4E-06	4.4E-05	8.2E-05	1.8E-04	5.0E-05	1.8E-06	7.2E-05	1.3E-04	2.3E-04	3.6E-04	4.8E-04	6.0E-04	5.3E-04	5.3E-04	3.8E-04	2.5E-04	1.1E-04
	5	1.4E-05	1.8E-04	2.0E-04	3.1E-05	7.4E-05	1.1E-04	1.7E-04	2.2E-04	3.0E-04	4.0E-04	5.0E-04	6.0E-04	5.3E-04	5.3E-04	3.8E-04	2.5E-04	1.1E-04
	6	8.7E-09	1.5E-06	2.4E-05	1.3E-04	2.1E-04	2.4E-04	2.8E-04	3.1E-04	3.8E-04	4.5E-04	5.3E-04	6.0E-04	5.3E-04	5.3E-04	3.8E-04	2.5E-04	1.1E-04
	7	8.7E-09	1.5E-06	5.7E-06	3.7E-05	6.8E-05	8.0E-05	1.0E-04	1.2E-04	1.5E-04	1.9E-04	2.4E-04	3.2E-04	3.6E-04	3.6E-04	3.8E-04	2.5E-04	1.1E-04
	8	8.7E-09	1.5E-06	5.7E-06	3.7E-05	4.7E-05	4.9E-05	5.5E-05	6.1E-05	7.4E-05	9.4E-05	1.2E-04	1.6E-04	1.9E-04	1.9E-04	2.7E-04	2.5E-04	1.1E-04
	9	8.7E-09	1.5E-06	5.7E-06	3.7E-05	6.8E-05	8.0E-05	7.6E-05	7.0E-05	6.4E-05	6.1E-05	6.3E-05	7.5E-05	8.4E-05	8.4E-05	1.2E-04	1.8E-04	1.1E-04
	10	8.7E-09	1.5E-06	5.7E-06	3.7E-05	6.8E-05	8.0E-05	1.0E-04	1.2E-04	1.2E-04	9.9E-05	8.2E-05	6.5E-05	6.0E-05	6.0E-05	6.0E-05	7.6E-05	1.1E-04

	11	8.7E-09	1.5E-06	5.7E-06	3.7E-05	6.8E-05	8.0E-05	1.0E-04	1.2E-04	1.3E-04	1.1E-04	9.1E-05	6.9E-05	6.3E-05	6.3E-05	5.8E-05	6.9E-05	1.1E-04
	12	8.7E-09	1.5E-06	5.7E-06	3.7E-05	6.8E-05	8.0E-05	1.0E-04	1.2E-04	2.2E-04	6.0E-04	7.3E-04	6.0E-04	5.3E-04	5.3E-04	3.8E-04	2.5E-04	1.1E-04
	13	8.7E-09	1.5E-06	5.7E-06	3.7E-05	6.8E-05	8.0E-05	1.0E-04	1.2E-04	1.5E-04	1.9E-04	4.3E-04	6.0E-04	5.3E-04	5.3E-04	3.8E-04	2.5E-04	1.1E-04
	14	8.7E-09	1.5E-06	5.7E-06	3.7E-05	6.8E-05	8.0E-05	1.0E-04	1.2E-04	1.5E-04	1.9E-04	2.4E-04	4.1E-04	5.2E-04	5.2E-04	3.8E-04	2.5E-04	1.1E-04
	15	8.7E-09	1.5E-06	5.7E-06	3.7E-05	6.8E-05	8.0E-05	1.0E-04	1.2E-04	1.5E-04	1.9E-04	2.4E-04	3.5E-04	4.4E-04	4.4E-04	3.8E-04	2.5E-04	1.1E-04
	16	1.5E-06	1.8E-05	3.2E-05	5.8E-05	5.8E-05	5.7E-05	5.2E-05	4.8E-05	3.7E-05	1.9E-05	2.2E-06	1.8E-04	3.8E-04	3.8E-04	3.8E-04	2.5E-04	1.1E-04
	17	1.9E-06	2.4E-05	4.2E-05	6.6E-05	6.2E-05	5.9E-05	5.3E-05	4.7E-05	3.2E-05	1.1E-05	1.3E-05	1.6E-04	3.2E-04	3.2E-04	3.2E-04	2.2E-04	1.1E-04
	18	1.9E-06	2.4E-05	4.2E-05	6.6E-05	6.2E-05	5.9E-05	5.3E-05	4.7E-05	3.2E-05	1.1E-05	1.3E-05	1.6E-04	3.2E-04	3.2E-04	3.2E-04	2.2E-04	1.1E-04
	19	1.9E-06	2.4E-05	4.2E-05	6.6E-05	6.2E-05	5.9E-05	5.3E-05	4.7E-05	3.2E-05	1.1E-05	1.3E-05	1.6E-04	3.2E-04	3.2E-04	3.2E-04	2.2E-04	1.1E-04
	20	1.9E-06	2.4E-05	4.1E-05	6.5E-05	6.1E-05	5.9E-05	5.2E-05	4.7E-05	3.3E-05	1.3E-05	1.1E-05	1.7E-04	3.2E-04	3.2E-04	3.2E-04	2.2E-04	1.1E-04
	21	1.9E-06	2.4E-05	4.1E-05	6.5E-05	6.3E-05	6.0E-05	5.5E-05	5.0E-05	3.7E-05	1.8E-05	9.9E-06	1.7E-04	3.3E-04	3.3E-04	3.2E-04	2.2E-04	1.1E-04
	22	1.9E-06	2.4E-05	4.1E-05	6.6E-05	6.6E-05	6.5E-05	6.0E-05	5.6E-05	4.5E-05	2.4E-05	1.5E-05	1.8E-04	3.3E-04	3.3E-04	3.2E-04	2.2E-04	1.1E-04
	23	2.0E-06	2.5E-05	4.3E-05	7.1E-05	7.4E-05	7.3E-05	7.1E-05	6.7E-05	5.8E-05	2.6E-05	2.4E-05	2.0E-04	3.3E-04	3.4E-04	3.2E-04	2.2E-04	1.1E-04
	24	2.1E-06	2.6E-05	4.6E-05	8.0E-05	8.6E-05	8.7E-05	8.6E-05	8.4E-05	6.7E-05	2.4E-05	3.6E-05	2.1E-04	3.4E-04	3.4E-04	3.2E-04	2.2E-04	1.1E-04
	26	2.5E-06	3.1E-05	5.6E-05	1.1E-04	1.3E-04	1.3E-04	1.2E-04	1.1E-04	7.7E-05	1.4E-05	6.4E-05	2.4E-04	3.5E-04	3.5E-04	3.2E-04	2.2E-04	1.1E-04
	27	2.8E-06	3.5E-05	6.3E-05	1.3E-04	1.5E-04	1.5E-04	1.3E-04	1.2E-04	7.8E-05	7.7E-06	7.7E-05	2.6E-04	3.6E-04	3.6E-04	3.2E-04	2.2E-04	1.1E-04
	28	3.1E-06	4.0E-05	7.3E-05	1.5E-04	1.6E-04	1.6E-04	1.4E-04	1.3E-04	7.9E-05	1.3E-06	9.0E-05	2.7E-04	3.6E-04	3.6E-04	3.2E-04	2.2E-04	1.1E-04
	29	3.5E-06	4.6E-05	8.4E-05	1.8E-04	1.8E-04	1.7E-04	1.5E-04	1.3E-04	7.9E-05	4.7E-06	1.0E-04	2.8E-04	3.7E-04	3.7E-04	3.2E-04	2.2E-04	1.1E-04
	30	4.0E-06	5.2E-05	9.7E-05	1.9E-04	1.9E-04	1.8E-04	1.6E-04	1.3E-04	7.8E-05	9.7E-06	1.1E-04	2.9E-04	3.7E-04	3.7E-04	3.2E-04	2.2E-04	1.1E-04
	31	4.6E-06	6.0E-05	1.1E-04	2.0E-04	2.0E-04	1.8E-04	1.6E-04	1.4E-04	7.8E-05	1.3E-05	1.2E-04	3.0E-04	3.7E-04	3.7E-04	3.2E-04	2.2E-04	1.1E-04
	32	4.6E-06	6.0E-05	1.1E-04	2.0E-04	2.0E-04	1.8E-04	1.6E-04	1.4E-04	7.8E-05	1.3E-05	1.2E-04	3.0E-04	3.7E-04	3.7E-04	3.2E-04	2.2E-04	1.1E-04
	33	4.6E-06	6.0E-05	1.1E-04	2.0E-04	2.0E-04	1.8E-04	1.6E-04	1.4E-04	7.8E-05	1.3E-05	1.2E-04	3.0E-04	3.7E-04	3.7E-04	3.2E-04	2.2E-04	1.1E-04

Divide the range into intervals of 2.75e-5. Table B.9 shows the frequency of occurrence of model instances in each interval at a location

Table B.9: Frequency of occurrence of 31 model instances in each interval at a 17 locations

Interval		Location																
Lower	Upper	1	2	3	4	5	6	7	8	9	10	11	13	14	15	16	17	18
0	2.75E-05	31	20	10	0	0	1	1	0	0	18	9	0	0	0	0	0	0
2.75E-05	0.000055	0	7	10	11	3	3	7	8	8	0	1	0	0	0	0	0	0
0.000055	8.25E-05	0	3	5	9	18	16	5	4	12	1	4	3	2	2	2	2	0
8.25E-05	0.00011	0	0	2	1	1	1	8	1	1	3	3	0	1	1	0	0	16
0.00011	0.000138	0	0	3	3	1	2	2	16	2	0	5	1	0	0	1	0	15
0.000138	0.000165	0	0	0	1	2	2	6	0	4	0	0	4	0	0	0	0	0
0.000165	0.000193	0	1	0	3	2	5	1	0	0	4	0	4	1	1	0	1	0
0.000193	0.00022	0	0	1	3	4	0	0	1	0	1	0	2	0	0	0	16	0
0.00022	0.000248	0	0	0	0	0	1	0	0	2	0	4	1	0	0	0	0	0
0.000248	0.000275	0	0	0	0	0	0	0	0	0	0	0	2	0	0	1	12	0
0.000275	0.000303	0	0	0	0	0	0	1	0	1	0	0	5	0	0	0	0	0
0.000303	0.00033	0	0	0	0	0	0	0	1	0	0	0	1	6	5	16	0	0
0.00033	0.000358	0	0	0	0	0	0	0	0	0	1	0	1	6	6	0	0	0
0.000358	0.000385	0	0	0	0	0	0	0	0	1	0	0	1	7	8	11	0	0
0.000385	0.000413	0	0	0	0	0	0	0	0	0	1	0	1	0	0	0	0	0
0.000413	0.00044	0	0	0	0	0	0	0	0	0	0	1	0	1	1	0	0	0
0.00044	0.000468	0	0	0	0	0	0	0	0	0	1	0	0	1	1	0	0	0
0.000468	0.000495	0	0	0	0	0	0	0	0	0	0	1	0	0	0	0	0	0
0.000495	0.000523	0	0	0	0	0	0	0	0	0	0	1	0	1	1	0	0	0
0.000523	0.00055	0	0	0	0	0	0	0	0	0	0	1	0	5	5	0	0	0
0.00055	0.000578	0	0	0	0	0	0	0	0	0	0	0	0	0	0	0	0	0
0.000578	0.000605	0	0	0	0	0	0	0	0	0	1	0	5	0	0	0	0	0
0.000605	0.000633	0	0	0	0	0	0	0	0	0	0	0	0	0	0	0	0	0
0.000633	0.00066	0	0	0	0	0	0	0	0	0	0	0	0	0	0	0	0	0
0.00066	0.000688	0	0	0	0	0	0	0	0	0	0	0	0	0	0	0	0	0

0.000688	0.000715	0	0	0	0	0	0	0	0	0	0	0	0	0	0	0	0	0
0.000715	0.000743	0	0	0	0	0	0	0	0	0	0	1	0	0	0	0	0	0
0.000743	0.00077	0	0	0	0	0	0	0	0	0	0	0	0	0	0	0	0	0
0.00077	0.000798	0	0	0	0	0	0	0	0	0	0	0	0	0	0	0	0	0
0.000798	0.000825	0	0	0	0	0	0	0	0	0	0	0	0	0	0	0	0	0

Probability of occurrence of model instances in each interval at different locations are given in Table B.10

Table B.10 Probability of occurrence of 31 model instances in each interval at 17 different locations

Interval		Location																
Lower	Upper	1	2	3	4	5	6	7	8	9	10	11	13	14	15	16	17	18
0	2.75E-05	1.00	0.65	0.32	0.00	0.00	0.03	0.03	0.00	0.00	0.58	0.29	0.00	0.00	0.00	0.00	0.00	0.00
2.75E-05	0.000055	0.00	0.23	0.32	0.35	0.10	0.10	0.23	0.26	0.26	0.00	0.03	0.00	0.00	0.00	0.00	0.00	0.00
0.000055	8.25E-05	0.00	0.10	0.16	0.29	0.58	0.52	0.16	0.13	0.39	0.03	0.13	0.10	0.06	0.06	0.06	0.06	0.00
8.25E-05	0.00011	0.00	0.00	0.06	0.03	0.03	0.03	0.26	0.03	0.03	0.10	0.10	0.00	0.03	0.03	0.00	0.00	0.52
0.00011	0.000138	0.00	0.00	0.10	0.10	0.03	0.06	0.06	0.52	0.06	0.00	0.16	0.03	0.00	0.00	0.03	0.00	0.48
0.000138	0.000165	0.00	0.00	0.00	0.03	0.06	0.06	0.19	0.00	0.13	0.00	0.00	0.13	0.00	0.00	0.00	0.00	0.00
0.000165	0.000193	0.00	0.03	0.00	0.10	0.06	0.16	0.03	0.00	0.00	0.13	0.00	0.13	0.03	0.03	0.00	0.03	0.00
0.000193	0.00022	0.00	0.00	0.03	0.10	0.13	0.00	0.00	0.03	0.00	0.03	0.00	0.06	0.00	0.00	0.00	0.52	0.00
0.00022	0.000248	0.00	0.00	0.00	0.00	0.00	0.03	0.00	0.00	0.06	0.00	0.13	0.03	0.00	0.00	0.00	0.00	0.00
0.000248	0.000275	0.00	0.00	0.00	0.00	0.00	0.00	0.00	0.00	0.00	0.00	0.00	0.06	0.00	0.00	0.03	0.39	0.00
0.000275	0.000303	0.00	0.00	0.00	0.00	0.00	0.00	0.03	0.00	0.03	0.00	0.00	0.16	0.00	0.00	0.00	0.00	0.00
0.000303	0.00033	0.00	0.00	0.00	0.00	0.00	0.00	0.00	0.03	0.00	0.00	0.00	0.03	0.19	0.16	0.52	0.00	0.00
0.00033	0.000358	0.00	0.00	0.00	0.00	0.00	0.00	0.00	0.00	0.00	0.03	0.00	0.03	0.19	0.19	0.00	0.00	0.00
0.000358	0.000385	0.00	0.00	0.00	0.00	0.00	0.00	0.00	0.00	0.03	0.00	0.00	0.03	0.23	0.26	0.35	0.00	0.00
0.000385	0.000413	0.00	0.00	0.00	0.00	0.00	0.00	0.00	0.00	0.00	0.03	0.00	0.03	0.00	0.00	0.00	0.00	0.00
0.000413	0.00044	0.00	0.00	0.00	0.00	0.00	0.00	0.00	0.00	0.00	0.00	0.03	0.00	0.03	0.03	0.00	0.00	0.00
0.00044	0.000468	0.00	0.00	0.00	0.00	0.00	0.00	0.00	0.00	0.00	0.03	0.00	0.00	0.03	0.03	0.00	0.00	0.00

0.000468	0.000495	0.00	0.00	0.00	0.00	0.00	0.00	0.00	0.00	0.00	0.00	0.03	0.00	0.00	0.00	0.00	0.00	0.00
0.000495	0.000523	0.00	0.00	0.00	0.00	0.00	0.00	0.00	0.00	0.00	0.00	0.03	0.00	0.03	0.03	0.00	0.00	0.00
0.000523	0.00055	0.00	0.00	0.00	0.00	0.00	0.00	0.00	0.00	0.00	0.00	0.03	0.00	0.16	0.16	0.00	0.00	0.00
0.00055	0.000578	0.00	0.00	0.00	0.00	0.00	0.00	0.00	0.00	0.00	0.00	0.00	0.00	0.00	0.00	0.00	0.00	0.00
0.000578	0.000605	0.00	0.00	0.00	0.00	0.00	0.00	0.00	0.00	0.00	0.03	0.00	0.16	0.00	0.00	0.00	0.00	0.00
0.000605	0.000633	0.00	0.00	0.00	0.00	0.00	0.00	0.00	0.00	0.00	0.00	0.00	0.00	0.00	0.00	0.00	0.00	0.00
0.000633	0.00066	0.00	0.00	0.00	0.00	0.00	0.00	0.00	0.00	0.00	0.00	0.00	0.00	0.00	0.00	0.00	0.00	0.00
0.00066	0.000688	0.00	0.00	0.00	0.00	0.00	0.00	0.00	0.00	0.00	0.00	0.00	0.00	0.00	0.00	0.00	0.00	0.00
0.000688	0.000715	0.00	0.00	0.00	0.00	0.00	0.00	0.00	0.00	0.00	0.00	0.00	0.00	0.00	0.00	0.00	0.00	0.00
0.000715	0.000743	0.00	0.00	0.00	0.00	0.00	0.00	0.00	0.00	0.00	0.00	0.03	0.00	0.00	0.00	0.00	0.00	0.00
0.000743	0.00077	0.00	0.00	0.00	0.00	0.00	0.00	0.00	0.00	0.00	0.00	0.00	0.00	0.00	0.00	0.00	0.00	0.00
0.00077	0.000798	0.00	0.00	0.00	0.00	0.00	0.00	0.00	0.00	0.00	0.00	0.00	0.00	0.00	0.00	0.00	0.00	0.00
0.000798	0.000825	0.00	0.00	0.00	0.00	0.00	0.00	0.00	0.00	0.00	0.00	0.00	0.00	0.00	0.00	0.00	0.00	0.00

To find the Shannon's entropy, p(x)log (p(x)) needs to be calculated for each interval at location. Sum of the negatives of p(x)log (p(x)) at a location gives the Shannon's entropy at that location. Table B.11 represent this data.

Table B.11: p(x)log (p(x)) values for each interval at a location

Interval		Location																
Lower	Upper	1	2	3	4	5	6	7	8	9	10	11	13	14	15	16	17	18
0	2.75E-05	0.00	-0.41	-0.53	NA	NA	-0.16	-0.16	NA	NA	-0.46	-0.52	NA	NA	NA	NA	NA	NA
2.75E-05	0.000055	NA	-0.48	-0.53	-0.53	-0.33	-0.33	-0.48	-0.50	-0.50	NA	-0.16	NA	NA	NA	NA	NA	NA
0.000055	8.25E-05	NA	-0.33	-0.42	-0.52	-0.46	-0.49	-0.42	-0.38	-0.53	-0.16	-0.38	-0.33	-0.26	-0.26	-0.26	-0.26	NA
8.25E-05	0.00011	NA	NA	-0.26	-0.16	-0.16	-0.16	-0.50	-0.16	-0.16	-0.33	-0.33	NA	-0.16	-0.16	NA	NA	-0.49
0.00011	0.000138	NA	NA	-0.33	-0.33	-0.16	-0.26	-0.26	-0.49	-0.26	NA	-0.42	-0.16	NA	NA	-0.16	NA	-0.51
0.000138	0.000165	NA	NA	NA	-0.16	-0.26	-0.26	-0.46	NA	-0.38	NA	NA	-0.38	NA	NA	NA	NA	NA
0.000165	0.000193	NA	-0.16	NA	-0.33	-0.26	-0.42	-0.16	NA	NA	-0.38	NA	-0.38	-0.16	-0.16	NA	-0.16	NA
0.000193	0.00022	NA	NA	-0.16	-0.33	-0.38	NA	NA	-0.16	NA	-0.16	NA	-0.26	NA	NA	NA	-0.49	NA

0.00022	0.000248	NA	NA	NA	NA	NA	-0.16	NA	NA	-0.26	NA	-0.38	-0.16	NA	NA	NA	NA	NA
0.000248	0.000275	NA	NA	NA	NA	NA	NA	NA	NA	NA	NA	NA	-0.26	NA	NA	-0.16	-0.53	NA
0.000275	0.000303	NA	NA	NA	NA	NA	NA	-0.16	NA	-0.16	NA	NA	-0.42	NA	NA	NA	NA	NA
0.000303	0.00033	NA	NA	NA	NA	NA	NA	NA	-0.16	NA	NA	NA	-0.16	-0.46	-0.42	-0.49	NA	NA
0.00033	0.000358	NA	NA	NA	NA	NA	NA	NA	NA	NA	-0.16	NA	-0.16	-0.46	-0.46	NA	NA	NA
0.000358	0.000385	NA	NA	NA	NA	NA	NA	NA	NA	-0.16	NA	NA	-0.16	-0.48	-0.50	-0.53	NA	NA
0.000385	0.000413	NA	NA	NA	NA	NA	NA	NA	NA	NA	-0.16	NA	-0.16	NA	NA	NA	NA	NA
0.000413	0.00044	NA	NA	NA	NA	NA	NA	NA	NA	NA	NA	-0.16	NA	-0.16	-0.16	NA	NA	NA
0.00044	0.000468	NA	NA	NA	NA	NA	NA	NA	NA	NA	-0.16	NA	NA	-0.16	-0.16	NA	NA	NA
0.000468	0.000495	NA	NA	NA	NA	NA	NA	NA	NA	NA	NA	-0.16	NA	NA	NA	NA	NA	NA
0.000495	0.000523	NA	NA	NA	NA	NA	NA	NA	NA	NA	NA	-0.16	NA	-0.16	-0.16	NA	NA	NA
0.000523	0.00055	NA	NA	NA	NA	NA	NA	NA	NA	NA	NA	-0.16	NA	-0.42	-0.42	NA	NA	NA
0.00055	0.000578	NA	NA	NA	NA	NA	NA	NA	NA	NA	NA	NA	NA	NA	NA	NA	NA	NA
0.000578	0.000605	NA	NA	NA	NA	NA	NA	NA	NA	NA	-0.16	NA	-0.42	NA	NA	NA	NA	NA
0.000605	0.000633	NA	NA	NA	NA	NA	NA	NA	NA	NA	NA	NA	NA	NA	NA	NA	NA	NA
0.000633	0.00066	NA	NA	NA	NA	NA	NA	NA	NA	NA	NA	NA	NA	NA	NA	NA	NA	NA
0.00066	0.000688	NA	NA	NA	NA	NA	NA	NA	NA	NA	NA	NA	NA	NA	NA	NA	NA	NA
0.000688	0.000715	NA	NA	NA	NA	NA	NA	NA	NA	NA	NA	NA	NA	NA	NA	NA	NA	NA
0.000715	0.000743	NA	NA	NA	NA	NA	NA	NA	NA	NA	NA	-0.16	NA	NA	NA	NA	NA	NA
0.000743	0.00077	NA	NA	NA	NA	NA	NA	NA	NA	NA	NA	NA	NA	NA	NA	NA	NA	NA
0.00077	0.000798	NA	NA	NA	NA	NA	NA	NA	NA	NA	NA	NA	NA	NA	NA	NA	NA	NA
0.000798	0.000825	NA	NA	NA	NA	NA	NA	NA	NA	NA	NA	NA	NA	NA	NA	NA	NA	NA
Entropy		0.00	1.38	2.22	2.35	1.99	2.23	2.61	1.86	2.41	2.12	2.99	3.41	2.88	2.87	1.60	1.44	1.00

Maximum entropy is obtained at Location 13. Hence the second sensor should be placed at Location 13. Therefore, Location 13 is the second element in the set Optimum_Location. Location 13 should be removed from the set Location_List. Also, there are four model instances completely distinguished through measurement at location 13. Hence, those four model instances should be removed from the set Sub_Models. Currently, Location_list has 16 elements, Sub_Models have 27 elements and Optimum_Locations has 2 element. Therefore remove the column corresponding location 13 and the rows corresponding to Model instances separated by location 13. Repeat the above steps until Sub_Models or Location_List becomes empty.

APPENDIX C

Data Sample from Field Implementation

This section gives snippets of data from the field implementation. Also Section C.5 gives a sample of how the system identification algorithm works.

C.1 Autolaunching

Table C.1 Strain data for auto launching operation

Location													
182	115	191	32	53	109	180	183	185	247	250	280	296	328
4.51E-05	1.15E-06	5.71E-07	1.31E-05	1.30E-05	7.35E-07	3.98E-05	4.43E-05	4.55E-05	3.74E-05	4.60E-05	1.82E-05	1.78E-05	1.67E-16
4.51E-05	1.15E-06	5.71E-07	1.31E-05	1.30E-05	7.35E-07	3.98E-05	4.43E-05	4.55E-05	3.74E-05	4.59E-05	1.82E-05	1.78E-05	2.33E-16
4.51E-05	1.15E-06	5.71E-07	1.31E-05	1.30E-05	7.35E-07	3.98E-05	4.43E-05	4.55E-05	3.73E-05	4.59E-05	1.81E-05	1.77E-05	3.99E-17
4.51E-05	1.15E-06	5.71E-07	1.31E-05	1.30E-05	7.35E-07	3.98E-05	4.43E-05	4.55E-05	3.72E-05	4.58E-05	1.80E-05	1.76E-05	3.62E-16
4.51E-05	1.15E-06	5.71E-07	1.31E-05	1.30E-05	7.35E-07	3.98E-05	4.43E-05	4.55E-05	3.72E-05	4.57E-05	1.80E-05	1.75E-05	8.81E-17
4.51E-05	1.15E-06	5.71E-07	1.31E-05	1.30E-05	7.35E-07	3.98E-05	4.43E-05	4.55E-05	3.71E-05	4.56E-05	1.79E-05	1.75E-05	4.35E-16
4.51E-05	1.15E-06	5.71E-07	1.31E-05	1.30E-05	7.35E-07	3.98E-05	4.43E-05	4.55E-05	3.70E-05	4.55E-05	1.78E-05	1.74E-05	4.27E-16
3.08E-05	8.19E-06	3.51E-05	1.68E-05	1.94E-05	9.82E-06	2.58E-05	3.07E-05	3.18E-05	3.74E-05	4.60E-05	1.82E-05	1.78E-05	1.67E-16
3.08E-05	8.19E-06	3.51E-05	1.68E-05	1.94E-05	9.82E-06	2.58E-05	3.07E-05	3.18E-05	3.74E-05	4.59E-05	1.82E-05	1.78E-05	2.33E-16
3.08E-05	8.19E-06	3.51E-05	1.68E-05	1.94E-05	9.82E-06	2.58E-05	3.07E-05	3.18E-05	3.73E-05	4.59E-05	1.81E-05	1.77E-05	3.99E-17
3.08E-05	8.19E-06	3.51E-05	1.68E-05	1.94E-05	9.82E-06	2.58E-05	3.07E-05	3.18E-05	3.72E-05	4.58E-05	1.80E-05	1.76E-05	3.62E-16
3.08E-05	8.19E-06	3.51E-05	1.68E-05	1.94E-05	9.82E-06	2.58E-05	3.07E-05	3.18E-05	3.72E-05	4.57E-05	1.80E-05	1.75E-05	8.81E-17
3.08E-05	8.19E-06	3.51E-05	1.68E-05	1.94E-05	9.82E-06	2.58E-05	3.07E-05	3.18E-05	3.71E-05	4.56E-05	1.79E-05	1.75E-05	4.35E-16
3.08E-05	8.19E-06	3.51E-05	1.68E-05	1.94E-05	9.82E-06	2.58E-05	3.07E-05	3.18E-05	3.70E-05	4.55E-05	1.78E-05	1.74E-05	4.27E-16
1.40E-06	7.38E-06	4.03E-06	7.24E-06	3.45E-06	7.12E-06	6.31E-07	2.10E-06	2.56E-06	3.74E-05	4.60E-05	1.82E-05	1.78E-05	1.67E-16
1.40E-06	7.38E-06	4.03E-06	7.24E-06	3.45E-06	7.12E-06	6.31E-07	2.10E-06	2.56E-06	3.74E-05	4.59E-05	1.82E-05	1.78E-05	2.33E-16
1.40E-06	7.38E-06	4.03E-06	7.24E-06	3.45E-06	7.12E-06	6.31E-07	2.10E-06	2.56E-06	3.73E-05	4.59E-05	1.81E-05	1.77E-05	3.99E-17

1.40E-06	7.38E-06	4.03E-06	7.24E-06	3.45E-06	7.12E-06	6.31E-07	2.10E-06	2.56E-06	3.72E-05	4.58E-05	1.80E-05	1.76E-05	3.62E-16
1.40E-06	7.38E-06	4.03E-06	7.24E-06	3.45E-06	7.12E-06	6.31E-07	2.10E-06	2.56E-06	3.72E-05	4.57E-05	1.80E-05	1.75E-05	8.81E-17
1.40E-06	7.38E-06	4.03E-06	7.24E-06	3.45E-06	7.12E-06	6.31E-07	2.10E-06	2.56E-06	3.71E-05	4.56E-05	1.79E-05	1.75E-05	4.35E-16
1.40E-06	7.38E-06	4.03E-06	7.24E-06	3.45E-06	7.12E-06	6.31E-07	2.10E-06	2.56E-06	3.70E-05	4.55E-05	1.78E-05	1.74E-05	4.27E-16
9.73E-06	5.39E-06	6.48E-05	7.24E-06	9.75E-07	5.50E-06	7.11E-06	1.01E-05	1.07E-05	2.65E-05	3.18E-05	9.04E-06	7.67E-06	5.30E-16
9.73E-06	5.39E-06	6.47E-05	7.24E-06	9.75E-07	5.50E-06	7.11E-06	1.01E-05	1.07E-05	2.64E-05	3.17E-05	8.99E-06	7.60E-06	3.66E-16
9.73E-06	5.39E-06	6.46E-05	7.24E-06	9.75E-07	5.50E-06	7.11E-06	1.01E-05	1.07E-05	2.63E-05	3.17E-05	8.93E-06	7.53E-06	2.66E-16
9.73E-06	5.39E-06	6.46E-05	7.24E-06	9.75E-07	5.50E-06	7.11E-06	1.01E-05	1.07E-05	2.63E-05	3.16E-05	8.88E-06	7.47E-06	7.07E-16
9.73E-06	5.39E-06	6.45E-05	7.24E-06	9.75E-07	5.50E-06	7.11E-06	1.01E-05	1.07E-05	2.62E-05	3.15E-05	8.82E-06	7.40E-06	7.50E-17
9.73E-06	5.39E-06	6.45E-05	7.24E-06	9.75E-07	5.50E-06	7.11E-06	1.01E-05	1.07E-05	2.62E-05	3.14E-05	8.76E-06	7.33E-06	3.65E-17
9.73E-06	5.39E-06	6.44E-05	7.24E-06	9.75E-07	5.50E-06	7.11E-06	1.01E-05	1.07E-05	2.61E-05	3.14E-05	8.71E-06	7.27E-06	8.03E-17
2.15E-05	7.26E-06	6.48E-05	2.43E-08	1.10E-05	8.25E-06	1.75E-05	2.17E-05	2.25E-05	2.65E-05	3.18E-05	9.04E-06	7.67E-06	5.30E-16
2.15E-05	7.26E-06	6.47E-05	2.43E-08	1.10E-05	8.25E-06	1.75E-05	2.17E-05	2.25E-05	2.64E-05	3.17E-05	8.99E-06	7.60E-06	3.66E-16
2.15E-05	7.26E-06	6.46E-05	2.43E-08	1.10E-05	8.25E-06	1.75E-05	2.17E-05	2.25E-05	2.63E-05	3.17E-05	8.93E-06	7.53E-06	2.66E-16
2.15E-05	7.26E-06	6.46E-05	2.43E-08	1.10E-05	8.25E-06	1.75E-05	2.17E-05	2.25E-05	2.63E-05	3.16E-05	8.88E-06	7.47E-06	7.07E-16
2.15E-05	7.26E-06	6.45E-05	2.43E-08	1.10E-05	8.25E-06	1.75E-05	2.17E-05	2.25E-05	2.62E-05	3.15E-05	8.82E-06	7.40E-06	7.50E-17
2.15E-05	7.26E-06	6.45E-05	2.43E-08	1.10E-05	8.25E-06	1.75E-05	2.17E-05	2.25E-05	2.62E-05	3.14E-05	8.76E-06	7.33E-06	3.65E-17
2.15E-05	7.26E-06	6.44E-05	2.43E-08	1.10E-05	8.25E-06	1.75E-05	2.17E-05	2.25E-05	2.61E-05	3.14E-05	8.71E-06	7.27E-06	8.03E-17
2.15E-05	7.26E-06	6.48E-05	2.43E-08	1.10E-05	8.25E-06	1.75E-05	2.17E-05	2.25E-05	2.65E-05	3.18E-05	9.04E-06	7.67E-06	5.30E-16
2.15E-05	7.26E-06	6.47E-05	2.43E-08	1.10E-05	8.25E-06	1.75E-05	2.17E-05	2.25E-05	2.64E-05	3.17E-05	8.99E-06	7.60E-06	3.66E-16
2.15E-05	7.26E-06	6.46E-05	2.43E-08	1.10E-05	8.25E-06	1.75E-05	2.17E-05	2.25E-05	2.63E-05	3.17E-05	8.93E-06	7.53E-06	2.66E-16
2.15E-05	7.26E-06	6.46E-05	2.43E-08	1.10E-05	8.25E-06	1.75E-05	2.17E-05	2.25E-05	2.63E-05	3.16E-05	8.88E-06	7.47E-06	7.07E-16
2.15E-05	7.26E-06	6.45E-05	2.43E-08	1.10E-05	8.25E-06	1.75E-05	2.17E-05	2.25E-05	2.62E-05	3.15E-05	8.82E-06	7.40E-06	7.50E-17
2.15E-05	7.26E-06	6.45E-05	2.43E-08	1.10E-05	8.25E-06	1.75E-05	2.17E-05	2.25E-05	2.62E-05	3.14E-05	8.76E-06	7.33E-06	3.65E-17
2.15E-05	7.26E-06	6.44E-05	2.43E-08	1.10E-05	8.25E-06	1.75E-05	2.17E-05	2.25E-05	2.61E-05	3.14E-05	8.71E-06	7.27E-06	8.03E-17
4.36E-07	1.14E-05	2.59E-06	2.22E-05	2.39E-06	1.13E-05	2.71E-06	4.51E-07	9.67E-07	4.15E-05	5.13E-05	2.16E-05	2.16E-05	2.10E-16
4.36E-07	1.14E-05	2.59E-06	2.22E-05	2.39E-06	1.13E-05	2.71E-06	4.51E-07	9.67E-07	4.14E-05	5.12E-05	2.16E-05	2.15E-05	6.38E-17
4.36E-07	1.14E-05	2.59E-06	2.22E-05	2.39E-06	1.13E-05	2.71E-06	4.51E-07	9.67E-07	4.14E-05	5.11E-05	2.15E-05	2.15E-05	3.24E-17
4.36E-07	1.14E-05	2.59E-06	2.22E-05	2.39E-06	1.13E-05	2.71E-06	4.51E-07	9.67E-07	4.13E-05	5.10E-05	2.14E-05	2.14E-05	1.57E-16
4.36E-07	1.14E-05	2.59E-06	2.22E-05	2.39E-06	1.13E-05	2.71E-06	4.51E-07	9.67E-07	4.12E-05	5.09E-05	2.14E-05	2.13E-05	1.52E-16

4.36E-07	1.14E-05	2.59E-06	2.22E-05	2.39E-06	1.13E-05	2.71E-06	4.51E-07	9.67E-07	4.12E-05	5.08E-05	2.13E-05	2.12E-05	3.95E-17
4.36E-07	1.14E-05	2.59E-06	2.22E-05	2.39E-06	1.13E-05	2.71E-06	4.51E-07	9.67E-07	4.11E-05	5.08E-05	2.12E-05	2.11E-05	3.97E-16
1.42E-05	7.92E-06	1.24E-05	9.66E-06	1.38E-05	6.71E-06	1.48E-05	1.31E-05	1.29E-05	8.90E-06	1.70E-05	3.50E-05	3.64E-05	2.37E-16
1.42E-05	7.92E-06	1.24E-05	9.66E-06	1.38E-05	6.71E-06	1.48E-05	1.31E-05	1.29E-05	8.90E-06	1.70E-05	3.49E-05	3.63E-05	1.48E-16
1.42E-05	7.92E-06	1.24E-05	9.66E-06	1.38E-05	6.71E-06	1.48E-05	1.31E-05	1.29E-05	8.90E-06	1.70E-05	3.48E-05	3.62E-05	1.74E-16
1.42E-05	7.92E-06	1.24E-05	9.66E-06	1.38E-05	6.71E-06	1.48E-05	1.31E-05	1.29E-05	8.90E-06	1.70E-05	3.47E-05	3.60E-05	9.86E-17
1.42E-05	7.92E-06	1.24E-05	9.66E-06	1.38E-05	6.71E-06	1.48E-05	1.31E-05	1.29E-05	8.90E-06	1.70E-05	3.46E-05	3.59E-05	2.19E-16
1.42E-05	7.92E-06	1.24E-05	9.66E-06	1.38E-05	6.71E-06	1.48E-05	1.31E-05	1.29E-05	8.90E-06	1.70E-05	3.45E-05	3.58E-05	1.84E-16
1.42E-05	7.92E-06	1.24E-05	9.66E-06	1.38E-05	6.71E-06	1.48E-05	1.31E-05	1.29E-05	8.90E-06	1.70E-05	3.44E-05	3.57E-05	6.26E-17
1.59E-05	3.77E-06	1.56E-05	9.66E-06	2.91E-05	5.89E-06	1.51E-05	1.52E-05	1.53E-05	7.03E-06	6.53E-06	2.47E-05	5.42E-05	1.68E-16
1.59E-05	3.77E-06	1.56E-05	9.66E-06	2.91E-05	5.89E-06	1.51E-05	1.52E-05	1.53E-05	7.03E-06	6.53E-06	2.47E-05	5.40E-05	7.61E-17
1.59E-05	3.77E-06	1.56E-05	9.66E-06	2.91E-05	5.89E-06	1.51E-05	1.52E-05	1.53E-05	7.03E-06	6.53E-06	2.47E-05	5.39E-05	1.07E-16
1.59E-05	3.77E-06	1.56E-05	9.66E-06	2.91E-05	5.89E-06	1.51E-05	1.52E-05	1.53E-05	7.03E-06	6.53E-06	2.47E-05	5.37E-05	1.20E-16
1.59E-05	3.77E-06	1.56E-05	9.66E-06	2.91E-05	5.89E-06	1.51E-05	1.52E-05	1.53E-05	7.03E-06	6.53E-06	2.47E-05	5.36E-05	9.12E-17
1.59E-05	3.77E-06	1.56E-05	9.66E-06	2.91E-05	5.89E-06	1.51E-05	1.52E-05	1.53E-05	7.03E-06	6.53E-06	2.47E-05	5.34E-05	5.91E-17
1.59E-05	3.77E-06	1.56E-05	9.66E-06	2.91E-05	5.89E-06	1.51E-05	1.52E-05	1.53E-05	7.03E-06	6.53E-06	2.47E-05	5.33E-05	8.73E-17
9.39E-06	2.04E-05	1.08E-05	9.66E-06	2.91E-05	2.33E-05	7.51E-06	9.46E-06	9.81E-06	1.24E-05	1.54E-05	4.06E-06	1.19E-05	3.19E-17
9.39E-06	2.04E-05	1.08E-05	9.66E-06	2.91E-05	2.33E-05	7.51E-06	9.46E-06	9.81E-06	1.24E-05	1.54E-05	4.06E-06	1.19E-05	1.03E-17
9.39E-06	2.04E-05	1.08E-05	9.66E-06	2.91E-05	2.33E-05	7.51E-06	9.46E-06	9.81E-06	1.24E-05	1.54E-05	4.06E-06	1.19E-05	3.21E-17
9.39E-06	2.04E-05	1.08E-05	9.66E-06	2.91E-05	2.33E-05	7.51E-06	9.46E-06	9.81E-06	1.24E-05	1.54E-05	4.06E-06	1.19E-05	7.10E-17
9.39E-06	2.04E-05	1.08E-05	9.66E-06	2.91E-05	2.33E-05	7.51E-06	9.46E-06	9.81E-06	1.24E-05	1.54E-05	4.06E-06	1.19E-05	1.19E-17
9.39E-06	2.04E-05	1.08E-05	9.66E-06	2.91E-05	2.33E-05	7.51E-06	9.46E-06	9.81E-06	1.24E-05	1.54E-05	4.06E-06	1.19E-05	5.34E-17
9.39E-06	2.04E-05	1.08E-05	9.66E-06	2.91E-05	2.33E-05	7.51E-06	9.46E-06	9.81E-06	1.24E-05	1.54E-05	4.06E-06	1.19E-05	3.48E-17
8.04E-06	2.29E-05	9.67E-06	9.66E-06	2.91E-05	6.25E-05	6.02E-06	8.24E-06	8.61E-06	1.25E-05	1.57E-05	2.33E-06	9.42E-06	2.70E-17
8.04E-06	2.29E-05	9.67E-06	9.66E-06	2.91E-05	6.25E-05	6.02E-06	8.24E-06	8.61E-06	1.25E-05	1.57E-05	2.33E-06	9.42E-06	6.46E-18
8.04E-06	2.29E-05	9.67E-06	9.66E-06	2.91E-05	6.25E-05	6.02E-06	8.24E-06	8.61E-06	1.25E-05	1.57E-05	2.33E-06	9.42E-06	8.06E-19
8.04E-06	2.29E-05	9.67E-06	9.66E-06	2.91E-05	6.25E-05	6.02E-06	8.24E-06	8.61E-06	1.25E-05	1.57E-05	2.33E-06	9.42E-06	2.24E-17
8.04E-06	2.29E-05	9.67E-06	9.66E-06	2.91E-05	6.25E-05	6.02E-06	8.24E-06	8.61E-06	1.25E-05	1.57E-05	2.33E-06	9.42E-06	1.39E-17
8.04E-06	2.29E-05	9.67E-06	9.66E-06	2.91E-05	6.25E-05	6.02E-06	8.24E-06	8.61E-06	1.25E-05	1.57E-05	2.33E-06	9.42E-06	1.94E-17
8.04E-06	2.29E-05	9.67E-06	9.66E-06	2.91E-05	6.25E-05	6.02E-06	8.24E-06	8.61E-06	1.25E-05	1.57E-05	2.33E-06	9.42E-06	1.29E-17

4.93E-05	5.14E-07	4.06E-05	9.66E-06	2.91E-05	6.25E-05	5.44E-05	4.46E-05	4.36E-05	9.17E-06	9.38E-06	5.43E-06	8.35E-06	7.46E-18
4.93E-05	5.14E-07	4.05E-05	9.66E-06	2.91E-05	6.25E-05	5.44E-05	4.46E-05	4.35E-05	9.14E-06	9.33E-06	5.48E-06	8.41E-06	1.91E-18
4.92E-05	5.14E-07	4.05E-05	9.66E-06	2.91E-05	6.25E-05	5.43E-05	4.45E-05	4.35E-05	9.10E-06	9.27E-06	5.52E-06	8.46E-06	4.28E-17
4.92E-05	5.14E-07	4.05E-05	9.66E-06	2.91E-05	6.25E-05	5.43E-05	4.45E-05	4.34E-05	9.06E-06	9.22E-06	5.57E-06	8.52E-06	3.36E-16
4.91E-05	5.14E-07	4.04E-05	9.66E-06	2.91E-05	6.25E-05	5.42E-05	4.44E-05	4.34E-05	9.02E-06	9.17E-06	5.61E-06	8.57E-06	3.78E-16
4.91E-05	5.14E-07	4.04E-05	9.66E-06	2.91E-05	6.25E-05	5.42E-05	4.44E-05	4.34E-05	8.98E-06	9.12E-06	5.66E-06	8.62E-06	4.23E-16
4.90E-05	5.14E-07	4.03E-05	9.66E-06	2.91E-05	6.25E-05	5.41E-05	4.43E-05	4.33E-05	8.95E-06	9.07E-06	5.70E-06	8.68E-06	4.45E-17
7.13E-07	6.63E-05	6.17E-05	9.67E-06	2.91E-05	6.25E-05	1.11E-07	6.63E-05	6.51E-05	2.43E-05	2.90E-05	7.23E-06	5.66E-06	5.95E-17
7.13E-07	6.63E-05	6.17E-05	9.67E-06	2.91E-05	6.25E-05	1.11E-07	6.62E-05	6.51E-05	2.42E-05	2.89E-05	7.17E-06	5.59E-06	4.28E-16
7.13E-07	6.63E-05	6.16E-05	9.67E-06	2.91E-05	6.25E-05	1.11E-07	6.62E-05	6.50E-05	2.42E-05	2.88E-05	7.12E-06	5.53E-06	7.77E-17
7.13E-07	6.63E-05	6.16E-05	9.67E-06	2.91E-05	6.25E-05	1.11E-07	6.61E-05	6.49E-05	2.41E-05	2.88E-05	7.06E-06	5.46E-06	6.95E-16
7.13E-07	6.63E-05	6.15E-05	9.67E-06	2.91E-05	6.25E-05	1.11E-07	6.60E-05	6.49E-05	2.41E-05	2.87E-05	7.01E-06	5.40E-06	1.37E-16
7.13E-07	6.63E-05	6.14E-05	9.67E-06	2.91E-05	6.25E-05	1.11E-07	6.60E-05	6.48E-05	2.40E-05	2.87E-05	6.96E-06	5.33E-06	2.18E-16
7.13E-07	6.63E-05	6.14E-05	9.67E-06	2.91E-05	6.25E-05	1.11E-07	6.59E-05	6.48E-05	2.40E-05	2.86E-05	6.90E-06	5.27E-06	6.17E-16
2.94E-08	6.63E-05	3.94E-07	9.67E-06	2.91E-05	6.25E-05	0.00014	1.42E-07	2.24E-07	3.43E-05	4.20E-05	1.56E-05	1.50E-05	4.84E-16
2.94E-08	6.63E-05	3.94E-07	9.67E-06	2.91E-05	6.25E-05	0.00014	1.42E-07	2.24E-07	3.43E-05	4.19E-05	1.56E-05	1.49E-05	3.72E-16
2.94E-08	6.63E-05	3.94E-07	9.67E-06	2.91E-05	6.25E-05	0.00014	1.42E-07	2.24E-07	3.42E-05	4.18E-05	1.55E-05	1.48E-05	1.59E-16
2.94E-08	6.63E-05	3.94E-07	9.67E-06	2.91E-05	6.25E-05	0.00014	1.42E-07	2.24E-07	3.41E-05	4.17E-05	1.54E-05	1.47E-05	3.14E-16
2.94E-08	6.63E-05	3.94E-07	9.67E-06	2.91E-05	6.25E-05	0.00014	1.42E-07	2.24E-07	3.41E-05	4.17E-05	1.54E-05	1.47E-05	2.16E-16
2.94E-08	6.63E-05	3.94E-07	9.67E-06	2.91E-05	6.25E-05	0.00014	1.42E-07	2.24E-07	3.40E-05	4.16E-05	1.53E-05	1.46E-05	7.18E-17
2.94E-08	6.63E-05	3.94E-07	9.67E-06	2.91E-05	6.25E-05	0.00014	1.42E-07	2.24E-07	3.40E-05	4.15E-05	1.52E-05	1.45E-05	2.39E-16
0.000148	6.64E-05	2.01E-07	9.67E-06	2.91E-05	6.25E-05	0.00014	0.000142	6.25E-07	3.67E-05	4.50E-05	1.76E-05	1.71E-05	2.94E-16
0.000148	6.64E-05	2.01E-07	9.67E-06	2.91E-05	6.25E-05	0.00014	0.000142	6.25E-07	3.66E-05	4.50E-05	1.75E-05	1.71E-05	2.53E-16
0.000148	6.64E-05	2.01E-07	9.67E-06	2.91E-05	6.25E-05	0.00014	0.000142	6.25E-07	3.65E-05	4.49E-05	1.75E-05	1.70E-05	5.43E-16
0.000148	6.64E-05	2.01E-07	9.67E-06	2.91E-05	6.25E-05	0.00014	0.000142	6.25E-07	3.65E-05	4.48E-05	1.74E-05	1.69E-05	2.91E-16
0.000148	6.64E-05	2.01E-07	9.67E-06	2.91E-05	6.25E-05	0.00014	0.000142	6.25E-07	3.64E-05	4.47E-05	1.73E-05	1.68E-05	1.64E-16
0.000148	6.64E-05	2.01E-07	9.67E-06	2.91E-05	6.25E-05	0.00014	0.000142	6.25E-07	3.64E-05	4.46E-05	1.73E-05	1.68E-05	4.57E-16
0.000148	6.64E-05	2.01E-07	9.67E-06	2.91E-05	6.25E-05	0.00014	0.000142	6.25E-07	3.63E-05	4.45E-05	1.72E-05	1.67E-05	6.69E-16
4.71E-05	2.20E-06	2.01E-07	1.31E-05	1.26E-05	2.61E-07	4.17E-05	4.63E-05	6.25E-07	3.67E-05	4.50E-05	1.76E-05	1.71E-05	2.94E-16
4.71E-05	2.20E-06	2.01E-07	1.31E-05	1.26E-05	2.61E-07	4.17E-05	4.63E-05	6.25E-07	3.66E-05	4.50E-05	1.75E-05	1.71E-05	2.53E-16

4.71E-05	2.20E-06	2.01E-07	1.31E-05	1.26E-05	2.61E-07	4.17E-05	4.63E-05	6.25E-07	3.65E-05	4.49E-05	1.75E-05	1.70E-05	5.43E-16
4.71E-05	2.20E-06	2.01E-07	1.31E-05	1.26E-05	2.61E-07	4.17E-05	4.63E-05	6.25E-07	3.65E-05	4.48E-05	1.74E-05	1.69E-05	2.91E-16
4.71E-05	2.20E-06	2.01E-07	1.31E-05	1.26E-05	2.61E-07	4.17E-05	4.63E-05	6.25E-07	3.64E-05	4.47E-05	1.73E-05	1.68E-05	1.64E-16
4.71E-05	2.20E-06	2.01E-07	1.31E-05	1.26E-05	2.61E-07	4.17E-05	4.63E-05	6.25E-07	3.64E-05	4.46E-05	1.73E-05	1.68E-05	4.57E-16
4.71E-05	2.20E-06	2.01E-07	1.31E-05	1.26E-05	2.61E-07	4.17E-05	4.63E-05	6.25E-07	3.63E-05	4.45E-05	1.72E-05	1.67E-05	6.69E-16

C.2 Segment Lifting

Table C.2 Strain data for segment lifting operation

Location													
182	115	191	32	53	109	180	183	185	247	250	280	296	328
4.96E-05	3.12E-06	2.01E-07	1.40E-05	1.28E-05	1.09E-06	4.41E-05	4.87E-05	6.25E-07	3.29E-05	4.04E-05	1.67E-05	1.69E-05	5.24E-17
4.96E-05	3.12E-06	2.01E-07	1.40E-05	1.28E-05	1.09E-06	4.41E-05	4.87E-05	6.25E-07	3.28E-05	4.03E-05	1.66E-05	1.68E-05	3.69E-16
4.96E-05	3.12E-06	2.01E-07	1.40E-05	1.28E-05	1.09E-06	4.41E-05	4.87E-05	6.25E-07	3.28E-05	4.02E-05	1.65E-05	1.67E-05	3.03E-16
4.96E-05	3.12E-06	2.01E-07	1.40E-05	1.28E-05	1.09E-06	4.41E-05	4.87E-05	6.25E-07	3.27E-05	4.02E-05	1.65E-05	1.66E-05	1.36E-16
4.96E-05	3.12E-06	2.01E-07	1.40E-05	1.28E-05	1.09E-06	4.41E-05	4.87E-05	6.25E-07	3.26E-05	4.01E-05	1.64E-05	1.66E-05	7.21E-17
4.96E-05	3.12E-06	2.01E-07	1.40E-05	1.28E-05	1.09E-06	4.41E-05	4.87E-05	6.25E-07	3.26E-05	4.00E-05	1.63E-05	1.65E-05	1.80E-16
4.96E-05	3.12E-06	2.01E-07	1.40E-05	1.28E-05	1.09E-06	4.41E-05	4.87E-05	6.25E-07	3.25E-05	3.99E-05	1.63E-05	1.64E-05	4.36E-16
5.01E-05	3.23E-06	2.01E-07	1.43E-05	1.29E-05	1.17E-06	4.45E-05	4.92E-05	6.25E-07	3.29E-05	4.04E-05	1.67E-05	1.69E-05	5.24E-17
5.01E-05	3.23E-06	2.01E-07	1.43E-05	1.29E-05	1.17E-06	4.45E-05	4.92E-05	6.25E-07	3.28E-05	4.03E-05	1.66E-05	1.68E-05	3.69E-16
5.01E-05	3.23E-06	2.01E-07	1.43E-05	1.29E-05	1.17E-06	4.45E-05	4.92E-05	6.25E-07	3.28E-05	4.02E-05	1.65E-05	1.67E-05	3.03E-16
5.01E-05	3.23E-06	2.01E-07	1.43E-05	1.29E-05	1.17E-06	4.45E-05	4.92E-05	6.25E-07	3.27E-05	4.02E-05	1.65E-05	1.66E-05	1.36E-16
5.01E-05	3.23E-06	2.01E-07	1.43E-05	1.29E-05	1.17E-06	4.45E-05	4.92E-05	6.25E-07	3.26E-05	4.01E-05	1.64E-05	1.66E-05	7.21E-17
5.01E-05	3.23E-06	2.01E-07	1.43E-05	1.29E-05	1.17E-06	4.45E-05	4.92E-05	6.25E-07	3.26E-05	4.00E-05	1.63E-05	1.65E-05	1.80E-16
5.01E-05	3.23E-06	2.01E-07	1.43E-05	1.29E-05	1.17E-06	4.45E-05	4.92E-05	6.25E-07	3.25E-05	3.99E-05	1.63E-05	1.64E-05	4.36E-16
5.35E-05	3.96E-06	2.01E-07	1.64E-05	1.41E-05	1.74E-06	4.77E-05	5.25E-05	6.25E-07	3.29E-05	4.04E-05	1.67E-05	1.69E-05	5.24E-17
5.35E-05	3.96E-06	2.01E-07	1.64E-05	1.41E-05	1.74E-06	4.77E-05	5.25E-05	6.25E-07	3.28E-05	4.03E-05	1.66E-05	1.68E-05	3.69E-16
5.35E-05	3.96E-06	2.01E-07	1.64E-05	1.41E-05	1.74E-06	4.77E-05	5.25E-05	6.25E-07	3.28E-05	4.02E-05	1.65E-05	1.67E-05	3.03E-16
5.35E-05	3.96E-06	2.01E-07	1.64E-05	1.41E-05	1.74E-06	4.77E-05	5.25E-05	6.25E-07	3.27E-05	4.02E-05	1.65E-05	1.66E-05	1.36E-16

5.35E-05	3.96E-06	2.01E-07	1.64E-05	1.41E-05	1.74E-06	4.77E-05	5.25E-05	6.25E-07	3.26E-05	4.01E-05	1.64E-05	1.66E-05	7.21E-17
5.35E-05	3.96E-06	2.01E-07	1.64E-05	1.41E-05	1.74E-06	4.77E-05	5.25E-05	6.25E-07	3.26E-05	4.00E-05	1.63E-05	1.65E-05	1.80E-16
5.35E-05	3.96E-06	2.01E-07	1.64E-05	1.41E-05	1.74E-06	4.77E-05	5.25E-05	6.25E-07	3.25E-05	3.99E-05	1.63E-05	1.64E-05	4.36E-16
8.19E-05	2.18E-05	2.01E-07	9.73E-06	2.26E-06	1.90E-05	7.48E-05	7.97E-05	6.25E-07	3.29E-05	4.04E-05	1.67E-05	1.69E-05	5.24E-17
8.21E-05	2.18E-05	2.01E-07	9.78E-06	2.27E-06	1.91E-05	7.49E-05	7.98E-05	6.25E-07	3.29E-05	4.04E-05	1.67E-05	1.69E-05	5.24E-17
8.23E-05	2.19E-05	2.01E-07	9.82E-06	2.28E-06	1.91E-05	7.51E-05	8.00E-05	6.25E-07	3.29E-05	4.04E-05	1.67E-05	1.69E-05	5.24E-17
8.19E-05	2.18E-05	2.01E-07	9.73E-06	2.26E-06	1.90E-05	7.48E-05	7.97E-05	6.25E-07	3.28E-05	4.03E-05	1.66E-05	1.68E-05	3.69E-16
8.21E-05	2.18E-05	2.01E-07	9.78E-06	2.27E-06	1.91E-05	7.49E-05	7.98E-05	6.25E-07	3.28E-05	4.03E-05	1.66E-05	1.68E-05	3.69E-16
8.23E-05	2.19E-05	2.01E-07	9.82E-06	2.28E-06	1.91E-05	7.51E-05	8.00E-05	6.25E-07	3.28E-05	4.03E-05	1.66E-05	1.68E-05	3.69E-16
8.19E-05	2.18E-05	2.01E-07	9.73E-06	2.26E-06	1.90E-05	7.48E-05	7.97E-05	6.25E-07	3.28E-05	4.02E-05	1.65E-05	1.67E-05	3.03E-16
8.21E-05	2.18E-05	2.01E-07	9.78E-06	2.27E-06	1.91E-05	7.49E-05	7.98E-05	6.25E-07	3.28E-05	4.02E-05	1.65E-05	1.67E-05	3.03E-16
8.23E-05	2.19E-05	2.01E-07	9.82E-06	2.28E-06	1.91E-05	7.51E-05	8.00E-05	6.25E-07	3.28E-05	4.02E-05	1.65E-05	1.67E-05	3.03E-16
8.19E-05	2.18E-05	2.01E-07	9.73E-06	2.26E-06	1.90E-05	7.48E-05	7.97E-05	6.25E-07	3.27E-05	4.02E-05	1.65E-05	1.66E-05	1.36E-16
8.21E-05	2.18E-05	2.01E-07	9.78E-06	2.27E-06	1.91E-05	7.49E-05	7.98E-05	6.25E-07	3.27E-05	4.02E-05	1.65E-05	1.66E-05	1.36E-16
8.23E-05	2.19E-05	2.01E-07	9.82E-06	2.28E-06	1.91E-05	7.51E-05	8.00E-05	6.25E-07	3.27E-05	4.02E-05	1.65E-05	1.66E-05	1.36E-16
8.19E-05	2.18E-05	2.01E-07	9.73E-06	2.26E-06	1.90E-05	7.48E-05	7.97E-05	6.25E-07	3.26E-05	4.01E-05	1.64E-05	1.66E-05	7.21E-17
8.21E-05	2.18E-05	2.01E-07	9.78E-06	2.27E-06	1.91E-05	7.49E-05	7.98E-05	6.25E-07	3.26E-05	4.01E-05	1.64E-05	1.66E-05	7.21E-17
8.23E-05	2.19E-05	2.01E-07	9.82E-06	2.28E-06	1.91E-05	7.51E-05	8.00E-05	6.25E-07	3.26E-05	4.01E-05	1.64E-05	1.66E-05	7.21E-17
8.19E-05	2.18E-05	2.01E-07	9.73E-06	2.26E-06	1.90E-05	7.48E-05	7.97E-05	6.25E-07	3.26E-05	4.00E-05	1.63E-05	1.65E-05	1.80E-16
8.21E-05	2.18E-05	2.01E-07	9.78E-06	2.27E-06	1.91E-05	7.49E-05	7.98E-05	6.25E-07	3.26E-05	4.00E-05	1.63E-05	1.65E-05	1.80E-16
8.23E-05	2.19E-05	2.01E-07	9.82E-06	2.28E-06	1.91E-05	7.51E-05	8.00E-05	6.25E-07	3.26E-05	4.00E-05	1.63E-05	1.65E-05	1.80E-16
8.19E-05	2.18E-05	2.01E-07	9.73E-06	2.26E-06	1.90E-05	7.48E-05	7.97E-05	6.25E-07	3.25E-05	3.99E-05	1.63E-05	1.64E-05	4.36E-16
8.21E-05	2.18E-05	2.01E-07	9.78E-06	2.27E-06	1.91E-05	7.49E-05	7.98E-05	6.25E-07	3.25E-05	3.99E-05	1.63E-05	1.64E-05	4.36E-16
8.23E-05	2.19E-05	2.01E-07	9.82E-06	2.28E-06	1.91E-05	7.51E-05	8.00E-05	6.25E-07	3.25E-05	3.99E-05	1.63E-05	1.64E-05	4.36E-16
8.34E-05	2.14E-05	2.01E-07	9.67E-06	2.34E-06	1.87E-05	7.57E-05	8.12E-05	6.25E-07	3.29E-05	4.04E-05	1.67E-05	1.69E-05	5.24E-17
8.36E-05	2.15E-05	2.01E-07	9.72E-06	2.35E-06	1.87E-05	7.59E-05	8.14E-05	6.25E-07	3.29E-05	4.04E-05	1.67E-05	1.69E-05	5.24E-17
8.38E-05	2.15E-05	2.01E-07	9.77E-06	2.36E-06	1.88E-05	7.61E-05	8.17E-05	6.25E-07	3.29E-05	4.04E-05	1.67E-05	1.69E-05	5.24E-17
8.34E-05	2.14E-05	2.01E-07	9.67E-06	2.34E-06	1.87E-05	7.57E-05	8.12E-05	6.25E-07	3.28E-05	4.03E-05	1.66E-05	1.68E-05	3.69E-16
8.36E-05	2.15E-05	2.01E-07	9.72E-06	2.35E-06	1.87E-05	7.59E-05	8.14E-05	6.25E-07	3.28E-05	4.03E-05	1.66E-05	1.68E-05	3.69E-16
8.38E-05	2.15E-05	2.01E-07	9.77E-06	2.36E-06	1.88E-05	7.61E-05	8.17E-05	6.25E-07	3.28E-05	4.03E-05	1.66E-05	1.68E-05	3.69E-16

8.34E-05	2.14E-05	2.01E-07	9.67E-06	2.34E-06	1.87E-05	7.57E-05	8.12E-05	6.25E-07	3.28E-05	4.02E-05	1.65E-05	1.67E-05	3.03E-16
8.36E-05	2.15E-05	2.01E-07	9.72E-06	2.35E-06	1.87E-05	7.59E-05	8.14E-05	6.25E-07	3.28E-05	4.02E-05	1.65E-05	1.67E-05	3.03E-16
8.38E-05	2.15E-05	2.01E-07	9.77E-06	2.36E-06	1.88E-05	7.61E-05	8.17E-05	6.25E-07	3.28E-05	4.02E-05	1.65E-05	1.67E-05	3.03E-16
8.34E-05	2.14E-05	2.01E-07	9.67E-06	2.34E-06	1.87E-05	7.57E-05	8.12E-05	6.25E-07	3.27E-05	4.02E-05	1.65E-05	1.66E-05	1.36E-16
8.36E-05	2.15E-05	2.01E-07	9.72E-06	2.35E-06	1.87E-05	7.59E-05	8.14E-05	6.25E-07	3.27E-05	4.02E-05	1.65E-05	1.66E-05	1.36E-16
8.38E-05	2.15E-05	2.01E-07	9.77E-06	2.36E-06	1.88E-05	7.61E-05	8.17E-05	6.25E-07	3.27E-05	4.02E-05	1.65E-05	1.66E-05	1.36E-16
8.34E-05	2.14E-05	2.01E-07	9.67E-06	2.34E-06	1.87E-05	7.57E-05	8.12E-05	6.25E-07	3.26E-05	4.01E-05	1.64E-05	1.66E-05	7.21E-17
8.36E-05	2.15E-05	2.01E-07	9.72E-06	2.35E-06	1.87E-05	7.59E-05	8.14E-05	6.25E-07	3.26E-05	4.01E-05	1.64E-05	1.66E-05	7.21E-17
8.38E-05	2.15E-05	2.01E-07	9.77E-06	2.36E-06	1.88E-05	7.61E-05	8.17E-05	6.25E-07	3.26E-05	4.01E-05	1.64E-05	1.66E-05	7.21E-17
8.34E-05	2.14E-05	2.01E-07	9.67E-06	2.34E-06	1.87E-05	7.57E-05	8.12E-05	6.25E-07	3.26E-05	4.00E-05	1.63E-05	1.65E-05	1.80E-16
8.36E-05	2.15E-05	2.01E-07	9.72E-06	2.35E-06	1.87E-05	7.59E-05	8.14E-05	6.25E-07	3.26E-05	4.00E-05	1.63E-05	1.65E-05	1.80E-16
8.38E-05	2.15E-05	2.01E-07	9.77E-06	2.36E-06	1.88E-05	7.61E-05	8.17E-05	6.25E-07	3.26E-05	4.00E-05	1.63E-05	1.65E-05	1.80E-16
8.34E-05	2.14E-05	2.01E-07	9.67E-06	2.34E-06	1.87E-05	7.57E-05	8.12E-05	6.25E-07	3.25E-05	3.99E-05	1.63E-05	1.64E-05	4.36E-16
8.36E-05	2.15E-05	2.01E-07	9.72E-06	2.35E-06	1.87E-05	7.59E-05	8.14E-05	6.25E-07	3.25E-05	3.99E-05	1.63E-05	1.64E-05	4.36E-16
8.38E-05	2.15E-05	2.01E-07	9.77E-06	2.36E-06	1.88E-05	7.61E-05	8.17E-05	6.25E-07	3.25E-05	3.99E-05	1.63E-05	1.64E-05	4.36E-16
8.58E-05	2.07E-05	2.01E-07	9.70E-06	2.62E-06	1.81E-05	7.77E-05	8.37E-05	6.25E-07	3.29E-05	4.04E-05	1.67E-05	1.69E-05	5.24E-17
8.61E-05	2.08E-05	2.01E-07	9.76E-06	2.65E-06	1.81E-05	7.80E-05	8.40E-05	6.25E-07	3.29E-05	4.04E-05	1.67E-05	1.69E-05	5.24E-17
8.64E-05	2.08E-05	2.01E-07	9.81E-06	2.67E-06	1.81E-05	7.82E-05	8.43E-05	6.25E-07	3.29E-05	4.04E-05	1.67E-05	1.69E-05	5.24E-17
8.58E-05	2.07E-05	2.01E-07	9.70E-06	2.62E-06	1.81E-05	7.77E-05	8.37E-05	6.25E-07	3.28E-05	4.03E-05	1.66E-05	1.68E-05	3.69E-16
8.61E-05	2.08E-05	2.01E-07	9.76E-06	2.65E-06	1.81E-05	7.80E-05	8.40E-05	6.25E-07	3.28E-05	4.03E-05	1.66E-05	1.68E-05	3.69E-16
8.64E-05	2.08E-05	2.01E-07	9.81E-06	2.67E-06	1.81E-05	7.82E-05	8.43E-05	6.25E-07	3.28E-05	4.03E-05	1.66E-05	1.68E-05	3.69E-16
8.58E-05	2.07E-05	2.01E-07	9.70E-06	2.62E-06	1.81E-05	7.77E-05	8.37E-05	6.25E-07	3.28E-05	4.02E-05	1.65E-05	1.67E-05	3.03E-16
8.61E-05	2.08E-05	2.01E-07	9.76E-06	2.65E-06	1.81E-05	7.80E-05	8.40E-05	6.25E-07	3.28E-05	4.02E-05	1.65E-05	1.67E-05	3.03E-16
8.64E-05	2.08E-05	2.01E-07	9.81E-06	2.67E-06	1.81E-05	7.82E-05	8.43E-05	6.25E-07	3.28E-05	4.02E-05	1.65E-05	1.67E-05	3.03E-16
8.58E-05	2.07E-05	2.01E-07	9.70E-06	2.62E-06	1.81E-05	7.77E-05	8.37E-05	6.25E-07	3.27E-05	4.02E-05	1.65E-05	1.66E-05	1.36E-16
8.61E-05	2.08E-05	2.01E-07	9.76E-06	2.65E-06	1.81E-05	7.80E-05	8.40E-05	6.25E-07	3.27E-05	4.02E-05	1.65E-05	1.66E-05	1.36E-16
8.64E-05	2.08E-05	2.01E-07	9.81E-06	2.67E-06	1.81E-05	7.82E-05	8.43E-05	6.25E-07	3.27E-05	4.02E-05	1.65E-05	1.66E-05	1.36E-16
8.58E-05	2.07E-05	2.01E-07	9.70E-06	2.62E-06	1.81E-05	7.77E-05	8.37E-05	6.25E-07	3.26E-05	4.01E-05	1.64E-05	1.66E-05	7.21E-17
8.61E-05	2.08E-05	2.01E-07	9.76E-06	2.65E-06	1.81E-05	7.80E-05	8.40E-05	6.25E-07	3.26E-05	4.01E-05	1.64E-05	1.66E-05	7.21E-17
8.64E-05	2.08E-05	2.01E-07	9.81E-06	2.67E-06	1.81E-05	7.82E-05	8.43E-05	6.25E-07	3.26E-05	4.01E-05	1.64E-05	1.66E-05	7.21E-17

8.58E-05	2.07E-05	2.01E-07	9.70E-06	2.62E-06	1.81E-05	7.77E-05	8.37E-05	6.25E-07	3.26E-05	4.00E-05	1.63E-05	1.65E-05	1.80E-16
8.61E-05	2.08E-05	2.01E-07	9.76E-06	2.65E-06	1.81E-05	7.80E-05	8.40E-05	6.25E-07	3.26E-05	4.00E-05	1.63E-05	1.65E-05	1.80E-16
8.64E-05	2.08E-05	2.01E-07	9.81E-06	2.67E-06	1.81E-05	7.82E-05	8.43E-05	6.25E-07	3.26E-05	4.00E-05	1.63E-05	1.65E-05	1.80E-16
8.58E-05	2.07E-05	2.01E-07	9.70E-06	2.62E-06	1.81E-05	7.77E-05	8.37E-05	6.25E-07	3.25E-05	3.99E-05	1.63E-05	1.64E-05	4.36E-16
8.61E-05	2.08E-05	2.01E-07	9.76E-06	2.65E-06	1.81E-05	7.80E-05	8.40E-05	6.25E-07	3.25E-05	3.99E-05	1.63E-05	1.64E-05	4.36E-16
8.64E-05	2.08E-05	2.01E-07	9.81E-06	2.67E-06	1.81E-05	7.82E-05	8.43E-05	6.25E-07	3.25E-05	3.99E-05	1.63E-05	1.64E-05	4.36E-16
8.91E-05	1.96E-05	2.01E-07	9.88E-06	3.23E-06	1.70E-05	8.05E-05	8.69E-05	6.25E-07	3.29E-05	4.04E-05	1.67E-05	1.69E-05	5.24E-17
8.95E-05	1.96E-05	2.01E-07	9.95E-06	3.27E-06	1.70E-05	8.09E-05	8.73E-05	6.25E-07	3.29E-05	4.04E-05	1.67E-05	1.69E-05	5.24E-17
8.99E-05	1.96E-05	2.01E-07	1.00E-05	3.31E-06	1.70E-05	8.12E-05	8.78E-05	6.25E-07	3.29E-05	4.04E-05	1.67E-05	1.69E-05	5.24E-17
8.91E-05	1.96E-05	2.01E-07	9.88E-06	3.23E-06	1.70E-05	8.05E-05	8.69E-05	6.25E-07	3.28E-05	4.03E-05	1.66E-05	1.68E-05	3.69E-16
8.95E-05	1.96E-05	2.01E-07	9.95E-06	3.27E-06	1.70E-05	8.09E-05	8.73E-05	6.25E-07	3.28E-05	4.03E-05	1.66E-05	1.68E-05	3.69E-16
8.99E-05	1.96E-05	2.01E-07	1.00E-05	3.31E-06	1.70E-05	8.12E-05	8.78E-05	6.25E-07	3.28E-05	4.03E-05	1.66E-05	1.68E-05	3.69E-16
8.91E-05	1.96E-05	2.01E-07	9.88E-06	3.23E-06	1.70E-05	8.05E-05	8.69E-05	6.25E-07	3.28E-05	4.02E-05	1.65E-05	1.67E-05	3.03E-16
8.95E-05	1.96E-05	2.01E-07	9.95E-06	3.27E-06	1.70E-05	8.09E-05	8.73E-05	6.25E-07	3.28E-05	4.02E-05	1.65E-05	1.67E-05	3.03E-16
8.99E-05	1.96E-05	2.01E-07	1.00E-05	3.31E-06	1.70E-05	8.12E-05	8.78E-05	6.25E-07	3.28E-05	4.02E-05	1.65E-05	1.67E-05	3.03E-16
8.91E-05	1.96E-05	2.01E-07	9.88E-06	3.23E-06	1.70E-05	8.05E-05	8.69E-05	6.25E-07	3.27E-05	4.02E-05	1.65E-05	1.66E-05	1.36E-16
8.95E-05	1.96E-05	2.01E-07	9.95E-06	3.27E-06	1.70E-05	8.09E-05	8.73E-05	6.25E-07	3.27E-05	4.02E-05	1.65E-05	1.66E-05	1.36E-16
8.99E-05	1.96E-05	2.01E-07	1.00E-05	3.31E-06	1.70E-05	8.12E-05	8.78E-05	6.25E-07	3.27E-05	4.02E-05	1.65E-05	1.66E-05	1.36E-16
8.91E-05	1.96E-05	2.01E-07	9.88E-06	3.23E-06	1.70E-05	8.05E-05	8.69E-05	6.25E-07	3.26E-05	4.01E-05	1.64E-05	1.66E-05	7.21E-17
8.95E-05	1.96E-05	2.01E-07	9.95E-06	3.27E-06	1.70E-05	8.09E-05	8.73E-05	6.25E-07	3.26E-05	4.01E-05	1.64E-05	1.66E-05	7.21E-17
8.99E-05	1.96E-05	2.01E-07	1.00E-05	3.31E-06	1.70E-05	8.12E-05	8.78E-05	6.25E-07	3.26E-05	4.01E-05	1.64E-05	1.66E-05	7.21E-17
8.91E-05	1.96E-05	2.01E-07	9.88E-06	3.23E-06	1.70E-05	8.05E-05	8.69E-05	6.25E-07	3.26E-05	4.00E-05	1.63E-05	1.65E-05	1.80E-16
8.95E-05	1.96E-05	2.01E-07	9.95E-06	3.27E-06	1.70E-05	8.09E-05	8.73E-05	6.25E-07	3.26E-05	4.00E-05	1.63E-05	1.65E-05	1.80E-16
8.99E-05	1.96E-05	2.01E-07	1.00E-05	3.31E-06	1.70E-05	8.12E-05	8.78E-05	6.25E-07	3.26E-05	4.00E-05	1.63E-05	1.65E-05	1.80E-16
8.91E-05	1.96E-05	2.01E-07	9.88E-06	3.23E-06	1.70E-05	8.05E-05	8.69E-05	6.25E-07	3.25E-05	3.99E-05	1.63E-05	1.64E-05	4.36E-16
8.95E-05	1.96E-05	2.01E-07	9.95E-06	3.27E-06	1.70E-05	8.09E-05	8.73E-05	6.25E-07	3.25E-05	3.99E-05	1.63E-05	1.64E-05	4.36E-16
8.99E-05	1.96E-05	2.01E-07	1.00E-05	3.31E-06	1.70E-05	8.12E-05	8.78E-05	6.25E-07	3.25E-05	3.99E-05	1.63E-05	1.64E-05	4.36E-16
9.30E-05	1.90E-05	2.01E-07	1.03E-05	4.22E-06	1.61E-05	8.40E-05	9.07E-05	6.25E-07	3.29E-05	4.04E-05	1.67E-05	1.69E-05	5.24E-17
9.35E-05	1.90E-05	2.01E-07	1.03E-05	4.29E-06	1.60E-05	8.45E-05	9.13E-05	6.25E-07	3.29E-05	4.04E-05	1.67E-05	1.69E-05	5.24E-17
9.41E-05	1.90E-05	2.01E-07	1.04E-05	4.35E-06	1.60E-05	8.49E-05	9.19E-05	6.25E-07	3.29E-05	4.04E-05	1.67E-05	1.69E-05	5.24E-17

9.30E-05	1.90E-05	2.01E-07	1.03E-05	4.22E-06	1.61E-05	8.40E-05	9.07E-05	6.25E-07	3.28E-05	4.03E-05	1.66E-05	1.68E-05	3.69E-16
9.35E-05	1.90E-05	2.01E-07	1.03E-05	4.29E-06	1.60E-05	8.45E-05	9.13E-05	6.25E-07	3.28E-05	4.03E-05	1.66E-05	1.68E-05	3.69E-16
9.41E-05	1.90E-05	2.01E-07	1.04E-05	4.35E-06	1.60E-05	8.49E-05	9.19E-05	6.25E-07	3.28E-05	4.03E-05	1.66E-05	1.68E-05	3.69E-16
9.30E-05	1.90E-05	2.01E-07	1.03E-05	4.22E-06	1.61E-05	8.40E-05	9.07E-05	6.25E-07	3.28E-05	4.02E-05	1.65E-05	1.67E-05	3.03E-16
9.35E-05	1.90E-05	2.01E-07	1.03E-05	4.29E-06	1.60E-05	8.45E-05	9.13E-05	6.25E-07	3.28E-05	4.02E-05	1.65E-05	1.67E-05	3.03E-16
9.41E-05	1.90E-05	2.01E-07	1.04E-05	4.35E-06	1.60E-05	8.49E-05	9.19E-05	6.25E-07	3.28E-05	4.02E-05	1.65E-05	1.67E-05	3.03E-16
9.30E-05	1.90E-05	2.01E-07	1.03E-05	4.22E-06	1.61E-05	8.40E-05	9.07E-05	6.25E-07	3.27E-05	4.02E-05	1.65E-05	1.66E-05	1.36E-16
9.35E-05	1.90E-05	2.01E-07	1.03E-05	4.29E-06	1.60E-05	8.45E-05	9.13E-05	6.25E-07	3.27E-05	4.02E-05	1.65E-05	1.66E-05	1.36E-16
9.41E-05	1.90E-05	2.01E-07	1.04E-05	4.35E-06	1.60E-05	8.49E-05	9.19E-05	6.25E-07	3.27E-05	4.02E-05	1.65E-05	1.66E-05	1.36E-16
9.30E-05	1.90E-05	2.01E-07	1.03E-05	4.22E-06	1.61E-05	8.40E-05	9.07E-05	6.25E-07	3.26E-05	4.01E-05	1.64E-05	1.66E-05	7.21E-17
9.35E-05	1.90E-05	2.01E-07	1.03E-05	4.29E-06	1.60E-05	8.45E-05	9.13E-05	6.25E-07	3.26E-05	4.01E-05	1.64E-05	1.66E-05	7.21E-17
9.41E-05	1.90E-05	2.01E-07	1.04E-05	4.35E-06	1.60E-05	8.49E-05	9.19E-05	6.25E-07	3.26E-05	4.01E-05	1.64E-05	1.66E-05	7.21E-17
9.30E-05	1.90E-05	2.01E-07	1.03E-05	4.22E-06	1.61E-05	8.40E-05	9.07E-05	6.25E-07	3.26E-05	4.00E-05	1.63E-05	1.65E-05	1.80E-16
9.35E-05	1.90E-05	2.01E-07	1.03E-05	4.29E-06	1.60E-05	8.45E-05	9.13E-05	6.25E-07	3.26E-05	4.00E-05	1.63E-05	1.65E-05	1.80E-16
9.41E-05	1.90E-05	2.01E-07	1.04E-05	4.35E-06	1.60E-05	8.49E-05	9.19E-05	6.25E-07	3.26E-05	4.00E-05	1.63E-05	1.65E-05	1.80E-16
9.30E-05	1.90E-05	2.01E-07	1.03E-05	4.22E-06	1.61E-05	8.40E-05	9.07E-05	6.25E-07	3.25E-05	3.99E-05	1.63E-05	1.64E-05	4.36E-16
9.35E-05	1.90E-05	2.01E-07	1.03E-05	4.29E-06	1.60E-05	8.45E-05	9.13E-05	6.25E-07	3.25E-05	3.99E-05	1.63E-05	1.64E-05	4.36E-16
9.41E-05	1.90E-05	2.01E-07	1.04E-05	4.35E-06	1.60E-05	8.49E-05	9.19E-05	6.25E-07	3.25E-05	3.99E-05	1.63E-05	1.64E-05	4.36E-16
9.74E-05	1.90E-05	2.01E-07	1.09E-05	5.61E-06	1.58E-05	8.80E-05	9.50E-05	6.25E-07	3.29E-05	4.04E-05	1.67E-05	1.69E-05	5.24E-17
9.80E-05	1.90E-05	2.01E-07	1.10E-05	5.71E-06	1.58E-05	8.86E-05	9.57E-05	6.25E-07	3.29E-05	4.04E-05	1.67E-05	1.69E-05	5.24E-17
9.87E-05	1.90E-05	2.01E-07	1.11E-05	5.82E-06	1.58E-05	8.92E-05	9.64E-05	6.25E-07	3.29E-05	4.04E-05	1.67E-05	1.69E-05	5.24E-17
9.74E-05	1.90E-05	2.01E-07	1.09E-05	5.61E-06	1.58E-05	8.80E-05	9.50E-05	6.25E-07	3.28E-05	4.03E-05	1.66E-05	1.68E-05	3.69E-16
9.80E-05	1.90E-05	2.01E-07	1.10E-05	5.71E-06	1.58E-05	8.86E-05	9.57E-05	6.25E-07	3.28E-05	4.03E-05	1.66E-05	1.68E-05	3.69E-16
9.87E-05	1.90E-05	2.01E-07	1.11E-05	5.82E-06	1.58E-05	8.92E-05	9.64E-05	6.25E-07	3.28E-05	4.03E-05	1.66E-05	1.68E-05	3.69E-16
9.74E-05	1.90E-05	2.01E-07	1.09E-05	5.61E-06	1.58E-05	8.80E-05	9.50E-05	6.25E-07	3.28E-05	4.02E-05	1.65E-05	1.67E-05	3.03E-16
9.80E-05	1.90E-05	2.01E-07	1.10E-05	5.71E-06	1.58E-05	8.86E-05	9.57E-05	6.25E-07	3.28E-05	4.02E-05	1.65E-05	1.67E-05	3.03E-16
9.87E-05	1.90E-05	2.01E-07	1.11E-05	5.82E-06	1.58E-05	8.92E-05	9.64E-05	6.25E-07	3.28E-05	4.02E-05	1.65E-05	1.67E-05	3.03E-16
9.74E-05	1.90E-05	2.01E-07	1.09E-05	5.61E-06	1.58E-05	8.80E-05	9.50E-05	6.25E-07	3.27E-05	4.02E-05	1.65E-05	1.66E-05	1.36E-16
9.80E-05	1.90E-05	2.01E-07	1.10E-05	5.71E-06	1.58E-05	8.86E-05	9.57E-05	6.25E-07	3.27E-05	4.02E-05	1.65E-05	1.66E-05	1.36E-16
9.87E-05	1.90E-05	2.01E-07	1.11E-05	5.82E-06	1.58E-05	8.92E-05	9.64E-05	6.25E-07	3.27E-05	4.02E-05	1.65E-05	1.66E-05	1.36E-16

9.74E-05	1.90E-05	2.01E-07	1.09E-05	5.61E-06	1.58E-05	8.80E-05	9.50E-05	6.25E-07	3.26E-05	4.01E-05	1.64E-05	1.66E-05	7.21E-17
9.80E-05	1.90E-05	2.01E-07	1.10E-05	5.71E-06	1.58E-05	8.86E-05	9.57E-05	6.25E-07	3.26E-05	4.01E-05	1.64E-05	1.66E-05	7.21E-17
9.87E-05	1.90E-05	2.01E-07	1.11E-05	5.82E-06	1.58E-05	8.92E-05	9.64E-05	6.25E-07	3.26E-05	4.01E-05	1.64E-05	1.66E-05	7.21E-17
9.74E-05	1.90E-05	2.01E-07	1.09E-05	5.61E-06	1.58E-05	8.80E-05	9.50E-05	6.25E-07	3.26E-05	4.00E-05	1.63E-05	1.65E-05	1.80E-16
9.80E-05	1.90E-05	2.01E-07	1.10E-05	5.71E-06	1.58E-05	8.86E-05	9.57E-05	6.25E-07	3.26E-05	4.00E-05	1.63E-05	1.65E-05	1.80E-16
9.87E-05	1.90E-05	2.01E-07	1.11E-05	5.82E-06	1.58E-05	8.92E-05	9.64E-05	6.25E-07	3.26E-05	4.00E-05	1.63E-05	1.65E-05	1.80E-16
9.74E-05	1.90E-05	2.01E-07	1.09E-05	5.61E-06	1.58E-05	8.80E-05	9.50E-05	6.25E-07	3.25E-05	3.99E-05	1.63E-05	1.64E-05	4.36E-16
9.80E-05	1.90E-05	2.01E-07	1.10E-05	5.71E-06	1.58E-05	8.86E-05	9.57E-05	6.25E-07	3.25E-05	3.99E-05	1.63E-05	1.64E-05	4.36E-16
9.87E-05	1.90E-05	2.01E-07	1.11E-05	5.82E-06	1.58E-05	8.92E-05	9.64E-05	6.25E-07	3.25E-05	3.99E-05	1.63E-05	1.64E-05	4.36E-16
0.000102	1.97E-05	2.01E-07	1.18E-05	7.44E-06	1.62E-05	9.23E-05	9.96E-05	6.25E-07	3.29E-05	4.04E-05	1.67E-05	1.69E-05	5.24E-17
0.000103	1.97E-05	2.01E-07	1.19E-05	7.60E-06	1.62E-05	9.30E-05	0.0001	6.25E-07	3.29E-05	4.04E-05	1.67E-05	1.69E-05	5.24E-17
0.000104	1.97E-05	2.01E-07	1.20E-05	7.75E-06	1.62E-05	9.38E-05	0.000101	6.25E-07	3.29E-05	4.04E-05	1.67E-05	1.69E-05	5.24E-17
0.000102	1.97E-05	2.01E-07	1.18E-05	7.44E-06	1.62E-05	9.23E-05	9.96E-05	6.25E-07	3.28E-05	4.03E-05	1.66E-05	1.68E-05	3.69E-16
0.000103	1.97E-05	2.01E-07	1.19E-05	7.60E-06	1.62E-05	9.30E-05	0.0001	6.25E-07	3.28E-05	4.03E-05	1.66E-05	1.68E-05	3.69E-16
0.000104	1.97E-05	2.01E-07	1.20E-05	7.75E-06	1.62E-05	9.38E-05	0.000101	6.25E-07	3.28E-05	4.03E-05	1.66E-05	1.68E-05	3.69E-16
0.000102	1.97E-05	2.01E-07	1.18E-05	7.44E-06	1.62E-05	9.23E-05	9.96E-05	6.25E-07	3.28E-05	4.02E-05	1.65E-05	1.67E-05	3.03E-16
0.000103	1.97E-05	2.01E-07	1.19E-05	7.60E-06	1.62E-05	9.30E-05	0.0001	6.25E-07	3.28E-05	4.02E-05	1.65E-05	1.67E-05	3.03E-16
0.000104	1.97E-05	2.01E-07	1.20E-05	7.75E-06	1.62E-05	9.38E-05	0.000101	6.25E-07	3.28E-05	4.02E-05	1.65E-05	1.67E-05	3.03E-16
0.000102	1.97E-05	2.01E-07	1.18E-05	7.44E-06	1.62E-05	9.23E-05	9.96E-05	6.25E-07	3.27E-05	4.02E-05	1.65E-05	1.66E-05	1.36E-16
0.000103	1.97E-05	2.01E-07	1.19E-05	7.60E-06	1.62E-05	9.30E-05	0.0001	6.25E-07	3.27E-05	4.02E-05	1.65E-05	1.66E-05	1.36E-16
0.000104	1.97E-05	2.01E-07	1.20E-05	7.75E-06	1.62E-05	9.38E-05	0.000101	6.25E-07	3.27E-05	4.02E-05	1.65E-05	1.66E-05	1.36E-16
0.000102	1.97E-05	2.01E-07	1.18E-05	7.44E-06	1.62E-05	9.23E-05	9.96E-05	6.25E-07	3.26E-05	4.01E-05	1.64E-05	1.66E-05	7.21E-17
0.000103	1.97E-05	2.01E-07	1.19E-05	7.60E-06	1.62E-05	9.30E-05	0.0001	6.25E-07	3.26E-05	4.01E-05	1.64E-05	1.66E-05	7.21E-17
0.000104	1.97E-05	2.01E-07	1.20E-05	7.75E-06	1.62E-05	9.38E-05	0.000101	6.25E-07	3.26E-05	4.01E-05	1.64E-05	1.66E-05	7.21E-17
0.000102	1.97E-05	2.01E-07	1.18E-05	7.44E-06	1.62E-05	9.23E-05	9.96E-05	6.25E-07	3.26E-05	4.00E-05	1.63E-05	1.65E-05	1.80E-16
0.000103	1.97E-05	2.01E-07	1.19E-05	7.60E-06	1.62E-05	9.30E-05	0.0001	6.25E-07	3.26E-05	4.00E-05	1.63E-05	1.65E-05	1.80E-16
0.000104	1.97E-05	2.01E-07	1.20E-05	7.75E-06	1.62E-05	9.38E-05	0.000101	6.25E-07	3.26E-05	4.00E-05	1.63E-05	1.65E-05	1.80E-16
0.000102	1.97E-05	2.01E-07	1.18E-05	7.44E-06	1.62E-05	9.23E-05	9.96E-05	6.25E-07	3.25E-05	3.99E-05	1.63E-05	1.64E-05	4.36E-16
0.000103	1.97E-05	2.01E-07	1.19E-05	7.60E-06	1.62E-05	9.30E-05	0.0001	6.25E-07	3.25E-05	3.99E-05	1.63E-05	1.64E-05	4.36E-16
0.000104	1.97E-05	2.01E-07	1.20E-05	7.75E-06	1.62E-05	9.38E-05	0.000101	6.25E-07	3.25E-05	3.99E-05	1.63E-05	1.64E-05	4.36E-16

0.000107	2.08E-05	2.01E-07	1.29E-05	8.98E-06	1.72E-05	9.69E-05	0.000104	6.25E-07	3.29E-05	4.04E-05	1.67E-05	1.69E-05	5.24E-17
0.000108	2.09E-05	2.01E-07	1.31E-05	9.18E-06	1.72E-05	9.78E-05	0.000105	6.25E-07	3.29E-05	4.04E-05	1.67E-05	1.69E-05	5.24E-17
0.000109	2.10E-05	2.01E-07	1.32E-05	9.37E-06	1.72E-05	9.87E-05	0.000106	6.25E-07	3.29E-05	4.04E-05	1.67E-05	1.69E-05	5.24E-17
0.000107	2.08E-05	2.01E-07	1.29E-05	8.98E-06	1.72E-05	9.69E-05	0.000104	6.25E-07	3.28E-05	4.03E-05	1.66E-05	1.68E-05	3.69E-16
0.000108	2.09E-05	2.01E-07	1.31E-05	9.18E-06	1.72E-05	9.78E-05	0.000105	6.25E-07	3.28E-05	4.03E-05	1.66E-05	1.68E-05	3.69E-16
0.000109	2.10E-05	2.01E-07	1.32E-05	9.37E-06	1.72E-05	9.87E-05	0.000106	6.25E-07	3.28E-05	4.03E-05	1.66E-05	1.68E-05	3.69E-16
0.000107	2.08E-05	2.01E-07	1.29E-05	8.98E-06	1.72E-05	9.69E-05	0.000104	6.25E-07	3.28E-05	4.02E-05	1.65E-05	1.67E-05	3.03E-16
0.000108	2.09E-05	2.01E-07	1.31E-05	9.18E-06	1.72E-05	9.78E-05	0.000105	6.25E-07	3.28E-05	4.02E-05	1.65E-05	1.67E-05	3.03E-16
0.000109	2.10E-05	2.01E-07	1.32E-05	9.37E-06	1.72E-05	9.87E-05	0.000106	6.25E-07	3.28E-05	4.02E-05	1.65E-05	1.67E-05	3.03E-16
0.000107	2.08E-05	2.01E-07	1.29E-05	8.98E-06	1.72E-05	9.69E-05	0.000104	6.25E-07	3.27E-05	4.02E-05	1.65E-05	1.66E-05	1.36E-16
0.000108	2.09E-05	2.01E-07	1.31E-05	9.18E-06	1.72E-05	9.78E-05	0.000105	6.25E-07	3.27E-05	4.02E-05	1.65E-05	1.66E-05	1.36E-16
0.000109	2.10E-05	2.01E-07	1.32E-05	9.37E-06	1.72E-05	9.87E-05	0.000106	6.25E-07	3.27E-05	4.02E-05	1.65E-05	1.66E-05	1.36E-16
0.000107	2.08E-05	2.01E-07	1.29E-05	8.98E-06	1.72E-05	9.69E-05	0.000104	6.25E-07	3.26E-05	4.01E-05	1.64E-05	1.66E-05	7.21E-17
0.000108	2.09E-05	2.01E-07	1.31E-05	9.18E-06	1.72E-05	9.78E-05	0.000105	6.25E-07	3.26E-05	4.01E-05	1.64E-05	1.66E-05	7.21E-17
0.000109	2.10E-05	2.01E-07	1.32E-05	9.37E-06	1.72E-05	9.87E-05	0.000106	6.25E-07	3.26E-05	4.01E-05	1.64E-05	1.66E-05	7.21E-17
0.000107	2.08E-05	2.01E-07	1.29E-05	8.98E-06	1.72E-05	9.69E-05	0.000104	6.25E-07	3.26E-05	4.00E-05	1.63E-05	1.65E-05	1.80E-16
0.000108	2.09E-05	2.01E-07	1.31E-05	9.18E-06	1.72E-05	9.78E-05	0.000105	6.25E-07	3.26E-05	4.00E-05	1.63E-05	1.65E-05	1.80E-16
0.000109	2.10E-05	2.01E-07	1.32E-05	9.37E-06	1.72E-05	9.87E-05	0.000106	6.25E-07	3.26E-05	4.00E-05	1.63E-05	1.65E-05	1.80E-16
0.000107	2.08E-05	2.01E-07	1.29E-05	8.98E-06	1.72E-05	9.69E-05	0.000104	6.25E-07	3.25E-05	3.99E-05	1.63E-05	1.64E-05	4.36E-16
0.000108	2.09E-05	2.01E-07	1.31E-05	9.18E-06	1.72E-05	9.78E-05	0.000105	6.25E-07	3.25E-05	3.99E-05	1.63E-05	1.64E-05	4.36E-16
0.000109	2.10E-05	2.01E-07	1.32E-05	9.37E-06	1.72E-05	9.87E-05	0.000106	6.25E-07	3.25E-05	3.99E-05	1.63E-05	1.64E-05	4.36E-16
0.000112	2.25E-05	2.01E-07	1.44E-05	9.73E-06	1.86E-05	0.000102	0.000109	6.25E-07	3.29E-05	4.04E-05	1.67E-05	1.69E-05	5.24E-17
0.000113	2.26E-05	2.01E-07	1.46E-05	9.95E-06	1.87E-05	0.000103	0.000111	6.25E-07	3.29E-05	4.04E-05	1.67E-05	1.69E-05	5.24E-17
0.000115	2.28E-05	2.01E-07	1.48E-05	1.02E-05	1.88E-05	0.000104	0.000112	6.25E-07	3.29E-05	4.04E-05	1.67E-05	1.69E-05	5.24E-17
0.000112	2.25E-05	2.01E-07	1.44E-05	9.73E-06	1.86E-05	0.000102	0.000109	6.25E-07	3.28E-05	4.03E-05	1.66E-05	1.68E-05	3.69E-16
0.000113	2.26E-05	2.01E-07	1.46E-05	9.95E-06	1.87E-05	0.000103	0.000111	6.25E-07	3.28E-05	4.03E-05	1.66E-05	1.68E-05	3.69E-16
0.000115	2.28E-05	2.01E-07	1.48E-05	1.02E-05	1.88E-05	0.000104	0.000112	6.25E-07	3.28E-05	4.03E-05	1.66E-05	1.68E-05	3.69E-16
0.000112	2.25E-05	2.01E-07	1.44E-05	9.73E-06	1.86E-05	0.000102	0.000109	6.25E-07	3.28E-05	4.02E-05	1.65E-05	1.67E-05	3.03E-16
0.000113	2.26E-05	2.01E-07	1.46E-05	9.95E-06	1.87E-05	0.000103	0.000111	6.25E-07	3.28E-05	4.02E-05	1.65E-05	1.67E-05	3.03E-16
0.000115	2.28E-05	2.01E-07	1.48E-05	1.02E-05	1.88E-05	0.000104	0.000112	6.25E-07	3.28E-05	4.02E-05	1.65E-05	1.67E-05	3.03E-16

0.000112	2.25E-05	2.01E-07	1.44E-05	9.73E-06	1.86E-05	0.000102	0.000109	6.25E-07	3.27E-05	4.02E-05	1.65E-05	1.66E-05	1.36E-16
0.000113	2.26E-05	2.01E-07	1.46E-05	9.95E-06	1.87E-05	0.000103	0.000111	6.25E-07	3.27E-05	4.02E-05	1.65E-05	1.66E-05	1.36E-16
0.000115	2.28E-05	2.01E-07	1.48E-05	1.02E-05	1.88E-05	0.000104	0.000112	6.25E-07	3.27E-05	4.02E-05	1.65E-05	1.66E-05	1.36E-16
0.000112	2.25E-05	2.01E-07	1.44E-05	9.73E-06	1.86E-05	0.000102	0.000109	6.25E-07	3.26E-05	4.01E-05	1.64E-05	1.66E-05	7.21E-17
0.000113	2.26E-05	2.01E-07	1.46E-05	9.95E-06	1.87E-05	0.000103	0.000111	6.25E-07	3.26E-05	4.01E-05	1.64E-05	1.66E-05	7.21E-17
0.000115	2.28E-05	2.01E-07	1.48E-05	1.02E-05	1.88E-05	0.000104	0.000112	6.25E-07	3.26E-05	4.01E-05	1.64E-05	1.66E-05	7.21E-17
0.000112	2.25E-05	2.01E-07	1.44E-05	9.73E-06	1.86E-05	0.000102	0.000109	6.25E-07	3.26E-05	4.00E-05	1.63E-05	1.65E-05	1.80E-16
0.000113	2.26E-05	2.01E-07	1.46E-05	9.95E-06	1.87E-05	0.000103	0.000111	6.25E-07	3.26E-05	4.00E-05	1.63E-05	1.65E-05	1.80E-16
0.000115	2.28E-05	2.01E-07	1.48E-05	1.02E-05	1.88E-05	0.000104	0.000112	6.25E-07	3.26E-05	4.00E-05	1.63E-05	1.65E-05	1.80E-16
0.000112	2.25E-05	2.01E-07	1.44E-05	9.73E-06	1.86E-05	0.000102	0.000109	6.25E-07	3.25E-05	3.99E-05	1.63E-05	1.64E-05	4.36E-16
0.000113	2.26E-05	2.01E-07	1.46E-05	9.95E-06	1.87E-05	0.000103	0.000111	6.25E-07	3.25E-05	3.99E-05	1.63E-05	1.64E-05	4.36E-16
0.000115	2.28E-05	2.01E-07	1.48E-05	1.02E-05	1.88E-05	0.000104	0.000112	6.25E-07	3.25E-05	3.99E-05	1.63E-05	1.64E-05	4.36E-16
0.000118	2.46E-05	2.01E-07	1.62E-05	9.88E-06	2.05E-05	0.000107	0.000114	6.25E-07	3.29E-05	4.04E-05	1.67E-05	1.69E-05	5.24E-17
0.000119	2.48E-05	2.01E-07	1.64E-05	1.01E-05	2.06E-05	0.000108	0.000116	6.25E-07	3.29E-05	4.04E-05	1.67E-05	1.69E-05	5.24E-17
0.00012	2.50E-05	2.01E-07	1.67E-05	1.03E-05	2.08E-05	0.000109	0.000117	6.25E-07	3.29E-05	4.04E-05	1.67E-05	1.69E-05	5.24E-17
0.000118	2.46E-05	2.01E-07	1.62E-05	9.88E-06	2.05E-05	0.000107	0.000114	6.25E-07	3.28E-05	4.03E-05	1.66E-05	1.68E-05	3.69E-16
0.000119	2.48E-05	2.01E-07	1.64E-05	1.01E-05	2.06E-05	0.000108	0.000116	6.25E-07	3.28E-05	4.03E-05	1.66E-05	1.68E-05	3.69E-16
0.00012	2.50E-05	2.01E-07	1.67E-05	1.03E-05	2.08E-05	0.000109	0.000117	6.25E-07	3.28E-05	4.03E-05	1.66E-05	1.68E-05	3.69E-16
0.000118	2.46E-05	2.01E-07	1.62E-05	9.88E-06	2.05E-05	0.000107	0.000114	6.25E-07	3.28E-05	4.02E-05	1.65E-05	1.67E-05	3.03E-16
0.000119	2.48E-05	2.01E-07	1.64E-05	1.01E-05	2.06E-05	0.000108	0.000116	6.25E-07	3.28E-05	4.02E-05	1.65E-05	1.67E-05	3.03E-16
0.00012	2.50E-05	2.01E-07	1.67E-05	1.03E-05	2.08E-05	0.000109	0.000117	6.25E-07	3.28E-05	4.02E-05	1.65E-05	1.67E-05	3.03E-16
0.000118	2.46E-05	2.01E-07	1.62E-05	9.88E-06	2.05E-05	0.000107	0.000114	6.25E-07	3.27E-05	4.02E-05	1.65E-05	1.66E-05	1.36E-16
0.000119	2.48E-05	2.01E-07	1.64E-05	1.01E-05	2.06E-05	0.000108	0.000116	6.25E-07	3.27E-05	4.02E-05	1.65E-05	1.66E-05	1.36E-16
0.00012	2.50E-05	2.01E-07	1.67E-05	1.03E-05	2.08E-05	0.000109	0.000117	6.25E-07	3.27E-05	4.02E-05	1.65E-05	1.66E-05	1.36E-16
0.000118	2.46E-05	2.01E-07	1.62E-05	9.88E-06	2.05E-05	0.000107	0.000114	6.25E-07	3.26E-05	4.01E-05	1.64E-05	1.66E-05	7.21E-17
0.000119	2.48E-05	2.01E-07	1.64E-05	1.01E-05	2.06E-05	0.000108	0.000116	6.25E-07	3.26E-05	4.01E-05	1.64E-05	1.66E-05	7.21E-17
0.00012	2.50E-05	2.01E-07	1.67E-05	1.03E-05	2.08E-05	0.000109	0.000117	6.25E-07	3.26E-05	4.01E-05	1.64E-05	1.66E-05	7.21E-17
0.000118	2.46E-05	2.01E-07	1.62E-05	9.88E-06	2.05E-05	0.000107	0.000114	6.25E-07	3.26E-05	4.00E-05	1.63E-05	1.65E-05	1.80E-16
0.000119	2.48E-05	2.01E-07	1.64E-05	1.01E-05	2.06E-05	0.000108	0.000116	6.25E-07	3.26E-05	4.00E-05	1.63E-05	1.65E-05	1.80E-16
0.00012	2.50E-05	2.01E-07	1.67E-05	1.03E-05	2.08E-05	0.000109	0.000117	6.25E-07	3.26E-05	4.00E-05	1.63E-05	1.65E-05	1.80E-16

0.000118	2.46E-05	2.01E-07	1.62E-05	9.88E-06	2.05E-05	0.000107	0.000114	6.25E-07	3.25E-05	3.99E-05	1.63E-05	1.64E-05	4.36E-16
0.000119	2.48E-05	2.01E-07	1.64E-05	1.01E-05	2.06E-05	0.000108	0.000116	6.25E-07	3.25E-05	3.99E-05	1.63E-05	1.64E-05	4.36E-16
0.00012	2.50E-05	2.01E-07	1.67E-05	1.03E-05	2.08E-05	0.000109	0.000117	6.25E-07	3.25E-05	3.99E-05	1.63E-05	1.64E-05	4.36E-16
0.000123	2.71E-05	2.01E-07	1.75E-05	9.29E-06	2.28E-05	0.000112	0.00012	6.25E-07	3.29E-05	4.04E-05	1.67E-05	1.69E-05	5.24E-17
0.000124	2.73E-05	2.01E-07	1.78E-05	9.48E-06	2.30E-05	0.000113	0.000121	6.25E-07	3.29E-05	4.04E-05	1.67E-05	1.69E-05	5.24E-17
0.000126	2.76E-05	2.01E-07	1.81E-05	9.67E-06	2.33E-05	0.000115	0.000122	6.25E-07	3.29E-05	4.04E-05	1.67E-05	1.69E-05	5.24E-17
0.000123	2.71E-05	2.01E-07	1.75E-05	9.29E-06	2.28E-05	0.000112	0.00012	6.25E-07	3.28E-05	4.03E-05	1.66E-05	1.68E-05	3.69E-16
0.000124	2.73E-05	2.01E-07	1.78E-05	9.48E-06	2.30E-05	0.000113	0.000121	6.25E-07	3.28E-05	4.03E-05	1.66E-05	1.68E-05	3.69E-16
0.000126	2.76E-05	2.01E-07	1.81E-05	9.67E-06	2.33E-05	0.000115	0.000122	6.25E-07	3.28E-05	4.03E-05	1.66E-05	1.68E-05	3.69E-16
0.000123	2.71E-05	2.01E-07	1.75E-05	9.29E-06	2.28E-05	0.000112	0.00012	6.25E-07	3.28E-05	4.02E-05	1.65E-05	1.67E-05	3.03E-16
0.000124	2.73E-05	2.01E-07	1.78E-05	9.48E-06	2.30E-05	0.000113	0.000121	6.25E-07	3.28E-05	4.02E-05	1.65E-05	1.67E-05	3.03E-16
0.000126	2.76E-05	2.01E-07	1.81E-05	9.67E-06	2.33E-05	0.000115	0.000122	6.25E-07	3.28E-05	4.02E-05	1.65E-05	1.67E-05	3.03E-16
0.000123	2.71E-05	2.01E-07	1.75E-05	9.29E-06	2.28E-05	0.000112	0.00012	6.25E-07	3.27E-05	4.02E-05	1.65E-05	1.66E-05	1.36E-16
0.000124	2.73E-05	2.01E-07	1.78E-05	9.48E-06	2.30E-05	0.000113	0.000121	6.25E-07	3.27E-05	4.02E-05	1.65E-05	1.66E-05	1.36E-16
0.000126	2.76E-05	2.01E-07	1.81E-05	9.67E-06	2.33E-05	0.000115	0.000122	6.25E-07	3.27E-05	4.02E-05	1.65E-05	1.66E-05	1.36E-16
0.000123	2.71E-05	2.01E-07	1.75E-05	9.29E-06	2.28E-05	0.000112	0.00012	6.25E-07	3.26E-05	4.01E-05	1.64E-05	1.66E-05	7.21E-17
0.000124	2.73E-05	2.01E-07	1.78E-05	9.48E-06	2.30E-05	0.000113	0.000121	6.25E-07	3.26E-05	4.01E-05	1.64E-05	1.66E-05	7.21E-17
0.000126	2.76E-05	2.01E-07	1.81E-05	9.67E-06	2.33E-05	0.000115	0.000122	6.25E-07	3.26E-05	4.01E-05	1.64E-05	1.66E-05	7.21E-17
0.000123	2.71E-05	2.01E-07	1.75E-05	9.29E-06	2.28E-05	0.000112	0.00012	6.25E-07	3.26E-05	4.00E-05	1.63E-05	1.65E-05	1.80E-16
0.000124	2.73E-05	2.01E-07	1.78E-05	9.48E-06	2.30E-05	0.000113	0.000121	6.25E-07	3.26E-05	4.00E-05	1.63E-05	1.65E-05	1.80E-16
0.000126	2.76E-05	2.01E-07	1.81E-05	9.67E-06	2.33E-05	0.000115	0.000122	6.25E-07	3.26E-05	4.00E-05	1.63E-05	1.65E-05	1.80E-16
0.000123	2.71E-05	2.01E-07	1.75E-05	9.29E-06	2.28E-05	0.000112	0.00012	6.25E-07	3.25E-05	3.99E-05	1.63E-05	1.64E-05	4.36E-16
0.000124	2.73E-05	2.01E-07	1.78E-05	9.48E-06	2.30E-05	0.000113	0.000121	6.25E-07	3.25E-05	3.99E-05	1.63E-05	1.64E-05	4.36E-16
0.000126	2.76E-05	2.01E-07	1.81E-05	9.67E-06	2.33E-05	0.000115	0.000122	6.25E-07	3.25E-05	3.99E-05	1.63E-05	1.64E-05	4.36E-16
0.000123	2.81E-05	2.01E-07	1.60E-05	7.55E-06	2.39E-05	0.000112	0.00012	6.25E-07	3.29E-05	4.04E-05	1.67E-05	1.69E-05	5.24E-17
0.000124	2.84E-05	2.01E-07	1.62E-05	7.68E-06	2.42E-05	0.000113	0.000121	6.25E-07	3.29E-05	4.04E-05	1.67E-05	1.69E-05	5.24E-17
0.000126	2.87E-05	2.01E-07	1.65E-05	7.81E-06	2.44E-05	0.000115	0.000123	6.25E-07	3.29E-05	4.04E-05	1.67E-05	1.69E-05	5.24E-17
0.000123	2.81E-05	2.01E-07	1.60E-05	7.55E-06	2.39E-05	0.000112	0.00012	6.25E-07	3.28E-05	4.03E-05	1.66E-05	1.68E-05	3.69E-16
0.000124	2.84E-05	2.01E-07	1.62E-05	7.68E-06	2.42E-05	0.000113	0.000121	6.25E-07	3.28E-05	4.03E-05	1.66E-05	1.68E-05	3.69E-16
0.000126	2.87E-05	2.01E-07	1.65E-05	7.81E-06	2.44E-05	0.000115	0.000123	6.25E-07	3.28E-05	4.03E-05	1.66E-05	1.68E-05	3.69E-16

0.000123	2.81E-05	2.01E-07	1.60E-05	7.55E-06	2.39E-05	0.000112	0.00012	6.25E-07	3.28E-05	4.02E-05	1.65E-05	1.67E-05	3.03E-16
0.000124	2.84E-05	2.01E-07	1.62E-05	7.68E-06	2.42E-05	0.000113	0.000121	6.25E-07	3.28E-05	4.02E-05	1.65E-05	1.67E-05	3.03E-16
0.000126	2.87E-05	2.01E-07	1.65E-05	7.81E-06	2.44E-05	0.000115	0.000123	6.25E-07	3.28E-05	4.02E-05	1.65E-05	1.67E-05	3.03E-16
0.000123	2.81E-05	2.01E-07	1.60E-05	7.55E-06	2.39E-05	0.000112	0.00012	6.25E-07	3.27E-05	4.02E-05	1.65E-05	1.66E-05	1.36E-16
0.000124	2.84E-05	2.01E-07	1.62E-05	7.68E-06	2.42E-05	0.000113	0.000121	6.25E-07	3.27E-05	4.02E-05	1.65E-05	1.66E-05	1.36E-16
0.000126	2.87E-05	2.01E-07	1.65E-05	7.81E-06	2.44E-05	0.000115	0.000123	6.25E-07	3.27E-05	4.02E-05	1.65E-05	1.66E-05	1.36E-16
0.000123	2.81E-05	2.01E-07	1.60E-05	7.55E-06	2.39E-05	0.000112	0.00012	6.25E-07	3.26E-05	4.01E-05	1.64E-05	1.66E-05	7.21E-17
0.000124	2.84E-05	2.01E-07	1.62E-05	7.68E-06	2.42E-05	0.000113	0.000121	6.25E-07	3.26E-05	4.01E-05	1.64E-05	1.66E-05	7.21E-17
0.000126	2.87E-05	2.01E-07	1.65E-05	7.81E-06	2.44E-05	0.000115	0.000123	6.25E-07	3.26E-05	4.01E-05	1.64E-05	1.66E-05	7.21E-17
0.000123	2.81E-05	2.01E-07	1.60E-05	7.55E-06	2.39E-05	0.000112	0.00012	6.25E-07	3.26E-05	4.00E-05	1.63E-05	1.65E-05	1.80E-16
0.000124	2.84E-05	2.01E-07	1.62E-05	7.68E-06	2.42E-05	0.000113	0.000121	6.25E-07	3.26E-05	4.00E-05	1.63E-05	1.65E-05	1.80E-16
0.000126	2.87E-05	2.01E-07	1.65E-05	7.81E-06	2.44E-05	0.000115	0.000123	6.25E-07	3.26E-05	4.00E-05	1.63E-05	1.65E-05	1.80E-16
0.000123	2.81E-05	2.01E-07	1.60E-05	7.55E-06	2.39E-05	0.000112	0.00012	6.25E-07	3.25E-05	3.99E-05	1.63E-05	1.64E-05	4.36E-16
0.000124	2.84E-05	2.01E-07	1.62E-05	7.68E-06	2.42E-05	0.000113	0.000121	6.25E-07	3.25E-05	3.99E-05	1.63E-05	1.64E-05	4.36E-16
0.000126	2.87E-05	2.01E-07	1.65E-05	7.81E-06	2.44E-05	0.000115	0.000123	6.25E-07	3.25E-05	3.99E-05	1.63E-05	1.64E-05	4.36E-16

C.3 Post tensioning

Table C.3 C Strain data for post tensioning operation

Location													
182	115	191	32	53	109	180	183	185	247	250	280	296	328
0.000123	2.81E-05	2.01E-07	1.60E-05	7.55E-06	2.39E-05	0.000112	0.00012	6.25E-07	3.29E-05	4.04E-05	1.67E-05	1.69E-05	5.24E-17
0.000124	2.84E-05	2.01E-07	1.62E-05	7.68E-06	2.42E-05	0.000113	0.000121	6.25E-07	3.29E-05	4.04E-05	1.67E-05	1.69E-05	5.24E-17
0.000126	2.87E-05	2.01E-07	1.65E-05	7.81E-06	2.44E-05	0.000115	0.000123	6.25E-07	3.29E-05	4.04E-05	1.67E-05	1.69E-05	5.24E-17
0.000123	2.81E-05	2.01E-07	1.60E-05	7.55E-06	2.39E-05	0.000112	0.00012	6.25E-07	3.28E-05	4.03E-05	1.66E-05	1.68E-05	3.69E-16
0.000124	2.84E-05	2.01E-07	1.62E-05	7.68E-06	2.42E-05	0.000113	0.000121	6.25E-07	3.28E-05	4.03E-05	1.66E-05	1.68E-05	3.69E-16
0.000126	2.87E-05	2.01E-07	1.65E-05	7.81E-06	2.44E-05	0.000115	0.000123	6.25E-07	3.28E-05	4.03E-05	1.66E-05	1.68E-05	3.69E-16
0.000123	2.81E-05	2.01E-07	1.60E-05	7.55E-06	2.39E-05	0.000112	0.00012	6.25E-07	3.28E-05	4.02E-05	1.65E-05	1.67E-05	3.03E-16
0.000124	2.84E-05	2.01E-07	1.62E-05	7.68E-06	2.42E-05	0.000113	0.000121	6.25E-07	3.28E-05	4.02E-05	1.65E-05	1.67E-05	3.03E-16

0.000126	2.87E-05	2.01E-07	1.65E-05	7.81E-06	2.44E-05	0.000115	0.000123	6.25E-07	3.28E-05	4.02E-05	1.65E-05	1.67E-05	3.03E-16
0.000123	2.81E-05	2.01E-07	1.60E-05	7.55E-06	2.39E-05	0.000112	0.00012	6.25E-07	3.27E-05	4.02E-05	1.65E-05	1.66E-05	1.36E-16
0.000124	2.84E-05	2.01E-07	1.62E-05	7.68E-06	2.42E-05	0.000113	0.000121	6.25E-07	3.27E-05	4.02E-05	1.65E-05	1.66E-05	1.36E-16
0.000126	2.87E-05	2.01E-07	1.65E-05	7.81E-06	2.44E-05	0.000115	0.000123	6.25E-07	3.27E-05	4.02E-05	1.65E-05	1.66E-05	1.36E-16
0.000123	2.81E-05	2.01E-07	1.60E-05	7.55E-06	2.39E-05	0.000112	0.00012	6.25E-07	3.26E-05	4.01E-05	1.64E-05	1.66E-05	7.21E-17
0.000124	2.84E-05	2.01E-07	1.62E-05	7.68E-06	2.42E-05	0.000113	0.000121	6.25E-07	3.26E-05	4.01E-05	1.64E-05	1.66E-05	7.21E-17
0.000126	2.87E-05	2.01E-07	1.65E-05	7.81E-06	2.44E-05	0.000115	0.000123	6.25E-07	3.26E-05	4.01E-05	1.64E-05	1.66E-05	7.21E-17
0.000123	2.81E-05	2.01E-07	1.60E-05	7.55E-06	2.39E-05	0.000112	0.00012	6.25E-07	3.26E-05	4.00E-05	1.63E-05	1.65E-05	1.80E-16
0.000124	2.84E-05	2.01E-07	1.62E-05	7.68E-06	2.42E-05	0.000113	0.000121	6.25E-07	3.26E-05	4.00E-05	1.63E-05	1.65E-05	1.80E-16
0.000126	2.87E-05	2.01E-07	1.65E-05	7.81E-06	2.44E-05	0.000115	0.000123	6.25E-07	3.26E-05	4.00E-05	1.63E-05	1.65E-05	1.80E-16
0.000123	2.81E-05	2.01E-07	1.60E-05	7.55E-06	2.39E-05	0.000112	0.00012	6.25E-07	3.25E-05	3.99E-05	1.63E-05	1.64E-05	4.36E-16
0.000124	2.84E-05	2.01E-07	1.62E-05	7.68E-06	2.42E-05	0.000113	0.000121	6.25E-07	3.25E-05	3.99E-05	1.63E-05	1.64E-05	4.36E-16
0.000126	2.87E-05	2.01E-07	1.65E-05	7.81E-06	2.44E-05	0.000115	0.000123	6.25E-07	3.25E-05	3.99E-05	1.63E-05	1.64E-05	4.36E-16

C.4 Span Lowering

Location													
182	115	191	32	53	109	180	183	185	247	250	280	296	328
7.50E-05	1.80E-05	2.01E-07	8.47E-06	3.31E-06	1.55E-05	6.85E-05	7.29E-05	6.25E-07	3.29E-05	4.04E-05	1.67E-05	1.69E-05	5.24E-17
7.50E-05	1.80E-05	2.01E-07	8.47E-06	3.31E-06	1.55E-05	6.85E-05	7.29E-05	6.25E-07	3.29E-05	4.04E-05	1.67E-05	1.69E-05	5.24E-17
7.50E-05	1.80E-05	2.01E-07	8.47E-06	3.31E-06	1.55E-05	6.85E-05	7.29E-05	6.25E-07	3.29E-05	4.04E-05	1.67E-05	1.69E-05	5.24E-17
7.50E-05	1.80E-05	2.01E-07	8.47E-06	3.31E-06	1.55E-05	6.85E-05	7.29E-05	6.25E-07	3.28E-05	4.03E-05	1.66E-05	1.68E-05	3.69E-16
7.50E-05	1.80E-05	2.01E-07	8.47E-06	3.31E-06	1.55E-05	6.85E-05	7.29E-05	6.25E-07	3.28E-05	4.03E-05	1.66E-05	1.68E-05	3.69E-16
7.50E-05	1.80E-05	2.01E-07	8.47E-06	3.31E-06	1.55E-05	6.85E-05	7.29E-05	6.25E-07	3.28E-05	4.03E-05	1.66E-05	1.68E-05	3.69E-16
7.50E-05	1.80E-05	2.01E-07	8.47E-06	3.31E-06	1.55E-05	6.85E-05	7.29E-05	6.25E-07	3.28E-05	4.02E-05	1.65E-05	1.67E-05	3.03E-16
7.50E-05	1.80E-05	2.01E-07	8.47E-06	3.31E-06	1.55E-05	6.85E-05	7.29E-05	6.25E-07	3.28E-05	4.02E-05	1.65E-05	1.67E-05	3.03E-16
7.50E-05	1.80E-05	2.01E-07	8.47E-06	3.31E-06	1.55E-05	6.85E-05	7.29E-05	6.25E-07	3.28E-05	4.02E-05	1.65E-05	1.67E-05	3.03E-16
7.50E-05	1.80E-05	2.01E-07	8.47E-06	3.31E-06	1.55E-05	6.85E-05	7.29E-05	6.25E-07	3.27E-05	4.02E-05	1.65E-05	1.66E-05	1.36E-16

7.50E-05	1.80E-05	2.01E-07	8.47E-06	3.31E-06	1.55E-05	6.85E-05	7.29E-05	6.25E-07	3.27E-05	4.02E-05	1.65E-05	1.66E-05	1.36E-16
7.50E-05	1.80E-05	2.01E-07	8.47E-06	3.31E-06	1.55E-05	6.85E-05	7.29E-05	6.25E-07	3.27E-05	4.02E-05	1.65E-05	1.66E-05	1.36E-16
7.50E-05	1.80E-05	2.01E-07	8.47E-06	3.31E-06	1.55E-05	6.85E-05	7.29E-05	6.25E-07	3.26E-05	4.01E-05	1.64E-05	1.66E-05	7.21E-17
7.50E-05	1.80E-05	2.01E-07	8.47E-06	3.31E-06	1.55E-05	6.85E-05	7.29E-05	6.25E-07	3.26E-05	4.01E-05	1.64E-05	1.66E-05	7.21E-17
7.50E-05	1.80E-05	2.01E-07	8.47E-06	3.31E-06	1.55E-05	6.85E-05	7.29E-05	6.25E-07	3.26E-05	4.01E-05	1.64E-05	1.66E-05	7.21E-17
7.50E-05	1.80E-05	2.01E-07	8.47E-06	3.31E-06	1.55E-05	6.85E-05	7.29E-05	6.25E-07	3.26E-05	4.00E-05	1.63E-05	1.65E-05	1.80E-16
7.50E-05	1.80E-05	2.01E-07	8.47E-06	3.31E-06	1.55E-05	6.85E-05	7.29E-05	6.25E-07	3.26E-05	4.00E-05	1.63E-05	1.65E-05	1.80E-16
7.50E-05	1.80E-05	2.01E-07	8.47E-06	3.31E-06	1.55E-05	6.85E-05	7.29E-05	6.25E-07	3.26E-05	4.00E-05	1.63E-05	1.65E-05	1.80E-16
7.50E-05	1.80E-05	2.01E-07	8.47E-06	3.31E-06	1.55E-05	6.85E-05	7.29E-05	6.25E-07	3.25E-05	3.99E-05	1.63E-05	1.64E-05	4.36E-16
7.50E-05	1.80E-05	2.01E-07	8.47E-06	3.31E-06	1.55E-05	6.85E-05	7.29E-05	6.25E-07	3.25E-05	3.99E-05	1.63E-05	1.64E-05	4.36E-16
7.50E-05	1.80E-05	2.01E-07	8.47E-06	3.31E-06	1.55E-05	6.85E-05	7.29E-05	6.25E-07	3.25E-05	3.99E-05	1.63E-05	1.64E-05	4.36E-16

C.6 System Identification Methodology C – Illustration

Figure C.1 shows the simplified sequence of system identification methodology C.

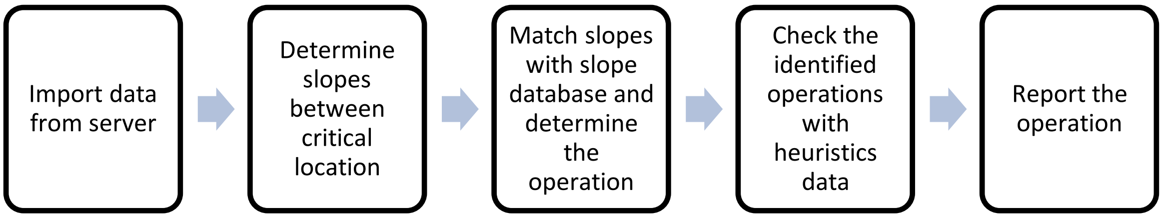

Figure C.1 : System Identification Methodology C Steps

Table C.5 shows a sample of data from the field data implementation downloaded from the server. This data was received after a data which was identified as Autolaunching.

Table C.4 Sample data from site

Location	182	115	191	32	53	109	180	183	185	247
Data	4.96E-05	3.12E-06	2.01E-07	1.40E-05	1.28E-05	1.09E-06	4.41E-05	4.87E-05	6.25E-07	3.28E-05

.

Once the data is imported from the server, Slopes between the readings at the critical locations are determined. The result is as shown in Table C.6

Table C.5 Slope Data

Slope Location A- Location B	182/115	115/191	191/32	32/53	53/109	109/180	180/183	183/185	185/247
Slope	1.59E+01	1.55E+01	1.44E-02	1.09E+00	1.17E+01	2.47E-02	9.06E-01	7.79E+01	1.91E-02

Search for the above slopes within an interval of +/- 2 * precision from the slope database

Table C.6 Slope data for Segment Lifting Case 18

Slope Location A- Location B	182/115	115/191	191/32	32/53	53/109	109/180	180/183	183/185	p185/247
Lower Limit	15.89744	15.52238	0.014346	1.093734	11.7431	0.024689	0.905511	77.91996	0.019027
Upper limit	15.89749	15.52244	0.014401	1.093789	11.74315	0.024744	0.905566	77.92002	0.019082

The slope data in Table C.6 lies in the interval corresponding to Segment lifting case 18 as shown in Table C.7. Hence it can be inferred that the current operation is segment lifting. Now we need to check the inferred data with heuristics condition. The previous data corresponded to Auto Launching. Therefore the current data can only be either Auto launching or segment lifting. The inferred data being segment lifting case 20, satisfies this condition. Hence report the activity as SEGMENT LIFTING.

CURRICULUM VITAE

Name:	RANJITH K. S.
Date of Birth:	13-12-1991

Educational Qualification

2013 Bachelor of Technology (B. Tech.)

Institution:	Government Engineering College Thrissur, University of Calicut
Specialization:	Civil Engineering

GENERAL TEST COMMITTEE

CHAIR PERSON:	Prof. K. Ananthanarayan Professor Department of Civil Engineering
GUIDE:	Dr. Benny Raphael Associate Professor Department of Civil Engineering
	Prof. Koshy Varghese Professor Department of Civil Engineering
MEMBERS:	Prof. V. Kamakoti . Professor Department of Computer Science and Engineering
	Dr. U. Saravanan Associate Professor Department of Civil Engineering